11-15-2015

Ecological strategies and disturbance response of tropical forest trees: insight from functional trait variation

Oyomoare Lolade Osazuwa-Peters
University of Missouri-St. Louis, oletkd@mail.umsl.edu

Ecological strategies and disturbance response of tropical forest trees: insight from functional trait variation

Oyomoare L. Osazuwa-Peters

M.Sc. Environmental Protection and Management, University of Edinburgh, Scotland, 2007
B.Sc., Botany, University of Benin, Nigeria, 2004

A dissertation submitted to the Graduate School at the University of Missouri-St. Louis in partial fulfillment of the requirements for the degree of Doctor of Philosophy in Biology with an emphasis in Ecology

May, 2015

Advisory Committee

Peter Stevens, Ph.D. (Advisor)

Amy Zanne, Ph.D. (Co-advisor)

Robert Marquis, Ph.D.

Iván Jiménez, Ph.D.

Acknowledgement

As many drops of water makes an ocean, I realize there are many who have made contributions by words or deeds, small or great, to my pursuit of a doctoral degree in the last five and a half years. To all of you, I say thank you, but due to limited space I can only mention some people.

Sincere thanks to my academic mentors who have patiently molded, guided and supported me in my advancement from an unadventurous, research-naïve first year graduate student to one who has successfully written and published peer-reviewed articles. For this, my advisor Dr. Amy Zanne, bears much of the credit, especially for her challenging me to develop my own intellectual identity, believing in my potential and what I can achieve even before I realized my own capabilities, and investing her and time and resources. Amy enjoys telling about when she encouraged me to explore the statistical computing software R for my data analysis. Even though I was initially hesitant and wanted to play safe with SPSS, Amy gently nudged me and did not give up in prodding me because she believed I could do it. Years later, as I write this page, I reflect on the fact that my entire dissertation analysis was done in R! Thanks Amy! On a different note, Amy earned my respect and admiration for her tolerance and respect for my rather unpopular stance towards widely accepted customs and holidays. I reckon this has not been always convenient for her in the last five and a half years, and yet she has respected my views and made allowances.

When Amy left UMSL in 2012, Dr. Peter Stevens became my advisor, and it has been a pleasant experience working with Peter. I call him the ‘face of kindness’, always looking out for my interest and success, always giving me valuable advice. What I find most endearing about Peter is his willingness to find solutions to whatever challenges I face, as well as read my paper as many times as possible, never tired of reading my drafts. Truly encouraging! There are others who patiently read as many drafts as I asked them to, and played pivotal roles in shaping and executing my dissertation research; Dr. Colin Chapman, so generous with his time and data representing decades of his hard-work. Dr. S. J. Wright, also generous with data and a patient teacher of even the simplest concepts that I had managed to forget! Dr. Wright made substantial contributions to the success of my first field season, providing field assistants, going to the field with me, showing me how to enter data in the long format that R loves, helping to resolve administrative issues, and welcoming my husband and I into his home while we were transiting through Gamboa, Panama. Dr. Iván Jiménez introduced me to the world of hypotheses and predictions, sampling distributions, and null models, unleashing the power of R before my eyes! Dr. Brad Oberle, another patient and effective teacher who showed me how to interpret statistical outputs from R. Dr. Robert Marquis, whose constructive comments and feedback during committee meetings were very helpful for anticipating comments from journal reviewers and editors.

I must not forget Dr. Patrick Osborne and the Whitney Harris World Ecology Center. They gave me this opportunity in the first place, and for this I am grateful. My research was mainly funded by the Whitney Harris World Ecology Center, with other

contributions from the Webster Grove Nature Study Society, and IDEA Wild. Dr. Patrick Osborne and his wife, Nancy Osborne, were supportive, especially with positive and encouraging words. Along with Renata Reinheimer, Patrick and Nancy Osborne helped me settle in during my first few weeks in St. Louis. Dr. David Kenfack too, always looking for opportunities for his African sister, setting up arrangements that led to two chapters in my dissertation. Folks at the Missouri Botanical Garden were very supportive, particularly Drs. Richard Keating and David Bogler; as well as the Smithsonian Tropical Research Institute, Panama, and the Kibale National Park, Uganda. My mentors in Nigeria, Drs. F. M. Ogbe, E. I. Aigbokhan, D. E. Vwioko, M. E. Osawaru, and other members of Department of Plant Biology and Biotechnology, University of Benin, Nigeria. You were the ones who spurred me on, and believed that the sky was my limit, giving me whatever support you could.

There were many behind the scenes; thanks to those who sorted out any administrative issues I encountered, Pat Hinton, Maryann Hempen, Kathy Burney-Miller; members of the Department of Biology, UMSL, especially friends that I have shared the graduate experience with including Jonathan Sweeney, Vania Torrez, Heritiana Ranarivelo, Maria Pil (and Junior Bagnara), Juan Carlos Penagos, Samoa Asigau, Mari Jaramillo, Rani Asmayarani, Leticia Guttierrez and most recently Leticia Soares my pal on the Certificate in University Teaching program, and Gyanpriya Maharaj who has made my teaching assistant experience on Human Anatomy and Physiology I smooth sailing. I also remember the field assistants I worked with in Panama, and Uganda (names mentioned in relevant articles); I really wouldn't have made it without them. And members of the

Zanne lab who had to listen to me practice numerous oral presentations including Darcy Young and Amy Milo. I must mention Maranda Evans, a special person and former member of the Zanne lab who was kind and practically helpful when I was so heavily pregnant and trying to set up a decomposition experiment.

And now my family; my Christian family, Delmar congregation at the local kingdom hall of Jehovah's witnesses, and the Mugalya Jones family in Fort Portal, Uganda. You played a big role in helping me keep my faith and hold on to my spiritual heritage. Belonging to two worlds that think differently was tough! But I have gone through this experience even surer of my convictions, and I thank my Christian family for helping me remain in Jehovah's loyal love! Now, my family; they have made the greatest sacrifices that words cannot capture, giving me financial and moral support, caring for my little man Owen Osazuwa-Peters these past few months. To my family, your love has been inspiring and sustaining! I say thank you to my parents, May and Osaretin Eruogun, and their entire household, Ayo Eruogun's family, Ekiomado Ohonyon's family, Rachel Iyageh's family (my backbone in America!), Uncle Jon Aibueku, and my family by marriage Godwin and Stella Osazuwa along with their household, particularly Osayomwanbor and Osakpolor Osazuwa.

I must end with a message of deep appreciation to my husband, Nosayaba Osazuwa-Peters, my fondest admirer and soulmate. Thanks for sharing my passion, giving me a reason to endure through these five and a half years and showing me how to enjoy life!

Table of contents **Page**

Acknowledgment ii
Dissertation abstract vii

Chapter 1 **1**
Radial variation in wood specific gravity of tropical tree species differing in growth-mortality strategies
Introduction 3
Methods 6
Results 13
Discussion 15
References 30
Supplementary material for chapter 1 36

Chapter 2 **38**
Anatomical underpinnings of wood density variation in tropical rainforest trees: insights from ontogeny
Introduction 40
Methods 46
Results 54
Discussion 57
References 79
Supplementary material for chapter 2 84

Chapter 3 **86**
Selective logging: does the imprint remain on tree structure and composition after 45 years?
Introduction 88
Methods 92
Results 100
Discussion 102
References 118
Supplementary material for chapter 3 124

Chapter 4 **127**
Selective logging: do rates of forest turnover in demography, species composition and functional traits decrease with time since disturbance? ─ A 45 year perspective
Introduction 129
Methods 135
Results 147
Discussion 150
References 160
Supplementary material for chapter 4 175

Dissertation abstract:

Tropical forests store ≈ 40% of terrestrial carbon, process six times as much carbon as is released through fossil fuel use, and are epicenters of biodiversity. Despite all that we know about tropical forests, there remains much to discover about variation in ecological strategies, differences in the way species acquire limited resources through dissimilarities in construction and allocation patterns. We also know little as to how this variation shapes the resilience of tropical tree communities to disturbance. These forests are increasingly threatened by global change stressors, such as anthropogenic land-use and climate change. Recent advances in ecological literature show that more insight into differences in ecological strategies among tropical forest species can be gained by going beyond species distributions to also examine functional trait variation. Functional traits are morphological and physiological traits that reflect allocation strategies thought to be important determinants of fitness. In the first two chapters of my dissertation, I quantified wood density and anatomical variation at multiple scales, and related this variation to ecological strategies of tropical forest tree species. The last two chapters examined effects of historical disturbance on the composition and temporal dynamics of tropical forest communities. In addition to wood density, other traits studied in these later chapters were maximum height and diameter. Across my dissertation, the scales spanned ranged from intra-individual, intra-specific, interspecific, community and temporal levels, across two tropical forests, the 50 ha CTFS plot in BCI, Panama, and the 5.2 ha long-term forest plots in Kibale National Park, Uganda. With the functional trait approach, my dissertation demonstrated several novel patterns, including 1) linear radial increases in

wood density are typical of fast-growth high mortality tropical tree species, while slow-growth low mortality species show a range of radial changes in wood density including non-linear trends 2) greater variation in ecological strategies when wood density is decomposed into anatomical components, with functional consequences for species growth and mortality of saplings but not adult trees, 3) persistence of the effects of selective logging on the taxonomic and structural composition but not functional composition of a tropical forest 45 years after, and 4) inadequacy of classical successional models that assume recovery to pre-disturbance conditions for predicting the effects of selective logging on tropical forest dynamics.

Chapter 1

Radial variation in wood specific gravity of tropical tree species differing in growth-mortality strategies

Oyomoare L. Osazuwa-Peters[1], S. Joseph Wright[2], and Amy E. Zanne[5, 6]

[1]Department of Biology, One University Boulevard, University of Missouri-St. Louis, St. Louis, Missouri, 63121, USA

[2]Smithsonian Tropical Research Institute, Apartado 0843 – 03092, Balboa, Panama

[3]Department of Biological Sciences, 2023 G St. NW, The George Washington University, Washington DC, 20052, USA

As published in:

Osazuwa-Peters, O. L., Wright, S. J., and Zanne, A. E. 2014. Radial variation in wood specific gravity of tropical tree species differing in growth-mortality strategies. *American Journal of Botany* 101(5): 803 – 811

Abstract

- *Premise of the study*: Wood specific gravity (WSG) mediates an interspecific tradeoff between growth and mortality and is a key measure for estimating carbon stocks. Most studies use species mean values to represent WSG, despite variation at different levels of biological organization. We examined sources of variation in WSG across four nested scales (segments within core, cores within trees, trees within species, and species), compared the pattern of radial variation in WSG among species differing in growth strategies, and investigated the effect of WSG radial variation on above-ground biomass estimates.
- *Methods*: We took two perpendicular cores from six individuals each of 20 tropical tree species representing a broad range of mean WSGs and growth-mortality strategies in a lowland tropical moist forest in Panama. Cores were divided into 1-cm segments, and WSG was determined for each segment.
- *Key results*: The bulk of the total variance in WSG was dominated by interspecies variation (88%) while variation due to measurement error, segments within cores and cores within trees (8%) was minimal. Radial variation in WSG, defined as change in WSG with increasing distance from the pith, was significant in 17 of the 20 species and included significant monotonic increases in six species and non-monotonic patterns in eleven species. Radial variation in WSG resulted in a small but significant bias in above-ground biomass estimates.

- *Conclusions*: Radial variation in WSG is related to a species' growth strategy, and though minimal relative to interspecific variation in WSG, can cause a downward bias when not incorporated into above-ground biomass estimates.

Keywords: above-ground biomass; growth-mortality trade off; Panama; wood density

Introduction

Trees in closed canopy forests exhibit a tradeoff between growth and mortality rates (Pacala et al. 1996; Gilbert et al. 2006; Poorter et al. 2008; Wright et al. 2010). At one extreme, light-demanding species are characterized by rapid growth rates under favorable light conditions but high mortality rates when shaded. At the other extreme, shade tolerant species are characterized by slow growth and low mortality rates under all light conditions. Wood specific gravity (WSG), a unit-less ratio of wood density compared to the density of water (Williamson and Wiemann 2010b), is well correlated with this growth-mortality tradeoff (Wright et al., 2010). Low WSG reduces wood construction costs enabling rapid growth rates in light-demanding species, while high WSG increases physical strength and pest resistance enabling low mortality rates at the price of greater construction costs and slower growth rates in shade-tolerant species (van Gelder et al., 2006; Chave et al., 2009).

Wood specific gravity can vary radially from pith to bark within individual trees (Wiemann and Williamson 1988, 1989; Woodcock and Shier, 2002; Nock et al., 2009; Hietz et al., 2013). This radial variation may be understood by considering how trees grow. As cambial activity adds new wood towards the outer edge of the tree, wood

corresponding to younger, earlier ontogenetic stages remains closer to the pith. Radial variation may reflect changing environmental conditions as well as changing demands placed on wood as trees age and/or increase in size. Radial variation in WSG estimated as the slope of WSG regressed on distance from pith is typically strongly correlated with tree age and not tree size, suggesting ontogenetic control of radial variation in WSG (Rueda and Williamson 1992; De Castro et al. 1993; Nock et al. 2009; Williamson and Wiemann 2010a, 2011; Williamson et al. 2012).

Radial variation in WSG may also be associated with the growth-mortality tradeoff (Woodcock and Shier, 2002). The growth-mortality tradeoff defines a species' life style or growth strategy, and radial variation in WSG can facilitate growth strategies through flexible responses to changing conditions and demands through ontogeny. Particularly for species on the fast growth, high mortality end of the growth-mortality spectrum, radial variation in WSG allows faster growth at juvenile stages such that plants can capitalize on light gaps and then construct the denser wood needed to withstand wind and other stressors at later and taller stages.

Four patterns of radial variation in WSG have been described in the literature. Radial increases from pith to bark result in a low-density core surrounded by a high-density exterior (Panshin and De Zeeuw 1980; Wiemann and Williamson 2012). This maximizes strength by placing the strongest material on the outside (Niklas 1997). Strength is also gained via an increased cross sectional area. In contrast, radial decreases from pith to bark result in a high-density core surrounded by a low-density exterior (Panshin and De Zeeuw 1980). Strength is gained mainly by an increased cross sectional

area (Larjavaara and Muller-Landau, 2010). The two remaining patterns of radial variation in WSG are non-linear. One non-linear pattern may involve an initial high WSG, followed by a decline, and then a steady increase to a constant or slowly increasing WSG (Gartner 1995). The second non-linear pattern involves an initial low WSG near the pith, followed by an increase, and then a leveling off or decline in rate of increase in WSG (Gartner 1995). The strongest documented radial gradients in WSG are increases from pith to bark among light-demanding tree species of wet tropical forests (Wiemann and Williamson 1988, 1989; Woodcock and Shier 2002; Williamson and Wiemann 2010a).

In addition to the potential fitness benefits for individual plants, radial variation in WSG has ecosystem-level consequences. Wood specific gravity, together with stem size, determines the amount of carbon sequestered in woody tissue (Chave et al., 2009; Fearnside 1997). WSG varies from about 0.08 to 1.39 among tree species (Zanne et al. 2009), meaning species differ seventeen fold in the amount of carbon they store at the same size. To accurately assess carbon pools and fluxes, it is important to understand the sources of WSG variation. This is especially pertinent for tropical forests because they harbor a huge diversity of tree species and are an important storehouse for carbon.

Most studies of radial gradients in WSG have focused on commercially important species or fast-growing pioneer species (Lachenbruch et al. 2011), while maximizing sampling replication across and within species. Here, we selected 20 canopy tree species from a wet tropical forest on Barro Colarado Island (BCI), Panama, including representatives of the full spectrum of growth and mortality rates (fast-growth, high

mortality to slow-growth, low mortality species), as well as the full range of average WSG (low to high WSG species) for this site, and included replicate samples for each individuals. Our goal was to quantify variation in WSG and address the following questions:

1. What is the contribution to overall variation in WSG of variation among segments within cores, among cores within individuals, among conspecific individuals and among species?

2. What is the contribution to overall variation in radial gradients in WSG of variation among cores within individuals, among conspecific individuals and among species?

3. What is the pattern of radial variation in WSG for each species?

4. Does radial variation in WSG vary among species with different growth-mortality strategies and/or different initial WSG values?

5. Does radial variation in WSG affect estimates of above-ground carbon storage?

Materials and methods

Study site—The Barro Colorado Nature Monument, Panama, supports 59 km^2 of tropical moist forest in the Holdridge Life Zone System. Annual rainfall averages 2600 mm with 10% falling during a four-month dry season, and annual temperature averages 27^oC (Leigh 1999).

Species positions on the growth-mortality tradeoff—Relative growth and mortality rates were determined for saplings (1 cm ≤ diameter at breast height (DBH) ≤ 5 cm) in a previous study for six censuses between 1982 and 2005 of the 50-ha Forest Dynamics Plot located on Barro Colorado Island (BCI) (9° 09' 17" N, 79° 50' 53" W) in the Barro Colorado Nature Monument (Wright et al. 2010). Relative growth rates under favorable conditions equaled 95th percentile relative growth rates (RGR_{95}; see Table 1 for definition of acronyms). Mortality rates under unfavorable conditions equaled mortality rates of the 25% of individuals with the slowest relative growth rates in the previous census interval (MRT_{25}). Using the function princomp in the stats package in R, we performed a principal components analysis on RGR_{95} and MRT_{25} and extracted species scores along the first component axis, to form the variable $RGR.MRT_{SAP}$.

Species regeneration in gaps— To further describe the species, we extracted the total number of recruits and the number located in low canopy sites or recent tree-fall gaps in the 50-ha plot for 15 of our 20 species from Wright et al. (2003). We used a Binomial Test to compare these numbers with the proportion of the 50-ha plot characterized by a low canopy (0.127) obtained from Welden et al. (1991).

Wood specific gravity—We selected 20 species that were widely distributed across the $RGR.MRT_{SAP}$ axis. We collected two cores from six adult individuals (minimum DBH = 20.5 cm) of each of these species (240 total cores) from forests greater than 100 years old located on the Gigante (9^{o} 07' 54" N, 79^{o} 50' 28" W) and Buena Vista (9° 11' 12" N, 79° 50' 32" W) peninsulas in the Barro Colorado Nature Monument between July 14 and August 12, 2010. Diameter at breast height was determined for each

individual, and a 5 mm diameter increment borer was used to extract two horizontal cores perpendicular to one another and from pith to bark. Cores were sealed in plastic straws, transported on ice to the nearby laboratory on BCI, and divided into 1-cm segments. For each 1-cm segment, fresh volume was measured with the water displacement method and dry mass was determined after drying to constant mass at 100^{o}C in a convection oven. WSG was calculated as dry mass divided by fresh volume divided by the density of water (ρ_{WATER} = 1 g/cm^3; Williamson and Wiemann 2010b), and distance to pith was recorded for each segment.

Analyses—Variance Components Analysis was used to evaluate the contribution of variation in WSG among segments within cores, cores within individuals, conspecific individuals and species to overall variation in WSG (Introduction: question 1). A random effects model with three nested levels of random effects (Species/Individuals/Cores) was used to estimate the proportion of variation in WSG associated with species, individuals and cores. The residual variation included variation associated with segments plus measurement error.

We used two metrics to quantify radial variation in WSG for each core:

1. Radial change (R_{O-I}) equaled WSG_O minus WSG_I, where WSG_I is mean WSG for the three 1-cm segments nearest to the pith (inner wood) and WSG_O is mean WSG for the three 1-cm segments nearest to the bark (outer wood) following Wiemann and Williamson (1989). R_{O-I} captures the difference between inner and outer wood.

2. Radial variance (R_{VAR}) equaled the variance of WSG for 1-cm segments from each core. R_{VAR} quantifies variation in WSG along a core, but not radial gradients.

A second variance components analysis evaluated the contributions of variation among cores within individuals, conspecific individuals within species and species to variation in $R_{O\text{-}I}$ and R_{VAR} (Introduction: question 2). A random effects model with two nested levels of random effects (Species/Individuals) was used to estimate the proportion of variation in radial gradient metrics associated with species and individuals. The residual variation included variation associated with cores plus measurement error.

We used linear mixed effects models to evaluate the pattern of radial variation in WSG for each species (Introduction: question 3). The fixed effect of radial position was quantified as distance to the pith (radial distance) for each segment. Because cores varied in length, radial distance was scaled to unit length by dividing each radial distance value by the length of the core to obtain proportional radial distance. The random effect incorporated the nested nature of the WSG data with segments nested within cores and cores nested within individuals for each species (random = ~1|Individual/Core). Linear mixed models are appropriate for nested data because they unambiguously model correlations among observations from the same unit (i.e., core and individual) by incorporating random effects in addition to the fixed effects (i.e., proportional radial distance) of interest. We evaluated mean, linear, and quadratic models, respectively, as follows:

$$WSG \sim \beta_0 \qquad \text{(Eq. 1)}$$

$$WSG \sim \beta_0 + \beta_1 \cdot Radial\ distance \quad \text{(Eq. 2)}$$

$$WSG \sim \beta_0 + \beta_1 \cdot Radial\ distance + \beta_2 \cdot Radial\ distance^2 \quad \text{(Eq. 3)}$$

where β_0, β_1, and β_2 are fitted coefficients.

We used Akaike's Information Criterion, corrected for finite sample sizes (AIC_c), which penalizes models with additional parameters, to select the best fit model (Burnham and Anderson 2002). We followed the general rule of thumb that $\Delta AIC_c \leq 2$ indicates no significant difference between models, and so the simpler model with fewer parameters is preferred. Larger ΔAIC_c values indicate that the model with the minimum AIC_c value had the best fit, with $\Delta AIC_c > 10$ providing overwhelming evidence for the model with the minimum AIC_c value. We used the lme function in the nlme package in R to perform these analyses (Pineheiro et al. 2009) and the aictab function in the AICcmodavg package to obtain ΔAIC_c values (Mazerolle 2013).

When the mean (Eq. 1) or the linear (Eq. 2) model provided the best fit for a species, the pattern of radial variation was unequivocal. When the quadratic model (Eq. 3) provided the best fit, we next determined whether the inflection point at which the WSG-radial distance slope equals zero (critical radial distance) fell within the range of possible values of proportional radial distance (zero to one). Setting the derivative of Eq. 3 equal to zero and rearranging,

$$Critical\ radial\ distance = {}^{-\beta_1}/_{2 \cdot \beta_2} \quad \text{(Eq. 4)}$$

We then calculated a 95% confidence interval (CI) for critical radial

distance by parametric bootstrapping which generates a random sample from a known distribution that best approximates the data and calculates the test statistic of interest (critical radial distance). We used the rmvnorm function in the mvtnorm package in R (Genz et al. 2012), with inputs β_1, β_2, and their variances and covariance estimated by the quadratic regression model, to implement the parametric bootstrap. The lower and upper confidence limits were extracted at the 0.025 and 0.975 quantiles of the bootstrapped distribution of critical radial distance values. Finally, we compared observed critical radial distances and their 95% CIs with the range of possible proportional radial distance values, which is zero to one. We concluded that the radial gradient is curvilinear if the 95% CI fell entirely within the observed range ($CI_{LOWER}>0$ and $CI_{UPPER}<1$), monotonically increasing ($\beta_1>0$) or decreasing ($\beta_1<0$) if the 95% CI fell entirely outside the observed range ($CI_{UPPER}<0$ or $CI_{LOWER}>1$), or uncertain if the 95% CI fell partially outside the observed range ($CI_{LOWER}<0$ or $CI_{UPPER}>1$).

To determine whether radial variation in WSG varies with species positions on the growth-mortality tradeoff ($RGR.MRT_{SAP}$) or with initial, juvenile WSG (WSG_I) (Introduction: question 4), we grouped the tree species into three categories based on the form of the WSG-radial distance relationships. We then carried out a linear discriminant analysis using the lda function in the MASS package in R (Venables and Ripley 2002). Linear discriminant analysis tests the extent to which a set of quantitative descriptors (predictors) can explain an independently pre-determined grouping that forms the qualitative response variable (Legendre and Legendre 2012). The response variable was the form of the WSG-radial distance relationship, while the quantitative descriptors were

WSG_I and $RGR.MRT_{SAP}$. To test for the overall significance of the linear discriminant model, we used Wilks' lambda to compare differences in $RGR.MRT_{SAP}$ and WSG_I among the predefined groups of WSG-radial distance relationship. Wilks' lambda tests if groups differ significantly in the position of their centroids, producing values ranging from near 0 (maximum dispersion of group centroids) to 1 (no dispersion among groups) (Legendre and Legendre 2012).

Lastly, we explored the effect of radial variation in WSG on above-ground biomass (Introduction: question 5). Above-ground biomass is estimated as the product of WSG and tree volume (Chave et al. 2005). For a fixed volume, relative values of WSG determine relative values of above-ground biomass. Thus, we compared mean WSG (WSG_{MEAN}) calculated as the average WSG over all segments for a species with area weighted mean WSG (WSG_A) calculated as follows:

$$WSG_A = \frac{1}{\pi \times DP_{max}^2} \times \int_{DP=0}^{1} 2 \times \pi \times DP \times \widehat{WSG} \qquad \text{(Eq. 5)}$$

where $\widehat{WSG}$ represents the best fit relationship between WSG and radial distance provided by equation 1, 2 or 3. Muller-Landau (2004) explains equation 5, and Williamson and Wiemann (2010b) apply it to linear radial gradients. A paired *t*-test was used to compare WSG_{MEAN} and WSG_A.

All analyses were conducted in R version 2.15.1 (R Core Team, 2012).

Results

We collected 240 cores from 120 individuals of 20 species, 19 genera and 12 families (Table 2). WSG_{MEAN} varied 3.4 fold from 0.260 for *Poulsenia armata* to 0.883 for *Tabebuia guayacan.* With the exception of *Tabebuia guayacan*, recruitment was significantly positively associated with recent tree-fall gaps for 14 of the 15 species for which data was available (Table 2).

Variance partitioning of WSG (question 1)—Variation among species, among conspecific individuals and between cores within individuals accounted for 88%, 4% and 1% of variation in WSG, respectively. Variation among segments within cores plus unknown measurement error accounted for the remaining 7% of variation in WSG.

Variance partitioning of radial variation in WSG (question 2)—Interspecific variation accounted for 32% and 21% of variation in $R_{O\text{-}I}$ and R_{VAR}, respectively. Variation among conspecific individuals accounted for 18% and 28%, respectively. Variation between cores within individuals plus unknown measurement error accounted for 50% and 51% of variation in $R_{O\text{-}I}$ and R_{VAR}, respectively (species average values of $R_{O\text{-}I}$ and R_{VAR} in Appendix S1; see Supplemental Data with the online version of this article).

Radial trends (question 3)—The radial gradient in WSG was best fit by the linear regression model for five species, all of which showed significant linear increases (Figs. 1B, C, F, G and N, Table 3, Appendix S2; see Supplemental Data with the online version of this article). The radial gradient in WSG was best fit by the quadratic regression model

for 12 species (Table 3, Appendix S2). Of these 12 species, eight were certainly non-monotonic involving an initial decrease and then an increase in WSG as radial distance increased (U-shaped) (Figs. 1E, H, I, J, K, L, O and Q), one was certainly monotonically increasing (Fig. 1D) because the 95% CI for critical radial distance was entirely above the largest possible value of one, and three had uncertain radial gradients (Figs. 1A, M and S) because the 95% CI for critical radial distance extended beyond the range of possible values. The three uncertain radial gradients appeared to be increasing from a low asymptotic value of WSG near the pith (Fig. 1A) or towards a high asymptotic value near the bark (Figs. 1M and S). The final three species (Figs. 1P, R and T) had no significant relationship between WSG and distance to the pith (Table 3).

Radial trends and the growth-mortality tradeoff (question 4) — Species' positions on the growth-mortality tradeoff were defined by a linear combination of RGR_{95} and MRT_{25} using Principal Components Analyses for saplings. The two component axes had eigenvalues of 1.5 and 0.5. The first component axis explained a substantial (77%) proportion of interspecific variation in growth and mortality rates. We therefore, used this first component axis to summarize interspecific variation in the growth-mortality tradeoff. Species positions along this axis equaled their extracted factor scores ($RGR.MRT_{SAP}$).

We excluded the three species with uncertain radial gradients and grouped the 17 remaining species into three categories based on the form of the WSG – radial distance relationship. Group I was composed of six species with monotonic increasing WSG-radial distance relationships. Group II was composed of eight species with U-shaped

WSG-radial distance relationships. Group III was composed of three species with insignificant WSG-radial distance relationships. The linear discriminant analysis was significant (Wilks lambda = 0.221, $P < 0.001$) and produced two discriminant functions. The first discriminant function achieved 93.5% separation, and the second achieved 6.5% separation. Groups I (increasing WSG-radial distance relationship) and III (insignificant WSG-radial distance relationship) were clearly separated by the first discriminant function, while Group II (U-shaped WSG-radial distance relationship) occupied an intermediate position, overlapping with Groups I and III. The absolute values of the loadings on both discriminant functions were largest for WSG_I (loadings on first and second linear discriminant function = 11.1 and -3.15, respectively) and smallest for $RGR.MRT_{SAP}$ (0.02 and -0.85, respectively). The first discriminant function represents a contrast between $RGR.MRT_{SAP}$ (r = -0.45; P = 0.069) and average WSG_I (r = 0.99; $P <$ 0.001).

Effect of radial variation in WSG on above-ground biomass estimates (question 5)—WSG_{MEAN} estimates were significantly lower than WSG_A estimates (paired t = - 4.31, df = 19, $P < 0.001$; Table 4).

Discussion

In a hierarchical partitioning of variation in WSG performed for 20 moist tropical forest species chosen to include a wide range of growth and mortality rates, most variation (88%) occurred among species. The only other study to partition variation in WSG focused on intra- and interspecific sources of variation for 32 temperate Australian

woody species and it also reported substantial (57–82%) variation among species (Onoda et al. 2010). The contributions of different sources of variation in functional traits at nested ecological scales have also been determined for leaf traits and promoted as a basis for prioritizing research efforts (Messier et al. 2010; Auger and Shipley 2012). Most of the variation in WSG can be captured at the interspecific level when resources have to be prioritized.

Radial variation in WSG is not necessarily uniform within a tree. A partitioning of variance showed that approximately 50% of the variance in two metrics of radial variation in WSG, $R_{O\text{-}I}$ and R_{VAR}, occurred between cores within individuals (or was due to measurement error). Tree growth is frequently asymmetrical around the trunk, as trees exhibit different extents of eccentricity (Williamson and Wiemann 2011). Thus, differences in the pattern of radial variation between two cores within a tree implies that tree responses to local environmental conditions such as mechanical perturbations due to wind vary across the stem (Niklas 1992, Pruyn et al. 2000, West 2009).

Radial trends—Although minimal relative to interspecific variation in WSG, variation among segments within cores was significantly related to the radial position or distance to the pith or center of the tree in 17 of the 20 study species (Fig. 1). From pith to bark, the significant radial gradients in WSG were monotonically increasing in six species with mean WSG ranging from low to intermediate (0.298 - 0.580), decreasing near the pith and then increasing closer to the bark (U-shaped) in eight species, and uncertain although non-linear in the final three species. This result corroborates reports from other studies on tropical forest trees, that radial increases are more common than

decreases, and that low WSG is not a mandatory requirement for radial increases to occur (Wiemann and Williamson 1989; Woodcock and Shier 2002; Heitz et al. 2013).

The significant non-linear, U-shaped pattern of radial variation in WSG found for eight species suggests that non-linear radial gradients in WSG are quite common in tropical forest trees (Williamson et al. 2012). Non-linear patterns of radial change in WSG have previously been described for many soft pines and softwoods of the Cupressaceae and some hardwoods e.g. *Populus tremuloides* (Zobel and van Buijtenen 1989). Fujimoto and Koga (2010) use a mixed effects quadratic regression model to show that WSG changes as a function of increasing age in a non-linear pattern, similar to the U-shaped pattern in our study, in Japanese larch (*Larix kaempferi*). The first description of a non-linear radial gradient in WSG for a tropical tree was given by Williamson et al. (2012) for *Schizolobium parahyba* a Neotropical pioneer that starts out with low initial WSG (0.15 - 0.20) that increases at an increasing rate with distance from the pith. Nevertheless, since earlier studies did not evaluate the prevalence of non-linear gradients in WSG among tropical species, we do not know how widespread non-linear radial gradients in WSG might be in tropical forest trees.

Ecological interpretation of radial changes in WSG —Woodcock and Shier (2002) assume that radial changes in WSG reflect shifts in resource allocation associated with changing structural requirements experienced by forest trees as they grow from the shaded understory into the sunlit canopy. Woodcock and Shier (2002) hypothesize that species that require the high light levels found in forest gaps to regenerate produce light wood to enable rapid growth as saplings in gaps and then gradually switch to denser

wood as they reach the canopy and face the stresses imposed by wind and their increasing size. This is consistent with our six species that show continuous increases in WSG (Figs. 1B, C, D, F, G and N). With the exception of *Simarouba amara*, these six species are among the most light-demanding species in the BCI forest. The first discriminant function returned by the linear discriminant analysis separated the six species with increasing radial gradients (Fig. 2). The high loading of WSG_I (or WSG near the pith) on this first discriminant function confirms that species starting out with low WSG have a higher potential to gradually switch investment from wood of low to high construction cost through the course of their ontogeny. Thus, the strategy of radially increasing WSG may be important to tropical pioneers that invest in rapid height increase, but need structural reinforcement on reaching the canopy with greater wind exposure (Putz et al.1983; Woodcock and Shier, 2002).

Woodcock and Shier (2002) also hypothesized that shade tolerant species produce dense wood initially to protect against pests and falling objects as saplings in the understory and then gradually switch to lighter wood as they reach the canopy. In this case, the switch to lighter wood increases strength by increasing cross sectional area (Woodcock and Shier, 2002; Larjavaara and Muller-Landau, 2010). Woodcock and Shier (2002) did not anticipate (but see Gartner 1995) the U-shaped pattern of radial variation in WSG that characterizes 40% of our study species (Fig. 1).

These U-shaped patterns are difficult to reconcile with the framework provided by Woodcock and Shier (2002), which assumes that saplings produce light wood when exposed to high light levels and dense wood when exposed to low light levels. In a U-

shaped pattern of radial variation, wood is relatively dense at the smallest and largest tree sizes and relatively light at intermediate tree sizes (Figs. 1E, H, I, J, K, L, O and Q). Most tree species have significantly greater numbers of recruits in gaps than expected by chance on BCI (Table 2; Welden et al., 1991; Wright et al. 2003). Yet, many of these same species produce relatively dense wood as saplings and lighter wood at intermediate sizes.

For this reason, we believe the inverse relationships between light levels and sapling wood density assumed by Woodcock and Shier (2002) may not hold for some of these species. Other alternatives are equally plausible. Many species have recruitment biased to gaps but are unable to grow rapidly enough to reach the canopy before gap closure (Wright et al. 2003). These species may allocate the enhanced resources available while gap conditions prevail to build the high density wood necessary to survive the low light, understory conditions that will almost inevitably follow. After gap closure, these species may produce relatively low density wood simply because fewer resources are available. Additional analyses are necessary to evaluate how growth rates actually change ontogenetically to evaluate this and other equally plausible alternatives.

Two of the three species that lacked significant radial gradients provide an interesting exception to the strong trend for significant radial gradients. *Luehea seemannii* (Fig. 1P) and *Platypodium elegans* (Fig. 1R) are the two most strongly buttressed species in our sample and are among the most strongly buttressed trees in central Panama. This suggests that buttresses might replace radial changes in WSG to facilitate tree responses to environmental and ontogenetic variation.

Radial variation in WSG and above-ground biomass estimates— Radial variation in WSG can cause discrepancies in estimates of carbon sequestration. Our simple comparison of WSG_{MEAN} and WSG_A showed that WSG_{MEAN} values were significantly lower than WSG_A values which account for radial variation in WSG. Although these discrepancies in WSG estimates were modest, varying from 0.02 to 5.75% among species, they were consistent in direction for 17 of 20 species, and largest for species with significant radial increases (Group I species) (Table 3). Failing to account for radial gradients will bias above-ground biomass estimates downwards (Nogueira et al. 2007; Nock et al. 2009; Williamson and Wiemann 2010a).

Conclusion— Radial variation in WSG is related to a species' growth strategy. Light-wooded, fast-growing, high-mortality species are characterized by radial increases in WSG, whereas slow-growing, low-mortality species show a range of radial patterns. Non-linear, U-shaped radial changes in WSG characterized 40 % of our study species. Additional studies of ontogenetic changes in light availability and radial growth rates are needed to understand the ecological causes of these unexpected U-shaped radial gradients in WSG in tropical trees. Additionally, radial variation in WSG is not necessarily uniform within a tree, which suggests that it is also involved in responses to extrinsic forces that vary across the growing stem. Finally, radial variation in WSG is also small compared with interspecific variation in WSG; however, the omission of radial variation in WSG from estimates of above-ground biomass is likely to bias those estimates downward modestly.

Acknowledgement

O. L. O. thanks Whitney Harris World Ecology Center for providing research funds; Ivan Jiménez for contributions to the statistical analysis; Helene Muller-Landau for providing the integral solution for area weighted mean estimates of wood specific gravity; Nosayaba Osazuwa-Peters, Sebastian Bernal, Omar Hernandez and Rufino Gonzalez for providing invaluable field and technical assistance; and Jon Aibueku for financial and David Kenfack for logistic support. M. C. Wiemann and three anonymous reviewers provided valuable comments on the manuscript.

Tables

Table 1. Acronyms referred to in main text and their meanings.

Acronym	Meaning
ΔAIC_c	Difference in Akaike's Information Criterion corrected for finite sample sizes
BCI	Barro Colorado Island
CI	95% confidence interval
DBH	Diameter at breast height
RGR_{95}	95^{th} percentile of the relative growth rate of saplings
MRT_{25}	Mortality rate of the 25% of saplings with the lowest relative growth rates in the previous census interval
$RGR.MRT_{SAP}$	Linear combination of RGR_{95} and MRT_{25} for saplings, obtained as extracted scores from the first axis of a principal component analysis.
R_{O-I}	Radial change, defined as WSG_O minus WSG_I
R_{VAR}	Radial variance, defined as the variance of WSG for 1-cm segments from each core
WSG	Wood specific gravity
WSG_A	Area weighted average WSG
WSG_I	Average WSG for the three 1 cm segments near the pith
WSG_{MEAN}	Average WSG over all segments for a species
WSG_O	Average WSG for the three 1 cm segments near the bark.

Table 2. Description of the 20 tropical forest canopy species including family, diameter at breast height (DBH) of sampled trees, and for 15 species, the proportion of recruits located in tree fall gaps. These proportions were significantly greater than the proportion of the forest in recent treefall gaps (0.127) for 14 of the 15 species (*P*-values).

Species	**Family**	**DBH mean (range) (cm)**	**Proportion of recruits in gaps (*P*)***
Apeiba membranacea	Malvaceae	42.3 (34.3 – 51.1)	
Astronium graveolens	Anacardaceae	28.0 (21.5 – 34.2)	0.381 (<0.01)
Calophyllum longifolium	Clusiaceae	37.9 (21.0 – 58.0)	0.271 (<0.01)
Cordia bicolor	Boraginaceae	29.6 (26.0 – 37.1)	
Guazuma ulmifolia	Malvaceae	31.2 (23.0 – 44.8)	0.714 (<0.01)
Inga marginata	Fabaceae	40.2 (25.6 – 52.2)	0.389 (<0.01)
Jacaranda copaia	Bignoniaceae	35.3 (24.5 – 41.6)	0.879 (<0.01)
Lacmellea panamensis	Apocynaceae	33.1 (28.5 – 37.0)	
Luehea seemannii	Malvaceae	49.6 (34.8 – 68.0)	0.745 (<0.01)
Platypodium elegans	Fabaceae	28.9 (21.0 – 37.1)	0.542 (<0.01)
Poulsenia armata	Moraceae	29.4 (21.0 – 46.4)	0.208 (<0.01)
Prioria copaifera	Fabaceae	37.1 (25.0 – 58.8)	0.207 (<0.01)

Simarouba amara	Simaroubaceae	33.8 (25.0 – 43.2)	0.291 (<0.01)
Spondias radlkoferi	Anacardiaceae	34.1 (28.8 – 40.2)	0.507 (<0.01)
Tabebuia guayacan	Bignoniaceae	23.8 (20.5 – 29.0)	0.286 (>0.05)
Tabebuia rosea	Bignoniaceae	32.9 (29.2 – 48.5)	0.262 (<0.01)
Tachigali versicolor	Fabaceae	29.6 (23.0 – 37.7)	0.218 (<0.01)
Triplaris cumingiana	Polygonaceae	28.2 (25.2 – 31.0)	
Virola sebifera	Myristicaceae	30.1 (27.3 – 33.7)	
Zanthoxylum ekmanii	Rutaceae	28.8 (23.0 – 34.9)	0.726 (<0.01)

*** From Wright et al. (2003).**

Table 3: Analyses of radial variation in wood specific gravity (WSG). The best fit model, (M=Mean, L=Linear, Q=Quadratic), parameter estimates for the best fit model, the critical radial distance or inflection point for species with best fit quadratic models, and the form of the WSG – radial distance relationship (I = increasing, N= no radial change, U = U-shaped, and O = uncertain nonlinear pattern). The mixed effects models included random effects for individual and core and were fit using Restricted Maximum Likelihood (REML). The fixed effect, radial distance, was scaled to unit length by dividing by the length of the core.

Species	**Best fit model**	β_0 **(95% CI)**	β_1 **(95% CI)**	β_2 **(95% CI)**	**Critical radial distance (95% CI)**	**WSG-radial distance relationship**
A. membranacea	L	0.27 (0.21, 0.33)	0.06 (0.03, 0.08)			I
A. graveolens	Q	0.83 (0.79, 0.86)	0.19 (0.06, 0.32)	-0.14 (-0.27, -0.02)	0.66(0.53, 1.12)	O
C. longifolium	Q	0.53 (0.49, 0.58)	-0.09 (-0.15, -0.03)	0.12 (0.06, 0.17)	0.38(0.20, 0.45)	U
C. bicolor	L	0.36 (0.34, 0.39)	0.15 (0.14, 0.17)			I
G. ulmifolia	Q	0.53 (0.49, 0.58)	-0.13 (-0.23, -0.03)	0.12 (0.03, 0.21)	0.57(0.45, 0.73)	U
I. marginata	Q	0.69 (0.66, 0.71)	-0.11 (-0.18, -0.04)	0.18 (0.12, 0.25)	0.29(0.16, 0.37)	U
J. copaia	Q	0.41 (0.37, 0.45)	-0.08 (-0.14, -0.02)	0.14 (0.09, 0.19)	0.28(0.11, 0.36)	U

L. panamensis	Q	0.51 (0.48, 0.54)	-0.08 (-0.13, -0.03)	0.16 (0.11, 0.20)	0.25(0.14, 0.32)	U
L. seemannii	M	0.66 (0.65, 0.67)				N
P. elegans	M	0.75 (0.71, 0.79)				N
P. armata	Q	0.26 (0.22, 0.29)	-0.09 (-0.19, 0.02)	0.11 (0.02, 0.20)	0.38 (-0.10, .49)	O
P. copaifera	Q	0.55 (0.52, 0.59)	-0.19 (-0.27, -0.11)	0.18 (0.11, 0.25)	0.52(0.32, 0.81)	U
S. amara	L	0.41 (0.39, 0.42)	0.04 (0.03, 0.05)			I
S. radlkoferi	L	0.28 (0.27, 0.30)	0.17 (0.15, 0.18)			I
T. guayacan	M	0.89 (0.87, 0.90)				N
T. rosea	Q	0.52 (0.46, 0.58)	0.15 (0.07, 0.23)	-0.09 (-0.16, -0.02)	0.86(0.69, 1.65)	O
T. versicolor	Q	0.60 (0.56, 0.64)	-0.12 (-0.23, -0.02)	0.14 (0.05, 0.24)	0.43(0.14, 0.52)	U
T. cumingiana	L	0.50 (0.45, 0.54)	0.17 (0.14, 0.20)			I
V. sebifera	Q	0.48 (0.46, 0.50)	-0.11 (-0.18, -0.04)	0.15 (0.08, 0.21)	0.37(0.25, 0.44)	U
Z. ekmanii	Q	0.27 (0.24, 0.31)	0.29 (0.20, 0.37)	-0.09 (-0.17, -0.01)	1.57(1.07, 5.22)	I

Table 4. Comparison of mean WSG (WSG_{MEAN}) calculated as the average WSG over all segments for a species, with area weighted mean WSG (WSG_A) and the percentage difference between the two estimates. WSG_{MEAN} and WSG_A are significantly different (paired t = - 4.31, df = 19, $P < 0.001$).

Species	WSG_{MEAN}	WSG_A	Difference (%)
A. membranacea	0.298	0.310	3.92
A. graveolens	0.876	0.881	0.53
C. longifolium	0.524	0.534	1.78
C. bicolor	0.443	0.465	4.70
G. ulmifolia	0.494	0.502	1.53
I. marginata	0.698	0.706	1.19
J. copaia	0.418	0.426	1.92
L. panamensis	0.524	0.535	2.05
L. seemannii	0.660	0.660	0.02
P. elegans	0.750	0.746	-0.47
P. armata	0.260	0.256	-1.64
P. copaifera	0.520	0.518	-0.43
S. amara	0.433	0.437	0.98
S. radlkoferi	0.372	0.395	5.75
T. guayacan	0.883	0.885	0.17
T. rosea	0.565	0.575	1.79
T. versicolor	0.583	0.590	1.15
T. cumingiana	0.580	0.607	4.51
V. sebifera	0.474	0.479	1.10
Z. ekmanii	0.396	0.419	5.50

Figures

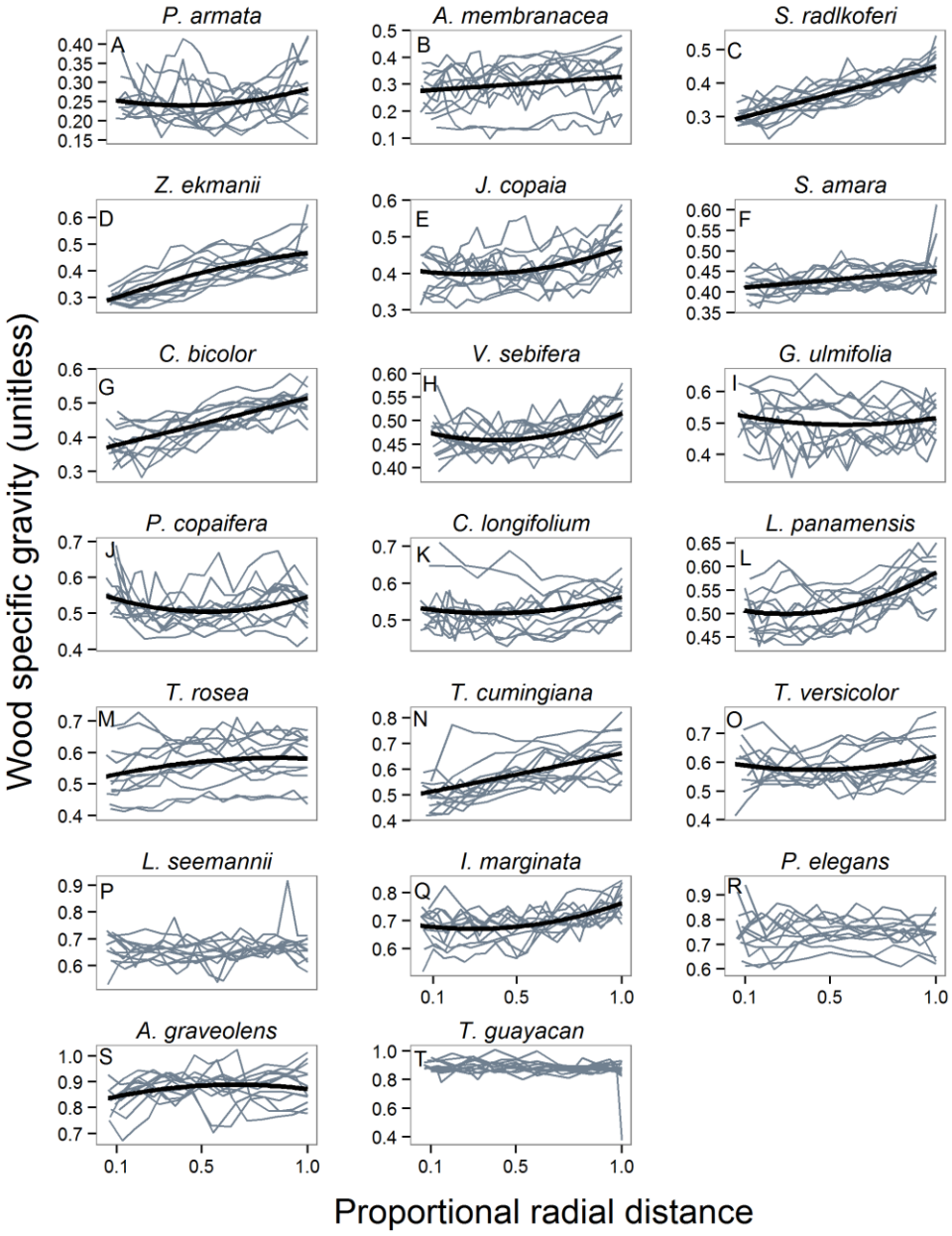

Fig. 1. Line-plots of wood specific gravity (WSG) on distance from pith scaled by core length (proportional radial distance) for twenty tree species from the Barro Colorado Nature Monument, Panama. Panels are ordered from smallest to largest by average species WSG. Each line connects WSG for contiguous 1-cm segments from a single core. Thick black lines represent best fit linear or quadratic regression models. From pith to bark, WSG increased monotonically for six species (panels B, C, D, F, G, N), decreased initially but subsequently increased for eight species (U-shaped; panels E, H, I, J, K, L, O, Q), and was uncertain for three species (panels A, M, and S). The relationship between WSG and proportional radial distance was insignificant for the three remaining species (panels P, R and T).

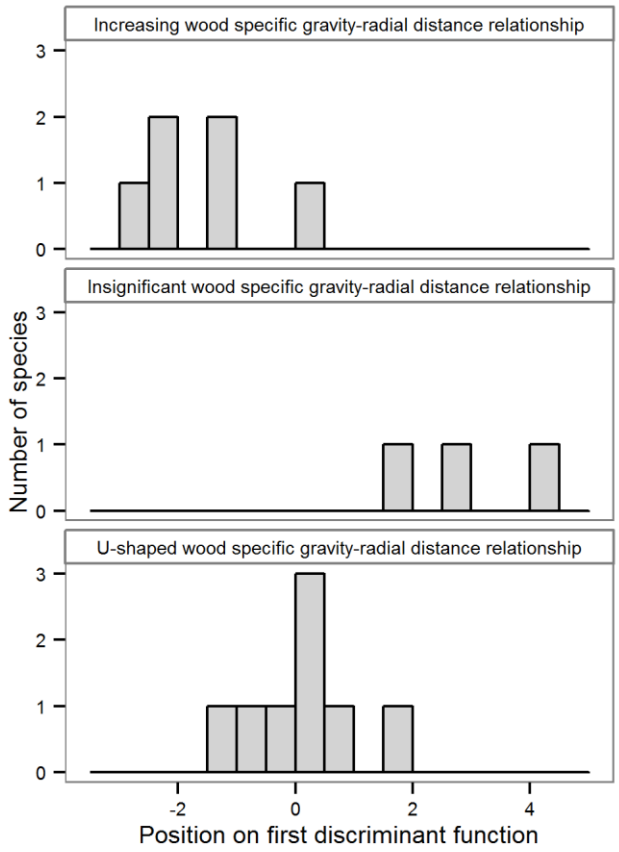

Fig. 2. Histograms of the first linear discriminant function values for three groups of species (n = 17) based on the form of WSG – radial distance relationship. This first discriminant function explained 93.5% of the differences among the three groups of species and was driven by a negative contrast between the linear combination of relative growth rates and mortality rates for saplings ($RGR.MRT_{SAP}$) and the average WSG near the pith (WSG_I). Species with "increasing WSG-radial distance relationship" are, with one exception, on the negative side of the first linear discriminant function, with large $RGR.MRT_{SAP}$ and low WSG_I. Species with "insignificant WSG-radial distance relationship" are exclusively on the positive side of the axis, with small $RGR.MRT_{SAP}$ and large WSG_I. And, species with "U-shaped WSG-radial distance relationship" are clustered around zero values with intermediate $RGR.MRT_{SAP}$ and WSG_I.

References

AUGER, S. AND SHIPLEY, B. (2012). Interspecific and intraspecific trait variation along short environmental gradients in an old-growth temperate forest. *Journal of Vegetation Science* 24: 419–428.

BURNHAM, K. P., AND ANDERSON D. R. (2002). Model selection and multi-model inference: a practical information-theoretic approach. New York, NY: Springer-Verlag.

CHAVE, J., ANDALO, C., BROWN, S., CAIRNS, M. A., CHAMBERS, J. Q., EAMUS, D., FÖLSTER, H., et al. (2005). Tree allometry and improved estimation of carbon stocks and balance in tropical forests. *Oecologia* 145: 87-99.

CHAVE, J., COOMES, D., JANSEN, S., LEWIS, S.L., SWENSON, N.G. AND ZANNE, A.E. (2009). Towards a worldwide wood economics spectrum. *Ecology Letters* 12: 351-366.

DE CASTRO, F., WILLIAMSON, G. B., AND MORAES DE JESUS, R. (1993). Radial variation in the wood specific gravity of *Joannesia princeps*: The role of age and diameter. *Biotropica* 25: 176 – 182.

FEARNSIDE, P. M. (1997). Wood density for estimating forest biomass in Brazilian Amazonia. *Forest Ecology and Management* 90: 59 – 87.

FUJIMOTO, T. AND KOGA, S. (2010). An application of mixed-effects model to evaluate the effects of initial spacing on radial variation in wood density in Japanese larch (*Larix kaempferi*). *Journal of Wood Science* 56: 7 – 14.

GARTNER, B. L. (1995). Patterns of xylem variation within a tree and their hydraulic and mechanical consequences. *In* Gartner, B. L [ed.], Plant Stems: Physiological and Functional Morphology , 125 – 149. Academic Press, San Diego, California, USA.

VAN GELDER, H.A., POORTER, L. AND STERCK, F.J. (2006). Wood mechanics, allometry, and life-history variation in a tropical rain forest tree community. *New Phytologist* 171: 367-378.

GENZ, A., TETSUHISA, F. B., XUEFEI MI, M., LEISCH, F., SCHEIPL, F., AND HOTHORN, T. (2012). mvtnorm: Multivariate Normal and t Distributions. R package version 0.9-9994. URL http://CRAN.R-project.org/package=mvtnorm.

GILBERT, B., WRIGHT, S.J., MULLER-LANDAU, H.C., KITAJIMA, K. and HERNÁNDÈZ, A. (2006). Life history trade-offs in tropical trees and lianas. *Ecology* 87: 1281-1288.

HACKE, U. G., SPERRY, J. S., POCKMAN, W. T., DAVIS, S. D., AND MCCULLOH K. A. (2001). Trends in wood density and structure are linked to prevention of xylem implosion by negative pressure. *Oecologia* 126: 457 – 461.

HIETZ, P., VALENCIA, R. AND WRIGHT, S. J. (2013). Strong radial variation in wood density follows a uniform pattern in two Neotropical rainforests. *Functional Ecology* 27: 684–692.

LACHENBRUCH, B., MOORE, J.R. AND EVANS, R. (2011). Radial variation in wood structure and function in woody plants, and hypotheses for its occurrence. *In* MEINZER, F.C., LACHENBRUCH, B. AND DAWSON, T.E [eds.], Size- and Age-Related Changes in Tree Structure and Function, 121–164. Springer Netherlands.

LARJAVAARA, M. AND MULLER-LANDAU, H.C. (2010). Rethinking the value of high wood density. *Functional Ecology* 24: 701-705.

LEGENDRE, P. AND LEGENDRE, L. (2012). Numerical ecology. 3rd Edition. Elsevier, The Netherlands.

LEIGH, E. G. (1999). Tropical forest ecology, a view from Barro Colorado Island. Oxford University Press, New York.

MAZEROLLE, M. J. (2013). AICcmodavg: Model selection and multimodel inference based on (Q)AIC(c). R package version 1.32. URL http://CRAN.R-project.org/package=AICcmodavg.

MESSIER, J., MCGILL, B. J., AND LECHOWICZ, M. J. (2010). How do traits vary across ecological scales? A case for trait-based ecology. *Ecology Letters* 13: 838–848.

MULLER-LANDAU, H. C. (2004). Interspecific and inter-site variation in wood specific gravity of tropical trees. *Biotropica* 36: 20 – 32.

NIKLAS, K.J. (1992). Plant biomechanics: an engineering approach to plant form and function. University of Chicago Press.

NIKLAS, K. J. (1997). Mechanical properties of black locust (*Robinia pseudoacacia* L.) wood. size- and age-dependent variations in sap and heartwood. *Annals of Botany* 79: 265 – 272.

NOCK, C.A., GEIHOFER, D., GRABNER, M., BAKER, P.J., BUNYAVEJCHEWIN, S. AND HIETZ, P. (2009). Wood density and its radial variation in six canopy tree species differing in shade-tolerance in western Thailand. *Annals of Botany* 104: 297-306.

NOGUEIRA, E., FEARNSIDE, P., NELSON, B. AND FRANCA, M. (2007). Wood density in forests of Brazil's "arc of deforestation": Implications for biomass and flux of carbon from land-use change in Amazonia. *Forest Ecology and Management* 248: 119-135.

ONODA, Y., RICHARDS, A. E., AND WESTOBY, M. (2010). The relationship between stem biomechanics and wood density is modified by rainfall in 32 Australian woody plant species. *New Phytologist* 185: 493 – 501.

PACALA, S. W., C. D. CANHAM, J. SAPONARA, J. A. SILANDER, R. K. KOBE, AND RIBBENS E. (1996). Forest models defined by field measurements: estimation, error analysis and dynamics. *Ecological Monographs* 66: 1–43.

PANSHIN, A. J., AND DE ZEEUW, C. (1980). Textbook of wood technology. McGraw-Hill Inc., US.

PINHEIRO, J., BATES, D., DEBROY, S., SARKAR, D., AND the R DEVELOPMENT CORE TEAM (2009). Nlme: Linear and Nonlinear Mixed Effects Models. R package version 2.9.1.

POORTER, L., WRIGHT, S. J., PAZ, H., ACKERLY, D. D., CONDIT, R., IBARRA-MANRIQUEZ, G., HARMS, K. E., ET AL. (2008). Are functional traits good predictors of demographic rates? Evidence from Neotropical forests. *Ecology* 89: 1908 – 1920.

PRUYN, M.L., EWERS III, B.J. AND TELEWSKI, F.W. (2000). Thigmomorphogenesis: changes in the morphology and mechanical properties of two *Populus* hybrids in response to mechanical perturbation. *Tree Physiology* 20: 535-540.

R CORE TEAM (2012). R: A language and environment for statistical computing. R Foundation for Statistical Computing, Vienna, Austria. ISBN 3-900051-07-0, URL http://www.R-project.org/.

RUEDA, R. AND WILLIAMSON, G.B. (1992). Radial and vertical wood specific gravity in *Ochroma pyramidale* (Cav. ex Lam.) Urb. (Bombacaceae). *Biotropica* 24: 512 – 518.

VENABLES, W. N. AND RIPLEY, B. D. (2002) Modern Applied Statistics with S. Fourth Edition. Springer, New York. ISBN 0-387-95457-0.

WELDEN, C. W., HEWETT, S. W., HUBBELL, S. P., AND FOSTER, R. B. (1991). Sapling survival, growth, and recruitment: relationship to canopy height in a neotropical forest. *Ecology* 72: 35–50.

WEST, P.W. (2009). Tree and Forest Measurement. 2nd Edition, Springer.

WIEMANN, M. C., AND WILLIAMSON, G. B. (1988). Extreme radial changes in wood specific gravity in some tropical pioneers. *Wood and Fiber Science* 20: 344 – 349.

WIEMANN, M.C. AND WILLIAMSON, G.B. (1989). Wood specific gravity gradients in tropical dry and montane rain forest trees. *American Journal of Botany* 76: 924-928.

WIEMANN, M.C. AND WILLIAMSON, G. B. (2012). Testing a novel method to approximate wood specific gravity of trees. *Forest Science* 58: 577 – 591.

WILLIAMSON, G. B. AND WIEMANN, M. C. (2010a). Age-dependent radial increases in wood specific gravity of tropical pioneers in Costa Rica. *Biotropica* 42: 590-597.

WILLIAMSON, G. B. AND WIEMANN, M. C. (2010b). Measuring wood specific gravity…correctly. *American Journal of Botany* 97: 519 -524.

WILLIAMSON, G. B. AND WIEMANN, M. C. (2011). Age versus size determination of radial variation in wood specific gravity: lessons from eccentrics. *Trees* 25: 585 – 591.

WILLIAMSON, B. G., WIEMANN, M. C., AND GEAGHAN, J. P. (2012). Radial wood allocation in *Schizolobium parahyba. American Journal of Botany* 99: 1010 – 1019.

WOODCOCK, D.W. AND SHIER, A.D. (2002). Wood specific gravity and its radial variations: the many ways to make a tree. *Trees* 16: 437 - 443.

WRIGHT, S. J, MULLER-LANDAU, H. C., CONDIT, R. AND HUBBELL, S. P. (2003). Gap-dependent recruitment, realized vital rates, and size distributions of tropical trees. *Ecology* 84: 3174-3185.

WRIGHT, S.J., KITAJIMA, K., KRAFT, N.J.B., REICH, P.B., WRIGHT, I.J., BUNKER, D.E., CONDIT, R. et al. (2010). Functional traits and the growth-mortality trade-off in tropical trees. *Ecology* 91: 3664-3674.

ZANNE A. E., LOPEZ-GONZALEZ, G., COOMES, D. A., ILIC, J., JANSEN, S., LEWIS, S. L., MILLER, R. B., SWENSON, N. G., WIEMANN, M.C., AND CHAVE, J. (2009) Data from: Towards a worldwide wood economics spectrum. Dryad Digital Repository. doi:10.5061/dryad.234

ZOBEL, B. H., AND VAN BUIJTENEN, J. P. (1989). Variation among and within trees. *In* ZOBEL, B. H., AND VAN BUIJTENEN, J. P., Wood Variation: Its Causes and Control, pp. 72 -131. Springer - Verlag.

Supplementary material for chapter 1

APPENDIX S1: Species average values for the two metrics of radial variation in wood specific gravity (WSG). R_{O-I} = difference between average WSG for outer wood (WSG_O) and inner wood (WSG_I), and R_{VAR} = variance of WSG for 1-cm segments from a single core.

Species	Average R_{O-I}	Average R_{VAR}
A. membranacea	0.0599	0.0032
A. graveolens	0.0343	0.0035
C. longifolium	0.0153	0.0011
C. bicolor	0.1160	0.0031
G. ulmifolia	-0.0085	0.0019
I. marginata	0.0770	0.0027
J. copaia	0.0744	0.0015
L. panamensis	0.0722	0.0014
L. seemannii	0.0087	0.0013
P. elegans	0.0035	0.0019
P. armata	0.0297	0.0022
P. copaifera	-0.0015	0.0020
S. amara	0.0253	0.0006
S. radlkoferi	0.1341	0.0031
T. guayacan	-0.0138	0.0024
T. rosea	0.0446	0.0017
T. versicolor	0.0299	0.0021
T. cumingiana	0.1392	0.0064
V. sebifera	0.0408	0.0013
Z. ekmanii	0.1407	0.0047

Appendix S2: Differences in Akaike information criterion (ΔAIC_c) for mean, linear, and quadratic models (see text equations 1, 2, and 3 respectively). ΔAIC_c is the difference between the model with the minimum AIC_c value and the AIC_c of the other candidate models. The model with the fewest parameters had best fit when $\Delta AIC_c \leq 2$.

Species	**Mean**	**Linear**	**Quadratic**
A. membranacea	17.2	0	1.70
A. graveolens	6.19	3.35	0
C. longifolium	33.7	15.1	0
C. bicolor	167	0	2.11
G. ulmifolia	2.68	4.47	0
I. marginata	97.8	26.4	0
J. copaia	95.3	23.1	0
L. panamensis	164	40.9	0
L. seemannii	0.46	0.08	0
P. elegans	0	2.1	3.1
P. armata	9.62	3.74	0
P. copaifera	19.9	21.9	0
S. amara	52.5	1.02	0
S. radlkoferi	267	1.69	0
T. guayacan	1.70	0	0.75
T. rosea	34.5	3.53	0
T. versicolor	10.4	6.28	0
T. cumingiana	85.2	0	1.50
V. sebifera	43.0	17.7	0
Z. ekmanii	183.8	3.31	0

Chapter 2

Anatomical underpinnings of wood density variation in tropical rainforest trees: insights from ontogeny

Oyomoare L. Osazuwa-Peters[1], S. Joseph Wright[2], and Amy E. Zanne[3, 4]

[1]Department of Biology, One University Boulevard, University of Missouri Saint Louis, Saint Louis, Missouri, 63121, USA

[2]Smithsonian Tropical Research Institute, Apartado 0843 – 03092, Balboa, Panama

[3]Department of Biological Sciences, 2023 G St. NW, The George Washington University, Washington DC, 20052, USA

[4]Center for Conservation and Sustainable Development, Missouri Botanical Garden, St. Louis, MO, 63166, USA

Manuscript draft to be submitted to *Functional Ecology*.

Abstract

1. Wood density is a key functional trait related to plant performance, and ecological strategy ─ the way that species acquire limited resources through dissimilarities in construction and allocation patterns. The same wood density value however can be achieved through different combinations of underlying anatomical components, suggesting that wood density's composite nature masks variation in ecological strategies among coexisting species. The functional basis of variation in wood density and its anatomical underpinnings can be investigated by examining ontogenetic changes within a tree since understorey juveniles and canopy-level adults experience different access to resources and environments.

2. We examined ontogenetic differences in wood trait variation and coordination, major anatomical drivers of wood density, and relationships between wood traits and species performance for 20 tree species from Barro Colorado Island, Panama. From species that varied widely along the growth-mortality tradeoff axis, we obtained wood segments from near the pith (juvenile wood) and from near the bark (adult wood) for three adults (≥ 20 cm diameter) per species. We quantified wood density, and two types of anatomical traits; 1) cell morphology (vessel diameter, vessel density, fiber wall thickness, and fiber lumen area), and 2) tissue fractions (vessel, parenchyma, fiber wall, and fiber lumen fractions). Species performance was measured (relative growth and mortality rates) for both juveniles and adults.

3. Overall, ontogeny accounted for considerable amounts of variation (36 – 67%) in vessel and parenchyma traits, but much less variation in fiber traits and wood density (17

– 26%). Anatomical traits showed strong coordination, with one axis capturing a contrast between fiber lumen fraction, fiber lumen area, and vessel diameter versus vessel density, fiber wall fraction and fiber wall thickness, while a second axis captured a contrast between vessel and parenchyma fraction. These coordination axes did not differ between juvenile and adult wood. Fiber wall and lumen were the most important anatomical traits underpinning wood density variation in both juvenile and adult wood. Finally, plant performance was strongly associated with vessel and fiber traits (but not wood density) in juveniles but not adults.

4. In sum, wood density does mask variation in ecological strategies, and juvenile wood holds the desired information on the functional consequences of a tree's anatomical configuration.

Key-words: trait co-variation, fiber, vessel, axial parenchyma, ray parenchyma, juveniles, adults, ecological strategy, species performance

Introduction

Wood density (dry mass/fresh volume) is a key functional trait related to several major aspects of a plant's ecology including biomechanical support, hydraulic transport, storage, defense, and successional status (Chave *et al.* 2009). To date, wood density has been found to be a significant but not particularly strong predictor of tree growth and mortality, measures of species performance. Wood density has at best explained between 29 - 41% of interspecific variation in growth and mortality rates of saplings of coexisting tree species (Chave *et al.* 2009; Poorter *et al.* 2010; Russo *et al.* 2010; Wright *et al.* 2010; Fan *et al.* 2012). It has been hypothesized that wood density's limited predictive ability

may be due to its links to multiple functional roles, so that it is unable to strongly predict any one function (Zieminska *et al.* 2013).

Wood density's link to multiple ecological functions results from its composite nature; it is derived from a combination of physical, chemical, and anatomical properties of cells (Chave *et al.* 2009). Prevailing understanding considers similar wood densities of species as indicative of similar ecological strategies ─ differences in the ways that species acquire limited resources through dissimilarities in construction and allocation patterns (Westoby *et al.* 2002; Chave *et al.* 2009; Wright *et al.* 2010). Low wood density species are considered to have a resource acquisitive strategy characterized by fast growth, high mortality and low stress tolerance, while high wood density species tend to the reverse. The same wood density value, however, can be achieved through different combinations of cell properties, suggesting that species with similar wood densities could in fact vary in ecological strategies if varying properties of cells impact whole plant functioning (Preston, Cornwell & DeNoyer 2006; Zanne *et al.* 2010; Russo *et al.* 2010; Zieminska *et al.* 2013; Lachenbruch & McCulloh 2014). If the composite nature of wood density masks variation in ecological strategies among coexisting species, better insight into wood structure and function may be found by examining the underlying anatomical components of wood density.

Key anatomical components of wood are vessels, fibers, and parenchyma, and these cell types can be directly related to specific ecological functions. In angiosperm wood, vessels are relatively large diameter conduits (5 - 400 μm) that are dead on maturity and have an open lumen for longitudinal water transport (Carlquist 2001; Sperry, Meinzer & McCulloh 2008; Cornwell *et al.* 2009; Zanne *et al.* 2010). Thus, vessel traits including

vessel area fraction, size and frequency, represent an axis of variation that appears to be decoupled from wood density (Martinez-Cabrera *et al.* 2009; Zanne *et al.* 2010), although moderate or weak relationships with wood density have also been reported (Preston *et al.* 2006; Poorter *et al.* 2010; Russo *et al.* 2010). The matrix outside of the vessel lumen area has strong influences on wood density, implicating fiber and parenchyma traits in wood density variation (Carlquist 2001; Jacobsen *et al.* 2007; Zanne *et al.* 2010; Zheng & Martínez-Cabrera 2013; Zieminska *et al.* 2013). Fibers function mainly in mechanical support and water storage (Carlquist 2001; Evert 2006); they have secondary walls of relatively constant density (Hacke *et al.* 2001) and are also dead at maturity (Pratt *et al.* 2007; Cornwell *et al.* 2009; Zanne *et al.* 2010). Axial and ray parenchyma are the living cells in sapwood that store nutrients and water, as well as allow for short distance transport (Carlquist 2001; Evert 2006), but die during heartwood formation (Taylor, Gartner & Morrell 2002).

Variation in wood density can be achieved anatomically by either altering cell morphology (cell wall thickness and lumen areas) or altering relative tissue proportions (area fraction in vessels, fiber wall, fiber lumen, and parenchyma) (Martinez-Cabrera *et al.* 2009; Lachenbruch & McCulloh 2014). Since lumens essentially have zero density, cell wall have positive density, and parenchyma being living cells have relatively less positive density (Zieminska *et al.* 2013), wood density should increase with increasing wall thickness, decreasing lumen area, and decreasing parenchyma fractions. However, the relative importance of these two mechanisms (cell morphology versus tissue fractions) for achieving intra- and inter-individual and interspecific variation in wood density has yet to be evaluated.

Insight into the anatomical influences on wood density can be hypothesized based on known variation and coordination (or co-variation) among anatomical traits. Coordination among anatomical traits may result from a physically enforced tradeoff or because such coordination is favored by available niches (Westoby *et al.* 2002), thus reflecting different resource allocation patterns (Chave *et al.* 2009). Hence, coordination among anatomical traits may be associated with variation in the composite trait wood density. Three major relationships between anatomical traits have been observed in past studies. 1) A negative relationship between vessel area and vessel density reflecting constant allocation to total vessel area with variation in vessel composition ranging from few large vessels to many small vessels (Zanne *et al.* 2010). 2) A negative relationship between fiber wall thickness and fiber lumen size (Roque & Tomazelo-Filho 2007), reflecting a tradeoff between mechanical support and water storage. 3) A negative relationship between fiber area fraction and parenchyma area fraction reflecting a tradeoff between mechanical support and nutrient storage (Pratt *et al.* 2007; Poorter *et al.* 2010; Fortunel *et al.* 2014).

Wood density and vessel anatomy are typically measured on adult wood. However, juvenile trees growing in the understorey experience different access to resources and different environments than their canopy level adults (Cavender-Bares & Bazzaz 2000; Thomas & Winner 2002). Investigations of wood density and anatomy variation within an individual at different ontogenetic stages can provide new insight into the functional consequences of these wood traits. Unlike animals that replace their cellular structure throughout their lives, trees retain their original wood structure, which largely remains unchanged with the exception of chemical deposition during heartwood formation

(Taylor *et al.* 2002; Lachenbruch, Moore & Evans 2011). Thus, ontogenetic changes in wood anatomy can be inferred from differences in wood properties between wood nearest the pith (produced as a juvenile) and wood nearest the bark of adult trees (Lachenbruch *et al.* 2011). Published evidence of ontogenetic shifts comes from only a few commercial softwoods (Lachenbruch *et al.* 2011). These data suggest that juvenile wood will have traits associated with lower specific conductivity and lower risk of embolism (e.g. smaller vessel fractions and smaller vessels) (Lachenbruch *et al.* 2011). However, the degree to which relationships among anatomical traits and between anatomical traits and wood density hold across ontogeny remains a largely unanswered question.

Due to the clear functional consequences of variation in anatomical properties, anatomy may show stronger ties to plant performance than has wood density. Growth rates are expected to increase with vessel area fraction and vessel size, which are associated with hydraulic conductivity, due to increased photosynthesis and carbon gain rates (Brodribb & Feild 2000; Chave *et al.* 2009) and to decrease with fiber wall thickness, due to increased stem construction costs (Poorter *et al.* 2010). In contrast, mortality rates should decrease with increasing fiber wall thickness due to increased mechanical strength and damage resistance, and with increasing parenchyma area fraction due to higher carbon and water storage potential (Poorter *et al.* 2010). The few studies that have investigated relationships between species' anatomical traits and growth and mortality rates have focused on vessel traits, showing a positive correlation between vessel diameter and growth rate (Poorter *et al.* 2010; Russo *et al.* 2010; Fan *et al.* 2012)

We have previously shown that wood density varies more among species, with much less variation among and within individuals of the same species (Osazuwa-Peters, Wright &

Zanne 2014). Here, we explore the ontogenetic, inter-individual and interspecific variation in anatomical traits underpinning wood density. We examined coordination among these anatomical traits and how these traits influence performance for 20 coexisting lowland rainforest species that were selected to represent the breadth of the growth-mortality tradeoff. We ask the following questions:

1. Wood traits – variation across taxonomic levels: How do anatomical traits vary ontogenetically within individuals, among conspecific individuals and among species? As with patterns of variation for wood density at different taxonomic levels (Osazuwa-Peters *et al.*, 2014), we expect interspecific variation to account for the bulk of variation in anatomical traits but that important variation will occur ontogenetically due to different environments experienced by plants as juveniles and as adults.

2. Anatomical trait coordination: a. Is there coordination among anatomical traits? b. Does this coordination differ with ontogeny? We anticipate negative relationships between vessel size and vessel density, fiber wall thickness and fiber lumen size, and fiber area fraction and parenchyma fraction. We have no *a priori* expectation that these patterns of coordination between traits should be different between juvenile and adult wood.

3. Anatomical underpinnings of wood density: a. What is the relative contribution to variation in wood density of i. cell morphology ii. tissue fractions and iii. anatomical traits overall? b. Does this relative contribution differ with ontogeny? c. Which anatomical traits are the best predictors of wood density? Given that past studies have found interspecific variation in wood density is largely independent of vessel and

parenchyma tissue fractions, but driven by the relative proportion of wall and lumen in the non-vessel lumen matrix (Zanne *et al.*, 2010; Zieminska *et al.*, 2013), we predict that wood density variation will be best explained by alterations of fiber cell morphology and the relative proportions in fiber wall and fiber lumen. We have no *a priori* expectation that this pattern should be different between juvenile and adult wood.

4. ***Wood traits and performance:*** a. Are particular anatomical traits more strongly associated with species performance than wood density? b. Does this pattern vary with ontogeny both in the performance traits and in the wood traits? Due to the composite nature of wood density and the relationship between anatomical traits and specific functions, anatomical traits will be better predictors of species performance than wood density. Based on the association of growth rate with hydraulic conductance, and with stem construction costs, we expect growth rates to increase with vessel fraction and diameter, and fiber lumen size, but decrease with fiber wall thickness. Mortality rates are expected to increase with fiber lumen size, fiber lumen fraction, and vessel lumen area, but to decrease with fiber wall thickness, fiber wall and parenchyma fractions, survival being greater with higher stem material strength and carbon storage potential. The direction of these associations between anatomical traits and species performance should be similar across ontogeny, albeit stronger in magnitude for juveniles. Stronger associations between anatomical traits and species performance is more likely for juvenile wood since understorey juveniles experience greater heterogeneity in environments than do sun-exposed, canopy adults (Webb & Peart 2000; Woodcock & Shier 2002). Thus, juvenile wood may exhibit greater interspecific variation in

performance and likely show greater interspecific variation in wood traits, resulting in stronger associations.

Materials and Methods

Samples for this study were collected from the Barro Colorado Nature Monument, Panama. In an earlier investigation on radial variation in wood density, 20 tropical tree species (Figs 1 and 2) that were widely distributed across the growth-mortality tradeoff and wood density spectra were selected (Osazuwa-Peters *et al.* 2014). For each of these species, two cores extending from bark to pith were extracted from 6 individuals > 20 cm diameter at breast height of each species (Osazuwa-Peters *et al.* 2014). For the present study, we selected from this pool of 240 cores one core from three individuals per species, resulting in 60 cores. From each core, two 1 cm wood segments were obtained; one segment within the first 3 cm near the pith (juvenile wood), and one segment within the last 3 cm near the bark (adult wood).

Data collection

Wood density

Wood density values for all 120 segments were obtained from Osazuwa-Peters et al. (2014). In that study, wood density was calculated as dry mass divided by fresh volume divided by the density of water (a.k.a. wood specific gravity in forestry literature; Williamson & Wiemann 2010). The fresh volume of each 1 cm segment was measured with the water-displacement method, and dry mass determined after drying to constant mass at 100^{o}C in a convection oven (Osazuwa-Peters, Zanne & PrometheusWiki contributors 2011).

Species performance

For all twenty species, relative growth and mortality rates were obtained from Wright *et al.*, (2010). Relative growth rates under favorable conditions equaled 95th percentile relative growth rates (RGR_{95}). Mortality rates under unfavorable conditions equaled mortality rates of the 25% of individuals with the slowest relative growth rates in the previous census interval (MRT_{25}). These rates were separately available for juveniles (RGR_{95SAP}, MRT_{25SAP}) and adult trees (RGR_{95TRE}, MRT_{25TRE}). Using the function *princomp* in the *stats* package in R (R Core Team 2014), RGR_{95} and MRT_{25} for saplings and large trees were linearly combined in a principal components analysis, and species scores along the first component axis were extracted to form the variables $RGR.MRT_{SAP}$, and $RGR.MRT_{TRE}$.

Anatomy

Thin anatomical wood sections, 15 – 40 μm thick, were taken from each 1 cm segment using a GSL 1 microtome (Gärtner, Lucchinetti & Schweingruber 2014). Sections were stained with cresyl violet acetate, a metachromatic dye (Keating 2014), to increase contrast. Images of stained sections were acquired with a Nikon Coolscope Digital Microscope at the Plant Anatomy Lab of the Missouri Botanical Garden, St. Louis, MO, USA. For each section, three images were captured at a coarse (4x) magnification to quantify vessel traits and three images were captured at a finer (20x) magnification to quantify fiber and parenchyma traits. The difference in image magnification for vessel traits vs. fiber and parenchyma traits was to avoid a bias of tissue area fractions towards vessels, particularly for species with large sized vessels that can dominate a 20x image.

Areas of cell types in each image were color coded in GIMP (version 2.8.0) using a Bamboo graphic tablet (Wacom Co. Ltd., Japan). Anatomical trait values for each 1 cm segment were obtained by averaging across the three images at a given magnification. Due to intergradation among cell types, particularly between dimorphic fibers and thick-walled parenchyma, longitudinal sections were prepared for four species to aid in identifying cell types (Carlquist 2014). In extreme cases of ambiguity between cell types, expert anatomists were consulted to confirm the identification of cell types. Eight images for which this ambiguity was unresolved were excluded from processing, and averages adjusted accordingly. Further analyses were conducted in ImageJ (http://imagej.nih.gov/ij/).

Vessel traits: to quantify vessel traits (vessel area fraction, vessel diameter (μm), and vessel density (#/μm^2)), the count, and diameter of whole and partial vessels (including vessel wall) within the entire image area were determined. Images that exhibited the edge effect in which one or more vessels were only partial in the image presented a challenge that was resolved by applying rules from the field of stereology (MBF BIOSCIENCE 2015). This involved defining a central image area surrounded by a buffer zone with a width slightly larger than the radius of the largest vessel for that species. All vessels with their centroids within the central image area were used in determining vessel count and vessel diameter so that only whole vessels were included. However, total area of vessels was based on all vessels whether entirely or partially within the total image area. Vessel area fraction at 4x was estimated as the total area of vessels divided by the total image area. Vessel density was estimated as the number of vessels divided by the total image area or the central image area for images that exhibited the edge effect.

Fiber traits: within each 20x image, fiber area was defined as area occupied by fiber cells. Also, the lumen area of an average of 133 (range: 25 - 347) individual fibers were used to estimate average fiber lumen area (μm^2) per image. Similarly, the double wall thickness for on average 60 (range: 30 – 73) pairs of fibers was determined by drawing lines that covered the length of the double wall of adjacent fibers; length was determined in ImageJ. Fiber double wall thickness was divided by 2 to obtain fiber wall thickness (μm).

Parenchyma traits: within each 20x image, parenchyma area was defined as the combined area occupied by axial and ray parenchyma.

Tissue fractions: were quantified as the fraction of a tissue per image area. Fractions determined at magnifications of 20x (fibers and parenchyma) were expressed as proportions of the image area at 4x. We multiplied the fraction of non-vessel area at 4x (i.e. 1 – vessel area fraction at 4x) by fiber fraction at 20x to get fiber fraction at 4x. Similarly, fraction of non-vessel area at 4x was multiplied by parenchyma fraction at 20x to get parenchyma fraction at 4x.

We further decomposed fiber fraction into fractions of fiber wall and fiber lumen area. To do this, we assumed, due to the absence of intercellular spaces, that fibers consist of a rectangular fiber wall layer surrounding a hollow fiber lumen. For each image, using average fiber cell measures of lumen area, lumen 'length' (measured as Feret's diameter in ImageJ), and wall thickness, we determined the fraction of a fiber cell area that is wall and lumen (see appendix 1 for details). Each of these fractions at the fiber cell level was multiplied by the total fiber fraction at the tissue level to obtain fiber wall fraction and fiber lumen fraction (See appendix 1 for details).

Data analysis

Distribution of data was examined for species performance, and separately for anatomical traits of juvenile and adult wood, using histogram plots. All variables were approximately normally distributed with the exception of RGR_{95SAP}, RGR_{95TRE}, and fiber lumen area for both juvenile and adult wood. Variables with non-normal distributions were natural log-transformed. Due to the constant-sum constraint exhibited by tissue fractions (parenchyma, vessel, fiber wall, and fiber lumen fractions) in our data-set (i.e. tissue fractions sum to 1), centered log ratio transformations of tissue fractions were used as input in the multivariate analyses (Aitchison 1983). Aitchison's centered log ratio transformation has been shown to successfully overcome the constant-sum constraint associated with compositional data, while using all fractions and without compromising interpretability (Aitchison 1983). Aitchison's centered log ratio transformation for compositional data was done with the *clr* function of the *Hotelling* package in R (Curran 2013).

1. Wood traits – variation across taxonomic levels: We performed a variance component analysis to assess the contributions to variation in wood traits (wood density and anatomical traits) from ontogenetic variation within an individual, intraspecific variation, and interspecific variation. This involved using a random-effects model with two nested levels of random effects (random=~1|Species/Individual) to estimate the proportion of variation in wood traits associated with species and individuals. The residual variation included variation associated with ontogeny plus measurement error.

2. Anatomical trait coordination: We performed principal components analyses (PCA) to evaluate relationships among anatomical traits separately for juvenile and adult wood, after scaling and centering the variables. We evaluated bivariate associations between wood anatomical traits separately for juvenile and adult wood with Pearson correlation tests. We evaluated differences between juvenile and adult wood for the strength and direction of correlations between vessel density and vessel diameter, fiber wall thickness and fiber lumen area, parenchyma fraction and fiber lumen fraction, and parenchyma fraction and fiber wall fraction. These bivariate correlations were dependent non-overlapping because sample pairs (i.e. juvenile and adult wood samples) were obtained from the same individual but none of the correlated variables were shared by juvenile and adult wood (e.g. different vessel density and diameter for juvenile and adult wood). Comparison of dependent non-overlapping correlation coefficients was done with the *cocor* function of the *cocor* package, which implements Fisher's *r*-to-*z*-transformation for testing the significance of the difference between two correlations (Diedenhofen & Diedenhofen 2015).

3. Anatomical underpinnings of wood density: We evaluated the relative contribution to variation in wood density of cell morphology and tissue fractions by partitioning the variation uniquely ([a] and [c] in Fig. 3) and jointly ([b] in Fig. 3) explained by cell morphology and tissue fractions in separate multiple regressions for juvenile and adult wood. This procedure termed 'variation partitioning' consists of six conceptual steps as described in Borcard, Gillet & Legendre (2011). First, multiple regression and forward selection is used to select explanatory variables separately for relationships between wood density and cell morphology and between wood density and tissue fractions.

Second, a redundancy analysis (RDA) is performed for one subset of the data (in this case cell morphology) to yield fraction [a+b] (see Fig. 3). Third, an RDA is performed for the other subset of the data (in this case tissue fractions) to yield [b+c]. Fourth, an RDA is performed for both subsets of the data together, yielding fraction [a+b+c]. Fifth, the adjusted R^2 of the three RDAs above is computed. Finally, estimates of the fractions of adjusted (adj) variation are computed by subtraction (e.g. fraction $[a]_{adj} = [a+b+c]_{adj} - [b+c]_{adj}$). To implement these steps with our dataset, three matrices were defined for each ontogenetic stage; 1) the response variable (wood density), 2) cell morphological traits (fiber lumen area, fiber wall thickness, vessel density, and vessel diameter), and 3) tissue fractions (parenchyma fraction, vessel fraction, fiber wall fraction, fiber lumen fraction).

The purpose of the forward selection procedure in step 1 was to determine a parsimonious set of predictor variables in order to avoid multi-colinearity. However, forward selection assesses the contributions of predictor variables as they are introduced into a regression model and depends largely on the order in which predictors are introduced into the model ((Ray-Mukherjee *et al.* 2014). Hence, we instead used a commonality analysis to identify the most parsimonious combination of wood traits for each matrix that best predicts the response variable. Commonality analysis is a multiple regression based method that explicitly addresses the multi-colinearity problem by partitioning the total variance ($\boldsymbol{R^2}$) explained in the response variable into unique and common contributions that each predictor makes to the total explained variance (Kraha *et al.* 2012; Ray-Mukherjee *et al.* 2014). Unique effects indicate the amount of variance in the response variable that is uniquely accounted for by a predictor, while common effects indicate the amount of variance due to two or more variables (Nimon 2010). Hence,

unique and common effects for each predictor variable are produced as coefficients in a commonality analysis. We used the commonality coefficients to select the most parsimonious combination of traits that best predict the response variable wood density, for the cell morphology matrix, and the tissue fraction matrix. For example, for juvenile wood, the simplest combination of cell morphological traits that predicted juvenile wood density was identified using the *regr* function of the *yhat* package in R (Nimon, Oswald & Roberts 2013). Each parsimonious set of traits for each matrix was then used as input in a variation partitioning analysis using the *varpart* function of the *vegan* package in R (Oksanen *et al.* 2015), which then estimates the unique and joint variances explained by each matrix (Borcard *et al.* 2011). Also, using a permutation method with the *anova.cca* function of the *vegan* package in R (Oksanen *et al.* 2015), the significance of the unique variances explained by each matrix was obtained. However, the significance of the joint variances cannot be determined using this method (Borcard *et al.* 2011). Lastly, we ran separate multiple regressions for wood density regressed on the parsimonious, and on the full combination of traits for cell morphology and for tissue fractions, in order to obtain $\boldsymbol{R^2}$ and standardized regression coefficients ($\boldsymbol{\beta}$) that quantify how much change in wood density results from a one-unit change in the predictor variables.

4. *Wood traits and performance:* We used Pearson correlation tests to evaluate the association between relative growth and mortality rates and wood density and anatomical traits, separately for juvenile and adult wood.

All statistical tests were implemented in R version 3.1.2 (R Core Team 2014), and *ggplot2* (Wickham & Chang 2014), *gridExtra* (Auguie 2012), and *corrplot* (Wei 2013) for graphics.

Results

Wood traits varied substantially across the 20 co-occurring tropical tree species (Figs 1 and 2) with similar patterns of variation irrespective of ontogenetic stage (Table 1). Fiber lumen area showed the largest variation among species, followed by fiber lumen fraction, vessel density and parenchyma fractions, respectively. The remaining traits, including wood density, had < 5-fold variation among species (Table 1).

1. Wood traits – variation across taxonomic levels: Interspecific variation explained the bulk of variation for most traits (Figs 4 and 5). However, ontogeny explained considerable variation in vessel traits (36 – 67%) and parenchyma fraction (39%), but smaller amounts of variation in fiber traits and wood density (17 – 26%; Fig. 4). Inter-individual variation was negligible for all traits (< 0.1%).

2. Anatomical trait coordination: To evaluate relationships among wood traits at different ontogenetic stages, data were analyzed separately for juvenile and adult wood using PCA (Fig. 6; Table 2). For juvenile wood, 47.0% and 22.1% of the variance was accounted for by the first and second PCA axes, respectively. The first PCA axis showed moderate negative loadings for fiber lumen area, vessel diameter, and fiber lumen fraction, and moderate positive loadings for vessel density, fiber wall fraction and fiber wall thickness. The second axis showed strong negative loadings for parenchyma fraction, and moderate positive loadings for vessel fraction, vessel density, and fiber lumen fraction. Patterns were generally similar for adult wood, with 45.8%, and 19.1% of variance explained by the first and second PCA axes, respectively. In adult wood, the same set of traits loaded modestly on the first axis as in juvenile wood, while the second

axis had strong negative loadings for parenchyma fraction and moderate positive loadings for vessel fraction and vessel density only.

In general, bivariate correlations between pairs of wood traits were similar across ontogeny. Fiber traits were strongly correlated with one another. Parenchyma fraction was strongly negatively associated with fiber lumen fraction. Vessel fraction was only weakly positively associated with vessel density; however, vessel density and vessel diameter were weakly to moderately associated with some fiber traits, and as expected, vessel density was strongly negatively associated with vessel diameter (Fig. 7). Bivariate correlation coefficients did not differ significantly between juvenile and adult wood for vessel density and diameter (z = -1.41, P = 0.92), fiber wall thickness and fiber lumen area (z = -0.63, P = 0.73), parenchyma fraction and fiber wall fraction (z = -0.76, P = 0.78), and parenchyma fraction and fiber lumen fraction (z = -1.06, P = 0.85).

3. Anatomical underpinnings of wood density: Of the four cell morphology traits considered, fiber lumen area accounted for the largest percentage of wood density variation (> 70%) for both juvenile and adult wood. This was followed by small but significant contributions from fiber wall thickness. For tissue fractions, fiber wall fraction was the most important trait for explaining both juvenile and adult wood density variation, followed by very small but significant contributions from fiber lumen fraction (Table 3). Similar amounts of variance in wood density were explained by the parsimonious and the full combination of traits (Table 3). Wood density decreased with increasing fiber lumen area and fraction, but increased with increasing fiber wall thickness and fraction (Table 3). The amount of variation in wood density uniquely explained by cell morphology was small and insignificant, while variance explained by

tissue fraction was also small but significant (Table 4). Together, cell morphology and tissue fractions jointly explained large amounts of variation in wood density for both juvenile and adult wood (Table 4).

4. *Wood traits and performance:* Whether measured for either saplings or large trees, growth (RGR_{95}) and mortality (MRT_{25}) rates as well as the linear combination (RGR.MRT) of these two rates were not significantly associated with either juvenile or adult wood density (Fig. 8). In contrast, when considering anatomical traits in juvenile wood, a number of moderate patterns were apparent. RGR_{95SAP} was moderately associated with juvenile wood fiber traits, negatively with fiber wall fraction and positively with fiber lumen area. Similarly, MRT_{25SAP} was moderately negatively associated with fiber wall fraction and vessel density, but positively associated with vessel diameter of juvenile wood (Fig. 8). Also, $RGR.MRT_{SAP}$ was negatively correlated with fiber wall fraction and positively correlated with vessel diameter of juvenile wood. In contrast for adult wood, there was only a marginally positive correlation between vessel diameter and MRT_{TRE}, and $RGR.MRT_{TRE}$ (Fig. 8).

Discussion

Variation in wood density, a key functional trait, can have consequences for whole-plant function, community dynamics, and ecosystem processes. However, the composite nature of wood density may mask variation in ecological strategies among co-occurring species with similar wood densities. Further, anatomical components of wood density may vary with ontogeny, as juvenile and adult trees experience different resource availability and environments. Here, we decompose wood density into its underlying anatomical

components, to explicitly test for ontogenetic differences in wood traits, coordination among wood traits, major anatomical drivers of wood density, and associations between wood traits and species performance. First, we found greater ontogenetic variation in vessel traits and parenchyma compared to fiber traits and wood density. Second, anatomical trait coordination did not differ with ontogeny. Third, variation in wood density was best explained by variation in fiber cell morphology and tissue fractions. Fourth, anatomical traits were more strongly associated with measures of species performance than with wood density. However, there was ontogenetic variation in the strength of these associations. Below, we discuss these results in detail.

Ontogenetic differences: Similar to wood density, most of the variation in anatomical traits can be captured at the interspecific level (Osazuwa-Peters *et al.* 2014). However, ontogeny explained between 17 and 67% of variation in individual wood traits. Developmental changes in response to different mechanical and hydraulic constraints experienced by saplings and adults may explain ontogenetic variation in wood traits. For example, juvenile trees have greater embolism resistance due to less developed root systems and lower capacity for water storage, while large trees have a higher specific conductivity due to greater resistance to water transport resulting from longer path lengths (Sperry *et al.* 2008; Lachenbruch *et al.* 2011). Similarly, resource availability and demands for maintaining structural integrity differ for juveniles because adult trees enjoy high light environment up in the canopy but have to deal with increased forces associated with self-weight and wind load (Read & Stokes 2006; Lachenbruch *et al.* 2011). Further, among species in our study, vessel and parenchyma traits had the largest variances attributable to ontogeny. This anatomical shift suggests that saplings are under selective

pressure to respond to non-trivial changes in hydraulic and storage demands by altering their wood anatomical properties as they grow. This ontogenetic plasticity in anatomical traits did not translate to differences in trait coordination or the identity of major drivers of wood density between juvenile and adult wood. But association between wood traits and whole-plant function varied with ontogeny.

Anatomical trait coordination: The first PCA axis (Fig. 6 & Table 2), defined by variation in fiber and vessel traits, separated species along the wood density spectrum ($R = 0.88$, $P < 0.0001$). On this axis, high wood density species had positive scores associated with higher fiber wall thickness and fraction and vessel density, while low wood density species had negative scores associated with higher fiber lumen area and fraction and vessel diameter. The second PCA axis captured variation in vessel and parenchyma fractions; species with positive scores on this axis had larger vessel fraction while species with negative scores on this axis had larger parenchyma fraction. Interestingly, from this second axis (Fig. 6) we determined that species differing in the traits captured on the first axis did not necessarily differ in position on the second axis, i.e. both species on the negative (low wood density) and positive (high wood density) sides of PCA axis 1 had high parenchyma fractions (negative side of PCA axis 2) and high vessel fractions (positive side of PCA axis 2). Hence, relatively high parenchyma fractions or to a lesser extent high vessel fractions (notice shortness of vessel fraction arrow in PCA biplots; Fig. 6) were not restricted to high or low wood density species. For example, both the slow growing, high wood density *Tabebuia guayacan* and the fast growing, low wood density, pioneer *Cordia bicolor* were close together on PCA axis 2 indicating similar parenchyma fractions. Consequently, parenchyma and vessel fractions

were largely decoupled from wood density variation in this study (Table 3) as in previous reports (Martinez-Cabrera *et al.* 2009; Martínez-Cabrera *et al.* 2011; Zieminska *et al.* 2013). This lends support to the notion that the integrative nature of wood density masks variation in ecological strategies among coexisting tropical trees. Thus, trees may have similar average wood density, but differ in hydraulic architecture and capacity for storage. Conversely, species may differ in ecological strategies as defined by wood density (e.g. fast-growth pioneer species vs. slow-growth late successional species), but exhibit similar hydraulic architecture and storage capacity.

As expected (see Introduction), there were strong tradeoffs between vessel diameter and vessel density, parenchyma and fiber lumen fractions, and fiber wall and lumen traits (Fig. 7). Overall, these negative correlations were similar in direction and strength to previous reports (Preston *et al.* 2006; Martinez-Cabrera *et al.* 2009; Poorter *et al.* 2010; Zanne *et al.* 2010; Martínez-Cabrera *et al.* 2011; Fortunel *et al.* 2014). However, our results contribute additional insight for trunk wood of tropical rainforest trees, because the only other study of such trees measured fiber fractions only and not traits related to fiber morphology i.e. wall thickness and lumen area (Poorter *et al.* 2010). Here, we show that trunk wood of tropical rainforest trees exhibited a similar coordination between morphology and fractions of fiber wall and lumen to that reported in shrubs (Martinez-Cabrera *et al.* 2009). However, there were moderate positive correlations between vessel morphological traits and fiber traits, parenchyma and fiber wall thickness, and strong positive correlations among fiber traits (Fig. 7). Positive correlations between vessel density and fiber wall fraction and thickness may be because fibers strengthen the matrix around vessels, thus helping to resist embolism (Jacobsen *et al.* 2005; Lachenbruch *et al.*

2011). Also, positive correlations between vessel diameter and fiber lumen may be attributed to the presumed roles of larger fiber and vessel lumens in water storage resulting in higher capacitance, so mitigating the need to invest in features that enhance resistance to embolism (Pratt *et al.* 2007; Sperry *et al.* 2008; Zanne *et al.* 2010). On the other hand, vessel fraction showed little coordination with other anatomical traits in juvenile wood, but moderate negative correlations with fiber lumen area and fraction in adult wood. This observation for adult wood indicates modest tradeoffs between hydraulic transport and mechanical support for adult trees but not for saplings, since small changes in vessel fraction can provide large increases in hydraulic conductivity with minimal effects on mechanical support (Zanne *et al.* 2010).

Fiber traits drive wood density variation: Fiber lumen area and fiber wall fraction were the major drivers of wood density variation, with smaller contributions from fiber wall thickness and fiber lumen fraction. This result is similar to several previous reports that have consistently identified fiber traits as strongly correlated with wood density including in shrubs (Jacobsen *et al.* 2007; Pratt *et al.* 2007; Martinez-Cabrera *et al.* 2009; Zieminska *et al.* 2013), branches and roots of Amazonian trees (Fortunel *et al.* 2014), and trunks of tropical cloud and dry forest trees (Aguilar-Rodríguez, Abundiz-Bonilla & Barajas-Morales 2001). However, we go beyond bivariate correlations between wood density and anatomical traits and use multiple regression analysis to show that fiber traits overall best predict variation in wood density. Fiber traits explained up to 82% of the variation in juvenile and adult wood density (Table 3). Fiber cells are the load-bearing cells in wood and their huge contribution to wood density variation implies that differential response to biomechanical pressures is the major factor determining wood

density variation. Fortunel *et al.* (2014) reached a similar conclusion that biophysical constraints must drive variation in wood density amongst the 113 Amazonian tropical tree species they examined; fiber traits mirrored variation in branch and root wood density across three environmentally contrasting habitats.

Also, fiber tissue fractions explained slightly more variation than fiber cell morphology, but the proportion of variance uniquely explained by each trait was quite small. More than 75% of the variance in wood density was jointly explained by tissue fractions and cell morphology. Tissue fractions relate to changes in the overall volume of cells, while cell morphology relates to changes in particular features of the cell such as lumen diameter or wall thickness (Lachenbruch & McCulloh 2014). Thus, changes in tissue fractions can occur along with changes in cell morphology, such that a change in fiber cell morphology may also cause a change in fraction or area occupied (e.g., thickening of fiber wall will result in greater fiber wall fraction). This corroborates the conclusion that cell morphological traits can provide more insightful understanding of wood density when combined with tissue fraction information (Zieminska *et al.* 2013).

Species performance: Perhaps the most compelling of our results are the correlations between measures of species performance and several anatomical traits and the absence of correlations between species performance and wood density (Fig. 8). We found these correlations because we paired relative growth and mortality rates for saplings with juvenile wood traits, and relative growth and mortality rates for large trees with adult wood traits. Our results advance what is known about anatomical traits and tree performance because previous studies focused on vessel traits and obtained anatomical trait measures from adult wood (Poorter *et al.* 2010; Russo *et al.* 2010; Fan *et al.* 2012).

In this study, whereas the integrative trait wood density was unrelated to species performance, sapling relative growth rates decreased with fiber wall fraction and increased with fiber lumen area. In contrast, mortality rates decreased with fiber wall fraction and vessel density, but increased with vessel diameter. In contrast, only the correlation between mortality rates and vessel diameter was marginally significant for adult wood (Fig. 8). Hence, these results suggest that the juvenile stage is more susceptible to the myriad hydraulic and mechanical stresses operating in the forest, and the quest to understand the functional significance of the anatomical basis of wood density should be focused on juvenile rather than adult wood.

The decoupling of wood density and measures of species performance for both saplings and adults corroborates the view that the same wood density can be achieved by different combinations of anatomical traits (Russo *et al.* 2010; Zieminska *et al.* 2013). The integrative nature of wood density masks the functional consequences of the different wood cell types for growth and mortality. However, when wood density is decomposed into its anatomical underpinnings, interesting associations with growth and mortality emerge. By prioritizing hydraulic efficiency, saplings of species that invest in large diameter vessels and low fiber wall fractions attain rapid growth, likely conferring a competitive advantage in light-limited environments. Such a strategy characterized by high transport efficiency and low structural costs is considered advantageous in highly productive, wet tropical environments (Choat *et al.* 2012). However, these species also suffered higher mortality as shown by the negative association between mortality rates and fiber wall fraction and positive association between mortality rates and fiber lumen fraction. Species that invest less in fiber wall may be more prone to mechanical damage

from wind and storms leading to higher mortality rates (Putz *et al.* 1983). On the other hand, hydraulic architecture, defined by the negative relationship between vessel density and diameter, was strongly associated with sapling mortality rates, so that species that prioritized hydraulic safety survived better. Adult trees exhibited a similar trend of hydraulic architecture translating to higher survival, albeit marginally. This result is relevant to the growth-hydraulic hypothesis that explains higher mortality rates of forest trees in resource-rich environments as a function of investments in efficient hydraulic architectures (Stephenson *et al.* 2011). A plant's hydraulic architecture largely determines its ability to resist embolism that block xylem conduits, reducing xylem pressure and water transport; for example, large vessels are conductively more efficient but potentially less resistant to drought-induced embolisms (Sperry *et al.* 2008). A continuous decline in xylem pressure and hydraulic capacity leads to hydraulic failure, causing tissue damage and plant death (Choat *et al.* 2012). Thus, hydraulic failure may have been an important mechanism in driving directional changes in species composition towards drought tolerant species that have been reported on Barro Colorado Island as a consequence of several unusual droughts and variation in rainfall patterns over the last six decades (Condit, Hubbell & Foster 1995; Feeley *et al.* 2011).

Conclusion

There has been much conjecture on the potential for the integrative functional trait wood density to mask variation in ecological strategies among coexisting tree species. Here, we approached this issue by examining ontogenetic differences in patterns of wood trait variation, coordination among wood traits, major drivers of wood density, and relationships with species performance. The key message from our study is that variation

in juvenile wood, and not adult wood, holds the desired information on the functional consequences of a tree's anatomical configuration. Multiple lines of evidence from this study (Fig. 4, 6 & 8) corroborate the notion that wood density masks variation in ecological strategies. There was variation in parenchyma and vessel fraction among species of similar wood densities and the association of species performance with hydraulic and mechanical wood traits but not with wood density. Lastly, biomechanical stresses in the environment of coexisting species must play a major role in wood density variation because fiber wall and lumen traits were the most important wood traits underpinning wood density variation. Future work should examine on a larger scale and across tropical forests the generality of the association between juvenile anatomical architecture and performance. Our results lead to the conclusion that wet tropical forests dominated by species that prioritize hydraulic efficiency will be susceptible to compositional changes driven by changing patterns in precipitation and mechanical stressors (e.g. wind storms).

Acknowledgement

O.L.O thanks the Whitney Harris World Ecology Center for research funding; the Smithsonian Tropical Research Institute for facilities and logistic support; the Missouri Botanical Garden for access to the Plant Anatomy lab; Richard Keating, Steven Jansen, Elizabeth Wheeler, Kasia Ziemińska, Juan Carlos Penagos Zuluaga, and David Bogler for advice on anatomical techniques and interpretation of anatomical images; and Peter Stevens and Brad Oberle for comments on earlier versions of manuscript. This research was funded in part by an NSF grant to AEZ (DEB-1302797).

Tables

Table 1: Summary characteristics of wood traits for juvenile and adult wood of 20 tropical tree species. Values are species mean minima (low), maxima (high), and their ratio (*n*-fold variation = maxima/minima).

Trait	Unit	Juvenile			Adult		
		Low	**High**	***n*-fold variation**	**Low**	**High**	***n*-fold variation**
Wood density	g/cm^3	0.21	0.87	4.14	0.30	0.90	3.00
Tissue fractions							
Parenchyma fraction		0.09	0.50	5.56	0.08	0.32	4.00
Vessel fraction		0.03	0.08	2.67	0.04	0.13	3.25
Fiber wall fraction		0.16	0.63	3.94	0.24	0.75	3.12
Fiber lumen fraction		0.03	0.59	19.67	0.01	0.41	41.00
Cell morphology							
Vessel diameter	μm	69.04	199.11	2.88	83.41	229.56	2.75
Vessel density	$vessels/\mu m^2$	1.86×10^{-6}	1.72×10^{-5}	9.26	1.42×10^{-6}	1.94×10^{-5}	13.72
Fiber lumen area	μm^2	4.63	641.93	138.65	1.74	443.18	254.7
Fiber wall thickness	μm	1.60	4.37	2.73	2.28	4.63	2.03

Table 2: Trait loadings on first and second axis of PCA for juvenile and adult wood. Absolute values of loadings ≥ 0.30 are considered moderate and ≥ 0.60 are considered strong, and these are indicated in bold. PC axis 1 captures a contrast between fiber and vessel traits, while PC axis 2 represents a contrast between parenchyma fraction and vessel traits.

Traits	**PC axis 1 (Fiber vessel contrast)**		**PC axis 2 (Parenchyma vessel contrast)**	
	Juvenile	**Adult**	**Juvenile**	**Adult**
Fiber lumen area	**-0.41**	**-0.38**	-0.05	-0.02
Vessel diameter	**-0.35**	**-0.33**	-0.29	-0.14
Vessel density	**0.35**	**0.32**	**0.37**	**0.43**
Fiber wall thickness	**0.43**	**0.43**	-0.24	-0.23
Parenchyma fraction	0.11	0.13	**-0.68**	**-0.65**
Vessel fraction	0.02	0.17	**0.36**	**0.54**
Fiber wall fraction	**0.46**	**0.45**	0.12	-0.04
Fiber lumen fraction	**-0.42**	**-0.46**	**0.33**	0.17

Table 3: Most parsimonious combination of cell morphology or tissue fraction traits that best predict the response variable, wood density, identified with a commonality analysis. Commonality analysis explicitly identifies multi-colinearity by quantifying the unique and common contributions that each predictor makes to the total variance explained in the response variable (Kraha *et al.* 2012; Ray-Mukherjee *et al.* 2014). Unique = proportion of variance in response variable uniquely explained by the predictor. Common = proportion of variance in response variable explained by the predictor that is also explained by one or more other predictors. Wood density regressed on the full set of traits to obtain adjusted R^2, and on the parsimonious set of traits to obtain adjusted R^2 and $\boldsymbol{\beta}$. Predictor variables in parsimonious model are in bold.

		Commonality coefficients				**Adjusted R^2**	
						Parsimonious model	**Full model**
	Trait	**Unique**	**Common**	**Total**	**β**		
Juvenile wood density							
Cell morphology	**Fiber lumen area**[##]	**0.25**	**0.51**	**0.76**	**-0.12*** **	**0.78**	
	Fiber wall thickness	**0.01**	**0.45**	**0.46**	**0.04***		
	Vessel diameter	0.01	0.26	0.27			
	Vessel density	0.0001	0.24	0.24			**0.79**
Tissue fractions	**Fiber wall fraction**[#]	**0**	**0.80**	**0.80**	**0.29*** **	**0.83**	

	Fiber lumen fraction#	**0**	**0.52**	**0.52**	**-0.07****		
	Vessel fraction#	0	0.001	0.001			**0.83**
	Parenchyma fraction#	0	0.001	0.001			
Adult wood density							
Cell morphology	**Fiber lumen area##**	**0.27**	**0.46**	**0.73**	**-0.08*****	**0.78**	
	Fiber wall thickness	**0.03**	**0.48**	**0.51**	**0.05*****		
	Vessel diameter	0.01	0.18	0.19			
	Vessel density	0.01	0.09	0.10			**0.78**
Tissue fractions	**Fiber wall fraction#**	**0**	**0.81**	**0.81**	**0.25*****	**0.83**	
	Fiber lumen fraction#	**0**	**0.56**	**0.56**	**-0.05****		
	Vessel fraction#	0	0.02	0.02			**0.83**
	Parenchyma fraction#	0	0.02	0.02			

Asterisks indicate level of significance (* = 0.05; ** = 0.01; *** = 0.001).

Natural log transformed variables are indicated by the superscript ##.

Center log ratio transformed variables are indicated by the superscript #.

Table 4: Joint and unique variances for cell morphological traits and tissue fractions as drivers of variation in wood density derived from a variation partitioning analysis based on a multiple regression of the most parsimonious combination of traits that best predicts wood density (see Table 3).

	Traits	R^2
Juvenile wood density		
Unique variances	Cell morphology	0.003
	Tissue fractions	0.057***
Joined variances		0.772
Unexplained variance		0.168
Adult wood density		
Unique variances	Cell morphology	0.010˙
	Tissue fractions	0.064***
Joined variances		0.767
Unexplained variance		0.159

Asterisks indicate level of significance (˙= 0.1, * = 0.05; ** = 0.01; *** = 0.001).

Figures

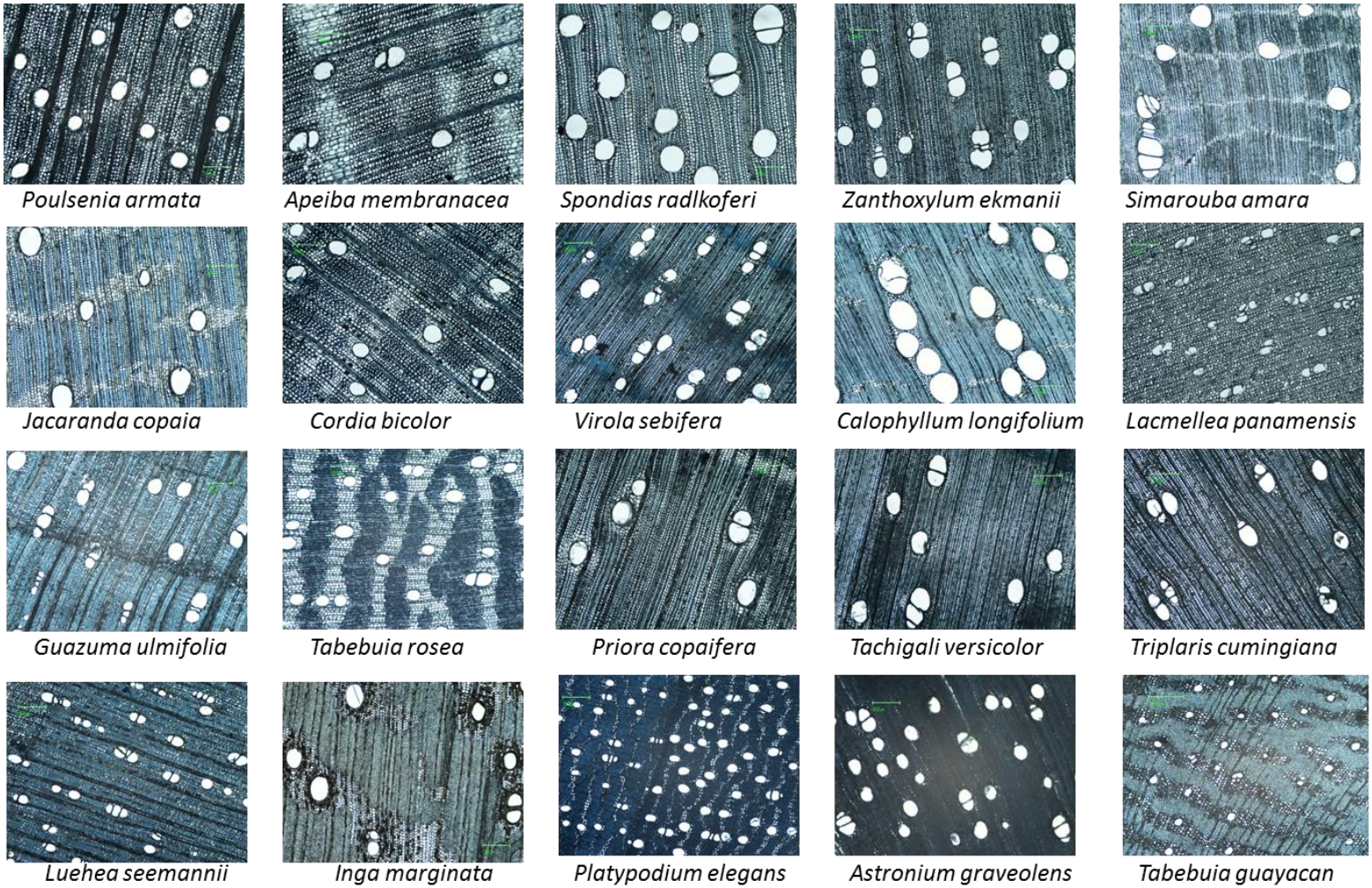

Figure 1: Images of transverse sections from wood of the twenty species examined (4x). Species arranged in order of increasing average wood density, left to right, top to bottom.

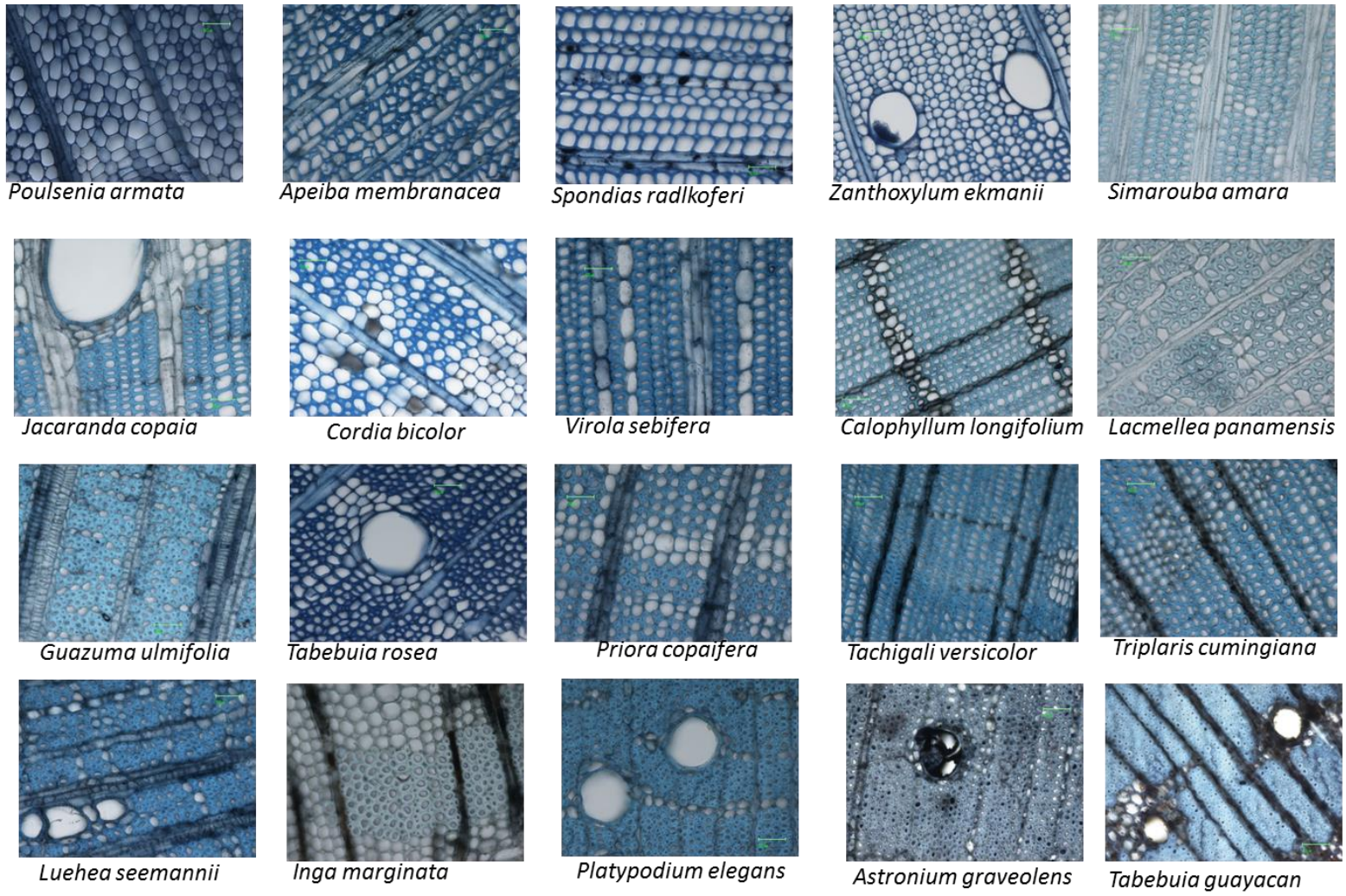

Figure 2: Images of transverse sections from wood of the twenty species examined (20x). Species arranged in order of increasing average wood density, left to right, top to bottom.

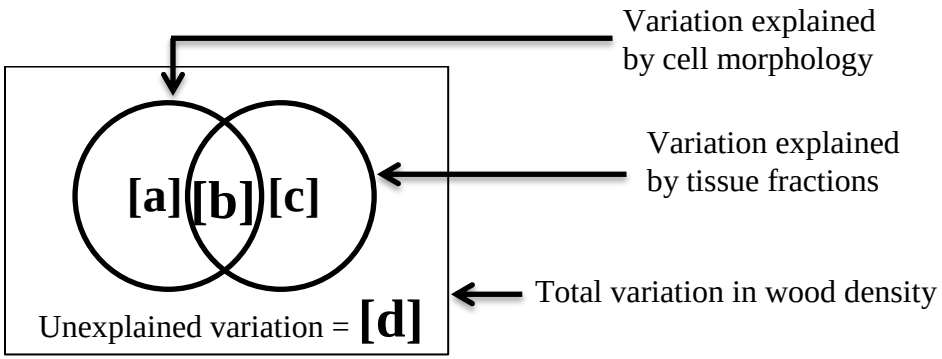

Figure 3: Venn diagram showing variation partitioning of a response variable between two sets of explanatory variables, cell morphology and tissue fractions. The rectangle represents the variation in the response variable, wood density. Fraction [a] and [c] are the unique variances explained by cell morphology and tissue fractions respectively, while [b] is the joined variance or the intersection of the amounts of variation explained by linear models for cell morphology and tissue fractions. Adapted from (Legendre 2008).

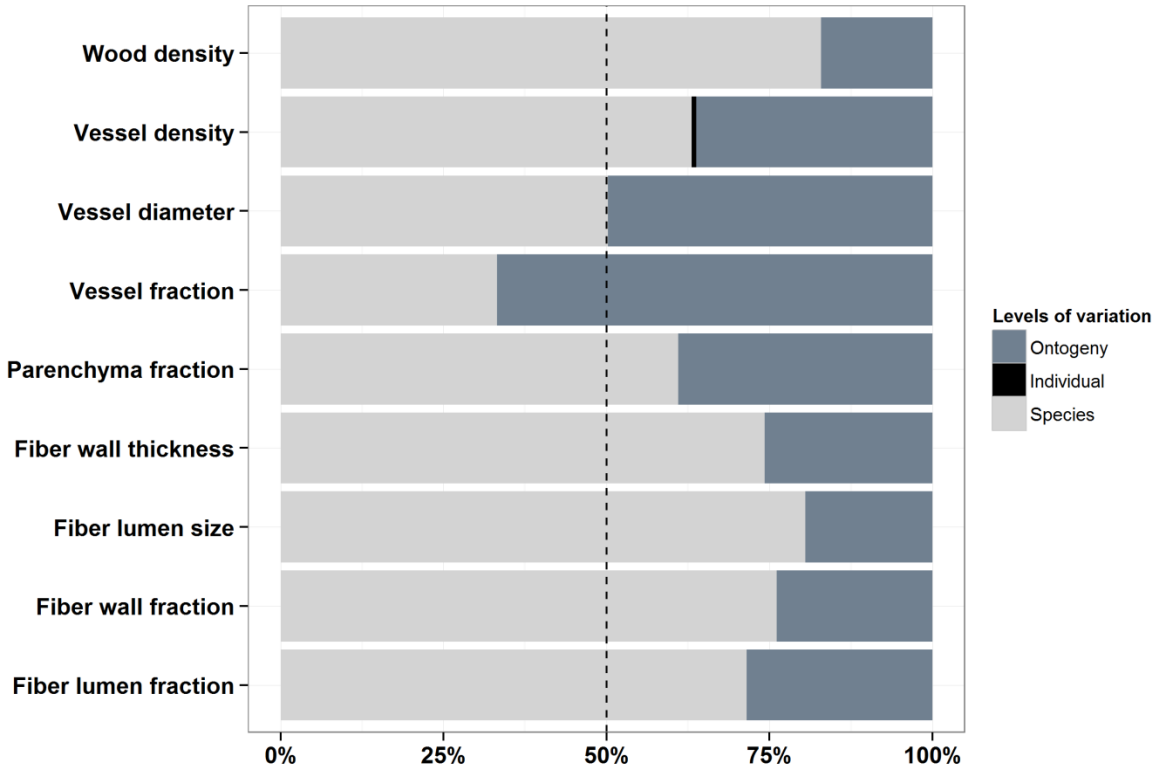

Figure 4: Proportion of variance explained by ontogeny, intraspecific, and interspecific levels of organization for eight anatomical traits and wood density.

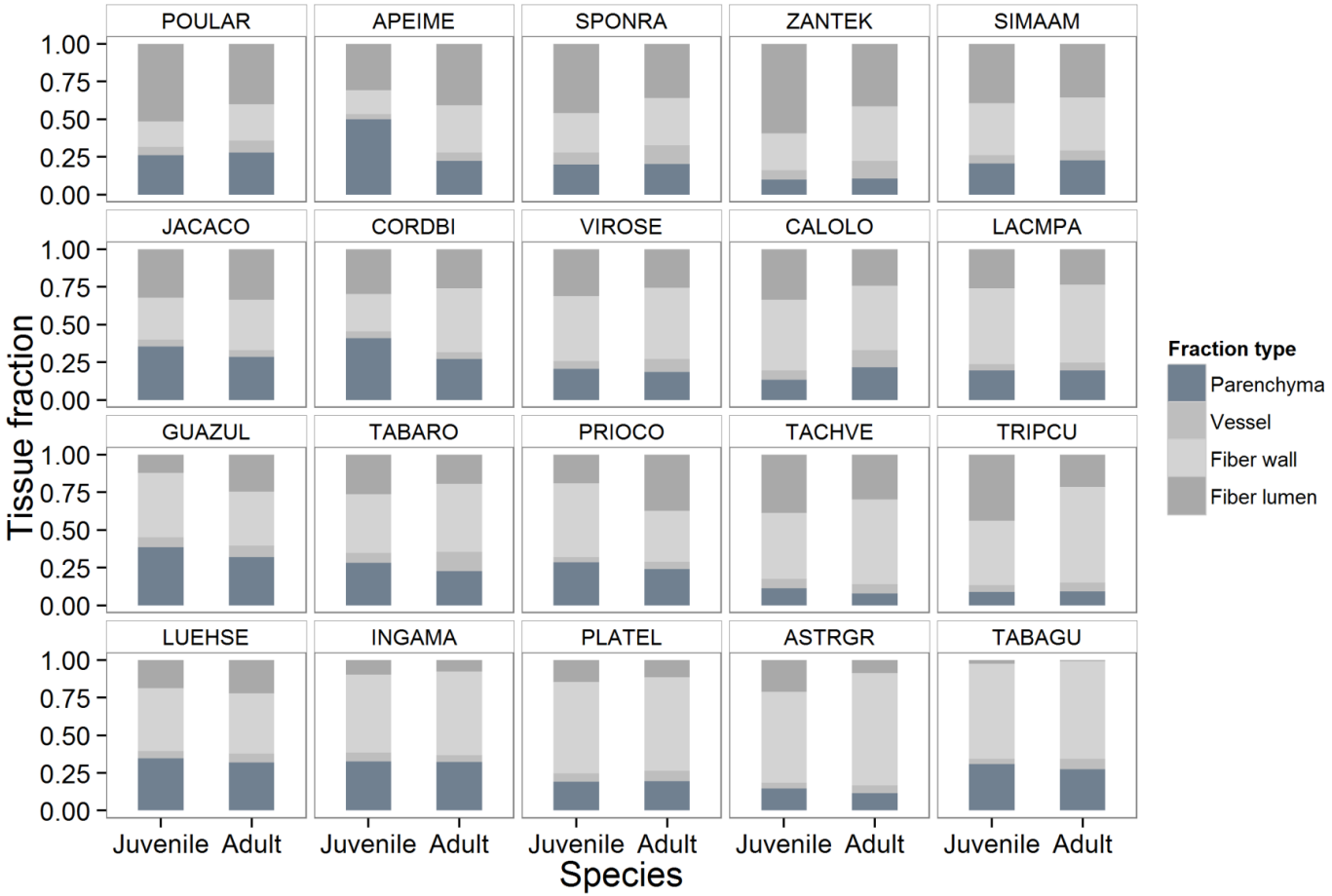

Figure 5: Ontogenetic differences in tissue fractions between juvenile and adult wood for each species. Species arranged in order of increasing average wood density, left to right, top to bottom. Each panel is labeled with a six letter acronym representing the first four letters of the genus and first two letters of the species binomial. See Fig. 1 or 2 for full binomial corresponding to each species acronym.

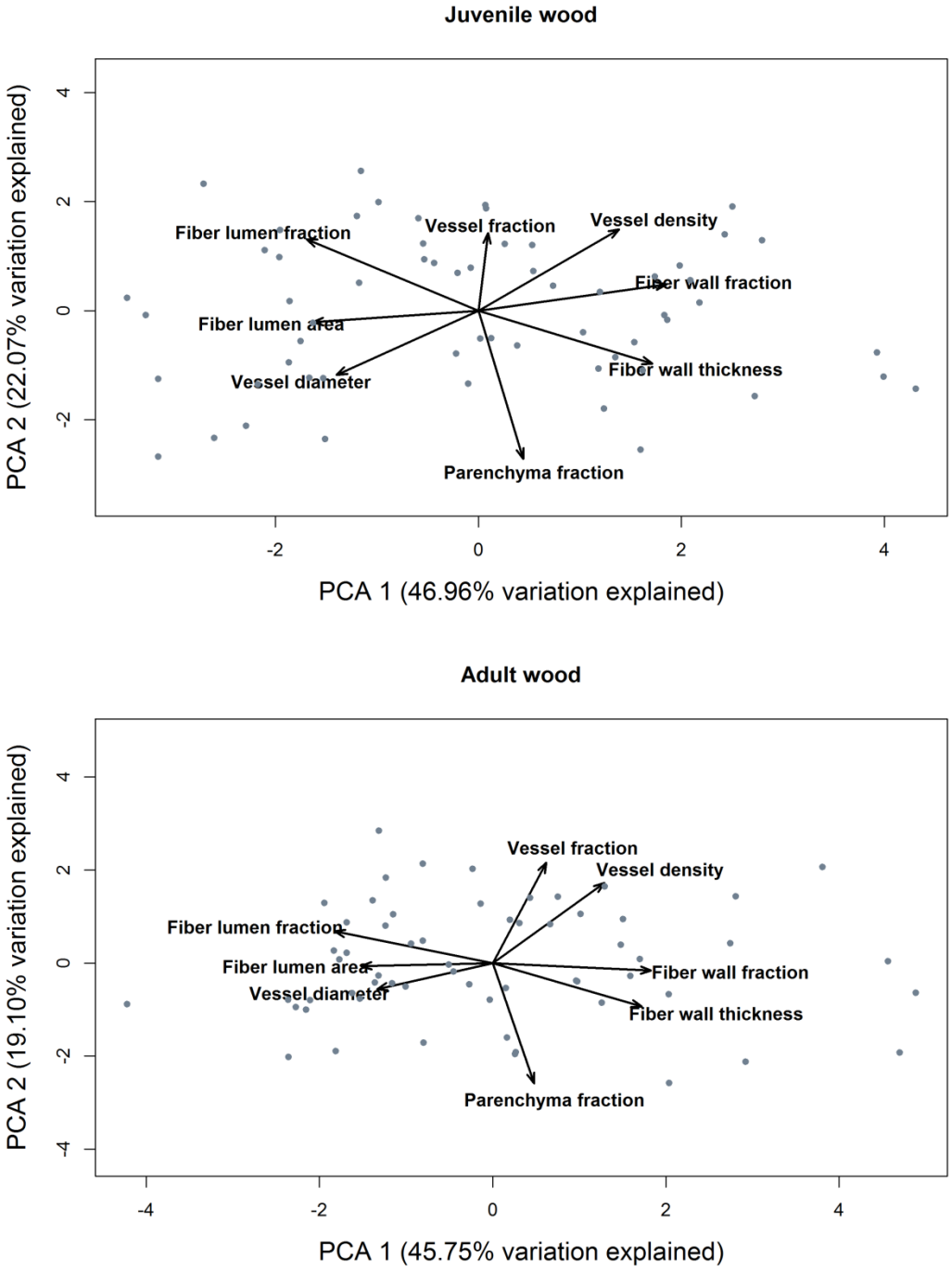

Figure 6: Principal component analyses showing relationships among wood traits for juvenile and adult wood.

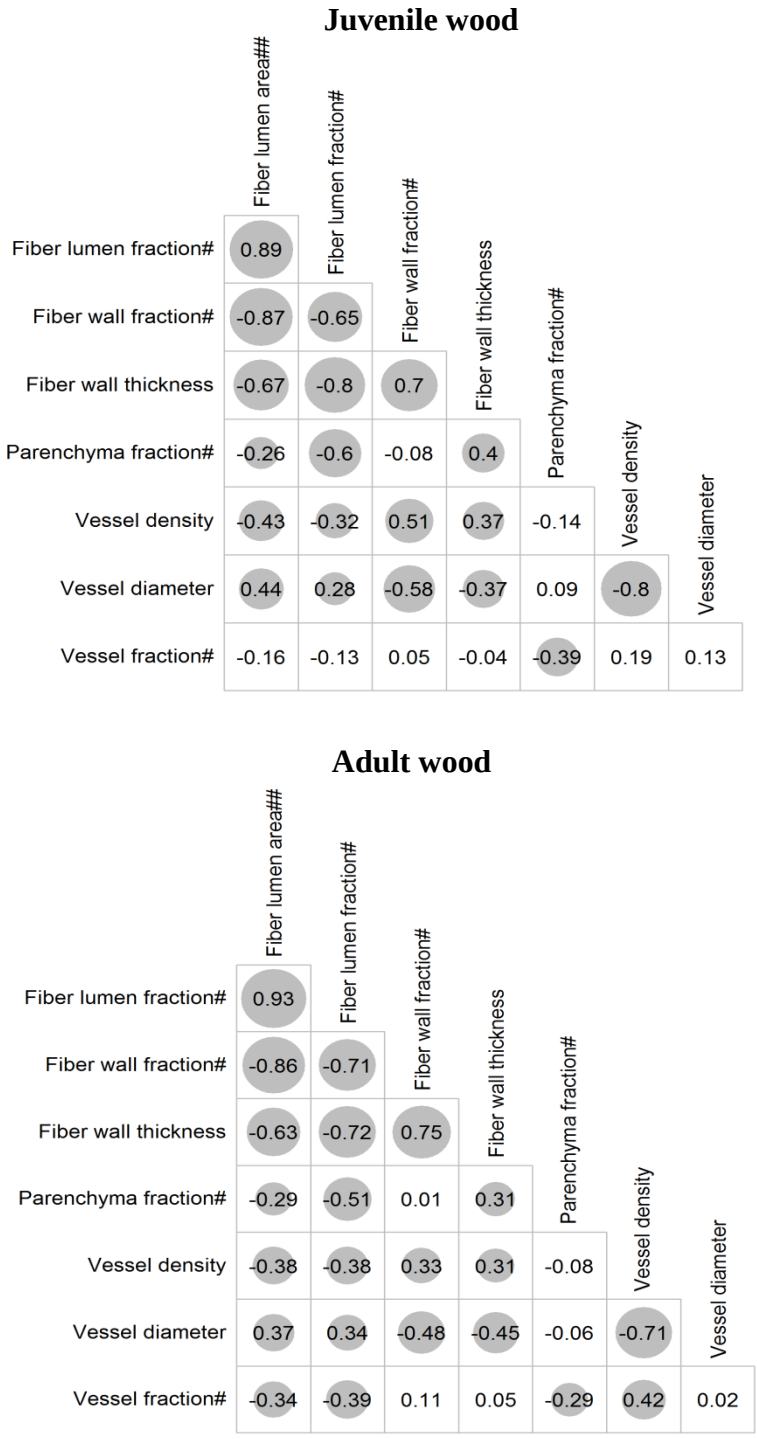

Figure 7: Bivariate correlations between pairs of anatomical traits. Centered log ratio transformation indicated by #, and natural log transformation indicated by ## in trait name. Presence of circle around correlation coefficient indicates correlation is significant at $P < 0.05$, and size of circle proportional to strength of correlation.

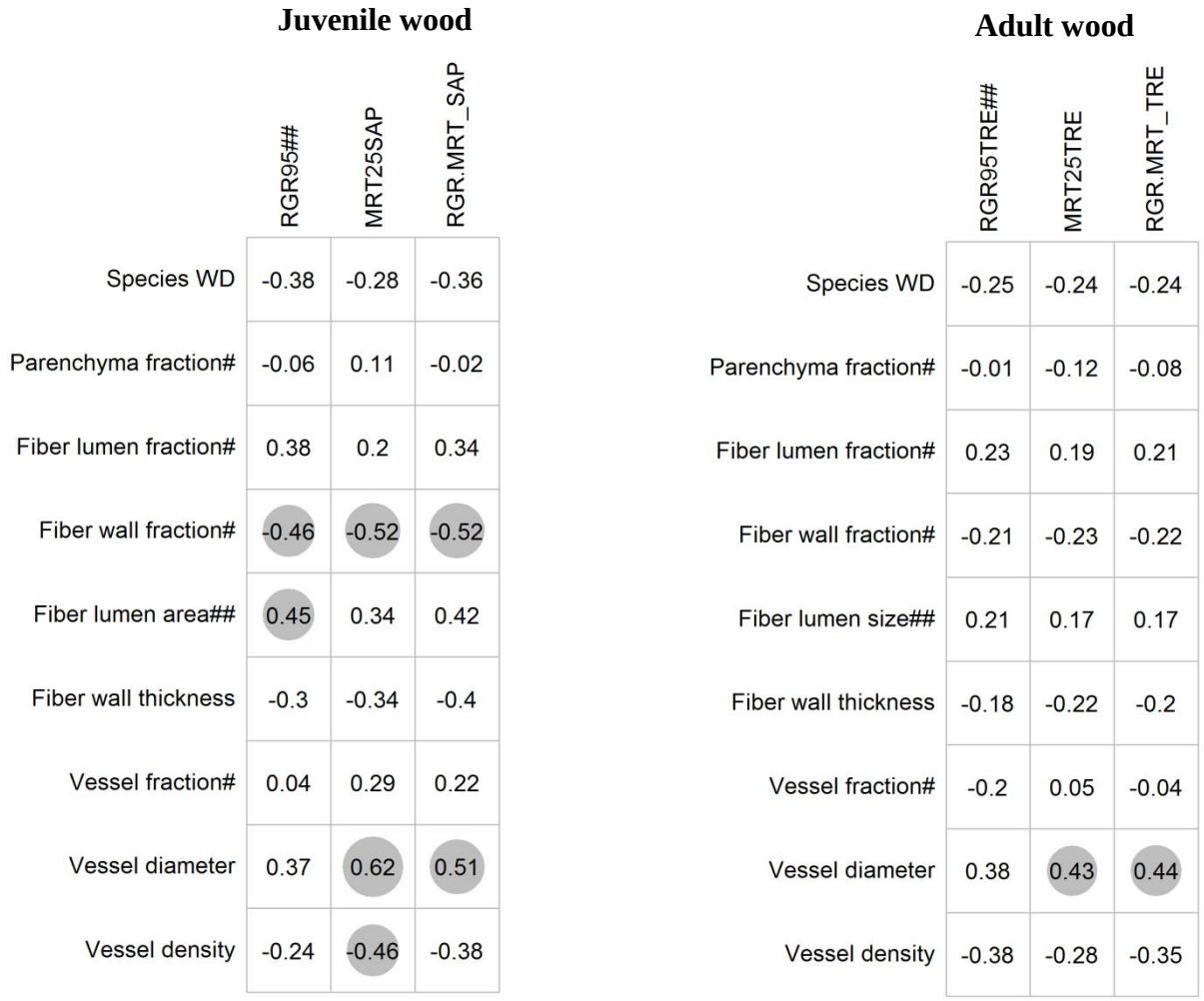

Figure 8: Associations between relative growth and mortality rates for saplings and juvenile wood density and anatomical traits, as well as between vital rates for large trees and adult wood density and anatomical traits. RGR_{95} = relative growth rates, MRT_{25} = mortality rates, RGR.MRT = linear combination of relative growth and mortality rates, SAP = saplings, and TRE = large trees. Centered log ratio transformation indicated by #, while natural log transformation indicated by ## in variable name. Presence of circle around correlation coefficient indicates correlation is significant, and size of circle proportional to strength of correlation. Juvenile wood correlations are significant at $P < 0.05$ while adult wood correlations are marginally significant at $P < 0.06$.

References

Aguilar-Rodríguez, S., Abundiz-Bonilla, L. & Barajas-Morales, J. (2001) Comparación de la gravedad específica y características anatómicas de la madera de dos comunidades vegetales en México. *Anales del Instituto de Biología, Universidad Autónoma de México, Serie Botánica* pp. 171–185.

Aitchison, J. (1983) Principal component analysis of compositional data. *Biometrika*, **70**, 57–65.

Auguie, B. (2012) *gridExtra: Functions in Grid Graphics*.

Borcard, D., Gillet, F. & Legendre, P. (2011) *Numerical Ecology with R*. Springer New York, New York, NY.

Brodribb, T.J. & Feild, T.S. (2000) Stem hydraulic supply is linked to leaf photosynthetic capacity: evidence from New Caledonian and Tasmanian rainforests. *Plant, Cell & Environment*, **23**, 1381–1388.

Carlquist, S. (2001) *Comparative Wood Anatomy*. Springer Berlin Heidelberg, Berlin, Heidelberg.

Carlquist, S. (2014) Fibre dimorphism: cell type diversification as an evolutionary strategy in angiosperm woods. *Botanical Journal of the Linnean Society*, **174**, 44–67.

Cavender-Bares, J. & Bazzaz, F.A. (2000) Changes in drought response strategies with ontogeny in Quercus rubra: implications for scaling from seedlings to mature trees. *Oecologia*, **124**, 8–18.

Chave, J., Coomes, D., Jansen, S., Lewis, S.L., Swenson, N.G. & Zanne, A.E. (2009) Towards a worldwide wood economics spectrum. *Ecology letters*, **12**, 351–366.

Choat, B., Jansen, S., Brodribb, T.J., Cochard, H., Delzon, S., Bhaskar, R., Bucci, S.J., Feild, T.S., Gleason, S.M., Hacke, U.G., Jacobsen, A.L., Lens, F., Maherali, H., Martínez-Vilalta, J., Mayr, S., Mencuccini, M., Mitchell, P.J., Nardini, A., Pittermann, J., Pratt, R.B., Sperry, J.S., Westoby, M., Wright, I.J. & Zanne, A.E. (2012) Global convergence in the vulnerability of forests to drought. *Nature*, **491**, 752–755.

Condit, R., Hubbell, S. & Foster, R. (1995) Mortality rates of 205 Neotropical tree and shrub species and the impact of a severe drought. *Ecological Monographs*, **65**, 419–439.

Cornwell, W.K., Cornelissen, J.H.C., Allison, S.D., Bauhus, J., Eggleton, P., Preston, C.M., Scarff, F., Weedon, J.T., Wirth, C. & Zanne, A.E. (2009) Plant traits and wood fates across the globe: rotted, burned, or consumed? *Global Change Biology*, **15**, 2431–2449.

Curran, J.M. (2013) Hotelling: Hotelling's T-squared test and variants. URL http://cran.r-project.org/web/packages/Hotelling/index.html [accessed 14 February 2015]

Diedenhofen, B. & Diedenhofen, M.B. (2015) Package 'cocor'. URL http://cran.stat.nus.edu.sg/web/packages/cocor/cocor.pdf [accessed 10 March 2015]

Evert, R.F. (2006) Xylem: Cell Types and Developmental Aspects. *Esau's Plant Anatomy* pp. 255–290. John Wiley & Sons, Inc.

Fan, Z.-X., Zhang, S.-B., Hao, G.-Y., Ferry Slik, J. w. & Cao, K.-F. (2012) Hydraulic conductivity traits predict growth rates and adult stature of 40 Asian tropical tree species better than wood density. *Journal of Ecology*, **100**, 732–741.

Feeley, K.J., Davies, S.J., Perez, R., Hubbell, S.P. & Foster, R.B. (2011) Directional changes in the species composition of a tropical forest. *Ecology*, **92**, 871–882.

Fortunel, C., Ruelle, J., Beauchêne, J., Fine, P.V.A. & Baraloto, C. (2014) Wood specific gravity and anatomy of branches and roots in 113 Amazonian rainforest tree species across environmental gradients. *New Phytologist*, **202**, 79–94.

Gärtner, H., Lucchinetti, S. & Schweingruber, F.H. (2014) New perspectives for wood anatomical analysis in dendrosciences: The GSL1-microtome. *Dendrochronologia*, **32**, 47–51.

Hacke, U.G., Sperry, J.S., Pockman, W.T., Davis, S.D. & McCulloh, K.A. (2001) Trends in wood density and structure are linked to prevention of xylem implosion by negative pressure. *Oecologia*, **126**, 457–461.

Jacobsen, A.L., Agenbag, L., Esler, K.J., Pratt, R.B., Ewers, F.W. & Davis, S.D. (2007) Xylem density, biomechanics and anatomical traits correlate with water stress in 17 evergreen shrub species of the Mediterranean-type climate region of South Africa. *Journal of Ecology*, **95**, 171–183.

Jacobsen, A.L., Ewers, F.W., Pratt, R.B., Paddock, W.A. & Davis, S.D. (2005) Do xylem fibers affect vessel cavitation resistance? *Plant Physiology*, **139**, 546–556.

Keating, R. (2014) *Preparing Plant Tissue for Light Microscopic Study: A Compendium of Simple Techniques, MSB 130*. Missouri Botanical Garden Press.

Kraha, A., Turner, H., Nimon, K., Zientek, L.R. & Henson, R.K. (2012) Tools to support interpreting multiple regression in the face of multicollinearity. *Frontiers in Psychology*, **3**.

Lachenbruch, B. & McCulloh, K.A. (2014) Traits, properties, and performance: how woody plants combine hydraulic and mechanical functions in a cell, tissue, or whole plant. *The New Phytologist*, **204**, 747–764.

Lachenbruch, B., Moore, J.R. & Evans, R. (2011) Radial variation in wood structure and function in woody plants, and hypotheses for its occurrence. *Size- and Age-Related Changes in Tree Structure and Function* (eds F.C. Meinzer, B. Lachenbruch & T.E. Dawson), pp. 121–164. Springer Netherlands, Dordrecht.

Legendre, P. (2008) Studying beta diversity: ecological variation partitioning by multiple regression and canonical analysis. *Journal of Plant Ecology*, **1**, 3–8.

Martinez-Cabrera, H.I., Jones, C.S., Espino, S. & Schenk, H.J. (2009) Wood anatomy and wood density in shrubs: responses to varying aridity along transcontinental transects. *American Journal of Botany*, **96**, 1388–1398.

Martínez-Cabrera, H.I., Schenk, H.J., Cevallos-Ferriz, S.R.S. & Jones, C.S. (2011) Integration of vessel traits, wood density, and height in angiosperm shrubs and trees. *American Journal of Botany*, **98**, 915–922.

MBF BIOSCIENCE. (2015) Counting Rules | Number | Stereology Information Center. URL http://www.stereology.info/counting-rules/ [accessed 21 February 2015]

Nimon, K. (2010) Regression commonality analysis: demonstration of an SPSS solution. *Multiple Linear Regression Viewpoints*, **36**, 10–17.

Nimon, K., Oswald, F. & Roberts, and J.K. (2013) yhat: Interpreting Regression Effects. URL http://cran.r-project.org/web/packages/yhat/index.html [accessed 4 March 2015]

Oksanen, J., Blanchet, G.F., Kindt, R., Legendre, P., Minchin, P.R., O'Hara, R.B., Simpson, G.L., Solymos, P., Stevens, M.H.H. & Wagner, H. (2015) vegan: Community Ecology Package. URL http://cran.r-project.org/web/packages/vegan/index.html [accessed 14 February 2015]

Osazuwa-Peters, O.L., Wright, S.J. & Zanne, A.E. (2014) Radial variation in wood specific gravity of tropical tree species differing in growth-mortality strategies. *American Journal of Botany*, **101**, 803–811.

Osazuwa-Peters, O.L., Zanne, A.E. & PrometheusWiki contributors. (2011) PrometheusWiki | Wood density protocol. URL http://prometheuswiki.publish.csiro.au/tiki-index.php?page=Wood+density+protocol [accessed 22 October 2013]

Poorter, L., McDonald, I., Alarcón, A., Fichtler, E., Licona, J.-C., Peña-Claros, M., Sterck, F., Villegas, Z. & Sass-Klaassen, U. (2010) The importance of wood traits and hydraulic conductance for the performance and life history strategies of 42 rainforest tree species. *New Phytologist*, **185**, 481–492.

Pratt, R.B., Jacobsen, A.L., Ewers, F.W. & Davis, S.D. (2007) Relationships among xylem transport, biomechanics and storage in stems and roots of nine Rhamnaceae species of the California chaparral. *The New Phytologist*, **174**, 787–798.

Preston, K.A., Cornwell, W.K. & DeNoyer, J.L. (2006) Wood density and vessel traits as distinct correlates of ecological strategy in 51 California coast range angiosperms. *New Phytologist*, **170**, 807–818.

Putz, F.E., Coley, P.D., Lu, K., Montalvo, A. & Aiello, A. (1983) Uprooting and snapping of trees: structural determinants and ecological consequences. *Canadian Journal of Forest Research*, **13**, 1011–1020.

Ray-Mukherjee, J., Nimon, K., Mukherjee, S., Morris, D.W., Slotow, R. & Hamer, M. (2014) Using commonality analysis in multiple regressions: a tool to decompose

regression effects in the face of multicollinearity (ed S Nakagawa). *Methods in Ecology and Evolution*, **5**, 320–328.

R Core Team. (2014) R: A language and environment for statistical computing. URL http://www.r-project.org/ [accessed 14 February 2015]

Read, J. & Stokes, A. (2006) Plant biomechanics in an ecological context. *American Journal of Botany*, **93**, 1546–1565.

Roque, R.M. & Tomazelo-Filho, M. (2007) Relationship between anatomical features and intra-ring wood density profiles in Gmelina arborea applying x-ray densitometry. *Cerne (Brazil)*.

Russo, S.E., Jenkins, K.L., Wiser, S.K., Uriarte, M., Duncan, R.P. & Coomes, D.A. (2010) Interspecific relationships among growth, mortality and xylem traits of woody species from New Zealand: tree growth, mortality and woody traits. *Functional Ecology*, **24**, 253–262.

Sperry, J.S., Meinzer, F.C. & McCulloh, K.A. (2008) Safety and efficiency conflicts in hydraulic architecture: scaling from tissues to trees. *Plant, Cell & Environment*, **31**, 632–645.

Stephenson, N.L., van Mantgem, P.J., Bunn, A.G., Bruner, H., Harmon, M.E., O'Connell, K.B., Urban, D.L. & Franklin, J.F. (2011) Causes and implications of the correlation between forest productivity and tree mortality rates. *Ecological Monographs*, **81**, 527–555.

Taylor, A.M., Gartner, B.L. & Morrell, J.J. (2002) Heartwood formation and natural durability - a review. *Wood and Fiber Science*, **34**, 587 – 611.

Thomas, S.C. & Winner, W.E. (2002) Photosynthetic differences between saplings and adult trees: an integration of field results by meta-analysis. *Tree Physiology*, **22**, 117–127.

Webb, C.O. & Peart, D.R. (2000) Habitat associations of trees and seedlings in a Bornean rain forest. *Journal of Ecology*, **88**, 464–478.

Wei, T. (2013) corrplot: Visualization of a correlation matrix. URL http://cran.r-project.org/web/packages/corrplot/index.html [accessed 14 February 2015]

Westoby, M., Falster, D.S., Moles, A.T., Vesk, P.A. & Wright, I.J. (2002) Plant Ecological Strategies: Some Leading Dimensions of Variation between Species. *Annual Review of Ecology and Systematics*, **33**, 125–159.

Wickham, H. & Chang, W. (2014) *ggplot2: An Implementation of the Grammar of Graphics*.

Williamson, G.B. & Wiemann, M.C. (2010) Measuring wood specific gravity...Correctly. *American Journal of Botany*, **97**, 519–524.

Woodcock, D. & Shier, A. (2002) Wood specific gravity and its radial variations: the many ways to make a tree. *Trees*, **16**, 437–443.

Wright, S.J., Kitajima, K., Kraft, N.J.B., Reich, P.B., Wright, I.J., Bunker, D.E., Condit, R., Dalling, J.W., Davies, S.J., Díaz, S., Engelbrecht, B.M.J., Harms, K.E.,

Hubbell, S.P., Marks, C.O., Ruiz-Jaen, M.C., Salvador, C.M. & Zanne, A.E. (2010) Functional traits and the growth–mortality trade-off in tropical trees. *Ecology*, **91**, 3664–3674.

Zanne, A.E., Westoby, M., Falster, D.S., Ackerly, D.D., Loarie, S.R., Arnold, S.E.J. & Coomes, D.A. (2010) Angiosperm wood structure: Global patterns in vessel anatomy and their relation to wood density and potential conductivity. *American Journal of Botany*, **97**, 207–215.

Zheng, J. & Martínez-Cabrera, H.I. (2013) Wood anatomical correlates with theoretical conductivity and wood density across China: evolutionary evidence of the functional differentiation of axial and radial parenchyma. *Annals of Botany*, **112**, 927–935.

Zieminska, K., Butler, D.W., Gleason, S.M., Wright, I.J. & Westoby, M. (2013) Fibre wall and lumen fractions drive wood density variation across 24 Australian angiosperms. *AoB PLANTS*, **5**, plt046–plt046.

Supporting information for chapter 2

Appendix 1: Decomposing fiber fraction at tissue level to fiber wall fraction and fiber lumen fraction.

Assumption: Fiber cells are rectangular in shape to satisfy the observation that fiber cells lack intercellular spaces.

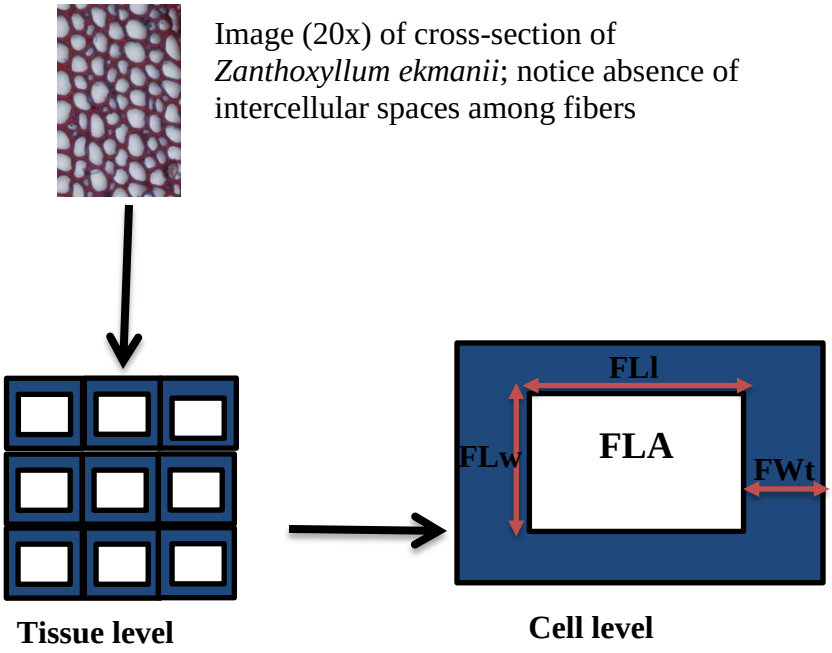

Appendix Figure 1: Conceptual representation of assumption and variables for decomposing fiber fraction at tissue level into fiber wall and fiber lumen fractions. See text below for meaning of acronyms.

Measured variables: At the level of a fiber cell, measures available included fiber lumen area (FLA), fiber lumen length (FLl), and cell wall thickness (FWt).

Variables estimated at cell level:

Fiber lumen width (FLw) was estimated as FLA divided by FLl.

$$FLw = \frac{FLA}{FLl} \quad \text{Eq. 1}$$

Fiber wall area (FWA) was then computed using the equation:

$$FWA = (4 * FWt^2 + 2 * (FLw + FLl) * FWt \quad \text{Eq. 2}$$

Fiber wall fraction equaled the ratio of FWA to total fiber area (sum of FWA and FLA).

$$Fiber\ wall\ fraction = \frac{FWA}{FWA+FLA} \quad \text{Eq. 3}$$

Similarly fiber lumen fraction equaled the ratio of FLA to total fiber area.

$$Fiber\ lumen\ fraction = \frac{FLA}{FWA+FLA} \quad \text{Eq. 4}$$

At the tissue level, total fraction of fiber was decomposed into fraction of fiber wall and fraction of fiber lumen by multiplying each fraction (i.e. fiber wall fraction, and fiber lumen fraction at the level of a fiber cell) by the independent measure of fiber fraction at the tissue level.

Chapter 3

Selective logging: does the imprint remain on tree structure and composition after 45 years?

Oyomoare L. Osazuwa-Peters[1], Colin A. Chapman[2] and Amy E. Zanne

[1]Department of Biology, One University Boulevard, University of Missouri-St. Louis, St. Louis, Missouri, 63121, USA

[2] Department of Anthropology and School of Environment, McGill University, Montreal, Quebec, H3A 2T7, Canada and Wildlife Conservation Society, Bronx, New York

[3]Department of Biological Sciences, 2023 G St. NW, The George Washington University, Washington DC, 20052, USA

As published in:

Osazuwa-Peters, O. L., Chapman, C. A., and Zanne, A. E. 2015. Selective logging: does the imprint remain on tree structure and composition after 45 years? *Conservation Physiology*

Abstract

Selective logging of tropical forests is increasing in extent and intensity. The duration over which impacts of selective logging persist however remains an unresolved question particularly for African forests. Here, we investigate the extent to which a past selective logging event continues to leave its imprint on different components of an East African forest 45 years later. We inventoried 2358 stems ≥ 10 cm diameter in 26 plots (200 x 10 m) within a 5.2 ha area in Kibale National Park (KNP), Uganda, in logged and unlogged forest. In these surveys, we characterized the forest light environment, taxonomic composition, functional trait composition using three traits ─ wood density, maximum height, and maximum diameter, and forest structure based on three measures ─ stem density, total basal area, and total aboveground (AGB) biomass. Selectively logged forest plots in KNP on average had higher light levels, different structure characterized by lower stem density, lower total basal area, and lower aboveground biomass, as well as a distinct taxonomic composition driven primarily by changes in species' relative abundance, than unlogged forests. Conversely, selectively logged forest plots were like unlogged plots in functional composition having similar community weighted mean values for wood density, maximum height and maximum diameter. This similarity in functional composition irrespective of logging history may be due to functional recovery of logged forest or background changes in functional attributes of unlogged forest. Despite the passage of 45 years, the legacy of selective logging on the tree community in KNP is still evident as indicated by distinct taxonomic and structural composition, and reduced carbon storage in logged, as compared to unlogged forests. The effects of

selective logging are exerted via influences on tree demography rather than functional trait composition.

Key words: Functional traits; historical logging event; Kibale National Park; light intensity; wood density

Introduction

Selective logging, the targeted harvesting of commercially valuable timber species in a single cutting cycle, is an increasingly important component of the human footprint on tropical forests; its extent and intensity are on the rise (Asner *et al.*, 2009; Gibson *et al.*, 2011). According to recent estimates, at least 390 million ha of tropical humid forests were selectively logged as of 2009 (Asner *et al.*, 2009), an area slightly larger than the size of India. These estimates are likely to be conservative because clandestine selective logging operations are extensive and largely undocumented. For example, more than half of the timber harvested from five major timber producing countries (Brazil, Cameroon, Ghana, Indonesia, and Malaysia) was illegally extracted in 2009 (Rands *et al.*, 2010). Selective logging is likely expanding due to rising global demands for timber products, providing large revenues for developing economies (Gibson *et al.*, 2011; Putz *et al.*, 2012).

The current prevalence and potential for continued expansion of selective logging has led to a call to better understand its impacts on tropical forests, particularly in terms of biodiversity conservation and carbon sequestration (Picard *et al.*, 2012). Several recent studies argue that its impacts are relatively benign in comparison to other uses of forests and selectively logged tropical forests have a high conservation value second only to

pristine tropical forests (Gibson *et al.*, 2011; Putz *et al.*, 2012; Ramage *et al.*, 2013). However, selective logging has known immediate impacts on the taxonomic, structural, and functional aspects of tropical forests. Taxonomically, selective logging can shift the composition and relative abundance of species (Baraloto *et al.*, 2012) including reducing species richness (Clark and Covey, 2012) and shifting the dominance of particular lineages (Berry *et al.*, 2010; Okuda *et al.*, 2003). Structural effects of selective logging include homogenizing canopy structure (Okuda *et al*., 2003), reducing stem density (Cannon *et al.*, 1998; Slik *et al.*, 2002; Hall *et al.*, 2003) and total basal area (Bonnell *et al.*, 2011), and losing large trees with a shift towards medium sized trees (Okuda *et al*., 2003; Bonnell *et al.*, 2011), consequently reducing aboveground biomass (Lasco *et al.*, 2006; Blanc *et al.*, 2009; Berry *et al.*, 2010; Lindner and Sattler, 2012). Lastly, the effect of selective logging on the capacity of tropical forests to maintain ecosystem function has been examined through characterizing shifts in dominance of pre-defined functional groups centered on plant attributes such as shade tolerance (Hall *et al.*, 2003), successional status (Bonnell *et al.*, 2011), or wood strength (Verburg and van Eijk-Bos, 2003). A handful of studies have used a more explicit continuous trait-based approach to demonstrate that tree communities respond to disturbance from selective logging by shifts in the range of functional trait values found in the community (Baraloto *et al.*, 2012; Carreño-Rocabado *et al.*, 2012; Mayfield *et al.*, 2010; Mouillot *et al.*, 2013)

Less clear than the immediate impacts of selective logging on tropical forests is the duration over which these impacts persist, given that trees are long lived and most studies are conducted within the first two decades after logging (Gibson *et al.*, 2011; Kormos and Zimmerman, 2014). Gibson *et al.* (2011) also highlight a regional bias in the tropical

land-use change literature, most of which focuses on Southeast Asian and Neotropical forests, with few studies in Africa. Yet, African forests differ from other tropical forests in several ways including having older soils (Richards, 1996), a smaller regional species pool (Richards, 1996; Chapman *et al.*, 1999), and historically fewer and smaller disturbances (Chapman *et al.*, 1999). The degree of logging damage in Africa is relatively lower than Southeast Asia and higher than the Neotropics (Picard *et al.*, 2012). To develop a comprehensive understanding of the long-term impacts of selective logging on the conservation value of tropical forests, we need more empirical studies exploring long-term effects on selectively logged African forests.

Here, we investigate the extent to which impacts of selective logging performed 45 years ago persist in an East African forest. We hypothesize that recovery from disturbance will be slow, such that imprints of selective logging will still be evident on the taxonomic, structural and functional components after almost half a century. We consider effects on understory light availability and community structural, taxonomic and functional composition. Understory light is strongly influenced by forest canopy structure-, and typically differs between old-growth and disturbed forests because their canopies are open to varying extents (Nicotra *et al.*, 1999). These different light conditions tend to favor different combinations of functional traits or ecological strategies, such that disturbed forests may be dominated by species with resource-acquisitive or disturbance-adapted strategies, leading additionally to taxonomic and structural differences. To capture such differences in functional composition between species in logged and unlogged plots, we focused on three traits. Wood density (WD; g/cm^3), a measure of a tree's dry carbon investment per unit volume, is a key indicator of the wood economic

spectrum due to its strong connection with several aspects of a plant's ecology including growth rate, carbon allocation, structural stability, hydraulic conductivity, and disease or pest resistance (Chave *et al*., 2009). The other two traits, plant maximum height (H_{MAX}; m) and maximum diameter at breast height (DBH_{MAX}; cm), are crucial components of a species' light competitive ability and carbon gain strategy (King *et al.*, 2006; Wright *et al.*, 2007; Moles *et al.*, 2009). Both WD and adult stature vary with species' light requirements and along a successional continuum (Chave *et al.*, 2009; Falster and Westoby, 2005).

We predict logged forest will have a (I) more open canopy and higher light levels (II) greater stem density, but less total basal area and aboveground biomass because higher light conditions will favor recruitment of more stems per unit area and unlogged forest will have more large trees (III) distinct tree size distribution with a relatively high frequency of mid-sized trees compared to the typical 'reverse J-shaped' tree size distributions for old-growth unlogged forest (Denslow, 1995) (IV) distinct taxonomic and functional composition since it is at an earlier stage of succession and dominated by species with a resource acquisitive strategy, whereas unlogged forests will be dominated by species with a resource conservative strategy. Prediction IV implies that logged forests will have lower community-weighted mean values for WD, H_{MAX}, and DBH_{MAX} compared to unlogged forest.

Materials and methods

Study site

This study was conducted in Kibale National Park (KNP; 795 km^2) in south-western Uganda (Chapman *et al.*, 2010a). It is composed predominantly of mature moist semi-deciduous and evergreen forest, but includes a variety of other habitats including grassland, woodland, lakes and wetlands, colonizing forest, and regrowth in areas previously planted with exotic trees (Chapman and Lambert, 2000). KNP receives an average of 1643 mm rainfall annually (1990 – 2013; Chapman and Chapman unpublished data collected at Makerere University Biological Field Station) with two rainy seasons from March to May and September to November (Chapman *et al.*, 2010a). Temperature ranges between a mean daily minimum of 15.5^{o}C and maximum of 23.7^{o}C. KNP is divided into compartments which were subjected to varying degrees of logging and have experienced different restoration efforts (Struhsaker, 1997; Chapman *et al.*, 2010a). Our study involved three compartments within KNP; i. K-30 (282 ha) is relatively disturbance free in recorded history, at least from humans, and is typically considered a mature old-growth forest, ii. K-14 (405 ha) was selectively logged between May and December 1969, but in a spatially heterogeneous manner, so that some areas (Mikana) experienced heavy logging with the removal and damage of up to 25% of all trees, while other areas were largely untouched (lightly logged areas), and iii. K-15 (347 ha) experienced high intensity selective logging between September 1968 and April 1969 resulting in removal and damage of up to 50% of all trees. All of these compartments have been classified as *Parinari* forest (Osmaston, 1959), are located closely together (within 1500 m), and prior

to logging exhibited high levels of structural similarity in cumulative basal area, canopy cover, and stem density (Kingston, 1967; Bonnell *et al.*, 2011).

Vegetation plots

Twenty-six permanent vegetation plots were randomly established within the existing trail system in KNP in December 1989. Each plot is 200 x 10 m, with a trail running down the middle of its length. The locations of the 26 plots were unevenly distributed across the three compartments: 11 plots were located in K-30, six were in the lightly logged areas and four were in the heavily logged (Mikana) parts of K-14, and five were in K-15. In this study, we assigned the 17 plots in K-30 and the lightly logged areas of K-14 to the unlogged plot category, while the 9 plots in the Mikana part of K-14 and in K-15 were assigned the logged category. The addition of plots in the lightly logged areas of K-14 to the unlogged plot category is informed by earlier works that established that the lightly logged forest suffered little damage from the logging event based on stump and gap enumeration (Kasenene, 1987; Chapman and Chapman, 1997; Bonnell *et al.*, 2011).

Data collection

a. Forest light intensity conditions

For 10 focal plots (five randomly selected from the 17 unlogged and five randomly selected from the 9 logged plots), light was measured from June – August 2011 between 9 a.m. and 2 p.m. Light intensity was measured on both sides of each plot extending from the dividing trail in the middle. Measures were taken at 10 m intervals underneath the forest canopy at 2 m above ground level as photo-synthetically active radiation (PAR) using a LI250 light meter and an LI-190SA quantum sensor (Licor, Lincoln, NE). This

photosynthetically active radiation was expressed relative to open light conditions, which were concurrently measured in the open at the Makerere University Biological Field Station using a HOBO light intensity data logger. This resulted in 42 light intensity measures per plot.

b. Forest composition and structure

All 26 plots were surveyed between March and May 2013. Surveys of each plot involved recording the DBH for all tree stems with DBH ≥10 cm (Chapman *et al.*, 2010a). Trees were identified using recognized taxonomic keys (Polhill, 1952; Hamilton, 1991; Katende *et al.*, 1995; Lwanga, 1996), and species names were updated using The Plant List (http://www.theplantlist.org/). Voucher specimens for all trees were given to Makerere University Biological Field Station and new specimens are currently being collected for the field stations' new herbarium. The resulting dataset contains information on stem number, species composition, and species relative abundances for each plot.

c. Species' functional traits

For the same 10 plots used for forest light intensity conditions, we measured WD and height for all species between June and August 2011. While many species found in the 10 focal plots were also found in the remaining 16 plots, this trait dataset excluded rare species which although present in one or more of the 26 vegetation plots did not occur in the focal plots. Field measured WD was available for only 60 species, height data for 58 species, and DBH for all 86 species in the 2013 census.

Diameter at breast height: tree trunk diameter was measured at 1.3 m above ground level for all stems ≥ 10 cm in the 26 plots during the 2013 census of vegetation plots. Species

DBH_{MAX} was the largest DBH value recorded of all individuals of a species in these 26 plots.

Wood density: wood samples were extracted at 1.3 m above ground level with a 12″ increment borer from up to 5 (or fewer when not available) upright adult individuals per species within each of the 10 focal plots (for a total of 687 trees). Extracted wood cores ranged from 4 – 8 cm in length, and each core was broken into 2 cm segments with the number of segments dependent on the length of the core. For each segment, fresh volume was determined using the water displacement method, and dry mass was determined after oven drying to constant mass at 105^{o}C (Osazuwa-Peters *et al.*, 2011). Wood density for each segment was computed as dry mass divided by fresh volume, and averaged over all segments that made up a core to determine a mean WD per tree. Species mean WD was then calculated as the average WD value of all individuals of a species pooled across the focal 10 plots. To obtain estimates for the remaining 26 unmeasured species found in the 16 non-focal plots, we obtained species-, genus-, or family-level (depending on availability) WD averages from the Global Wood Density database subset to African region only (Zanne *et al.*, 2009). This African-region subset of the Global Wood Density Database contained wood density values for 6 of the missing species, as well as genus-level wood density values for 9 species and family-level wood density values for the remaining 11 species.

Tree height: Height was measured as the distance between the base and top of a tree for ≥ 5 (or fewer when unavailable) healthy adult individuals per species within each focal plot using a vertex hypsometer (Vertex IV, Haglöf Sweden). Height values were obtained for 892 trees in the ten plots. A species' maximum height was then determined as the greatest

height recorded across all individuals of a species (King *et al.*, 2006) from the pool of the 10 plots. DBH measures were available for 622 of the 892 stems with height data. Height was regressed on DBH for this subset to obtain a forest-wide regression that was then used to interpolate height for species with DBH but missing height values. The regression (R^2 = 0.31, P < 0.01) relationship was as follows:

$$\widehat{H_{MAX}} = 9.753326 + (0.052898 * DBH_{MAX}) \quad \text{Eq. (1)}$$

This relationship was used to predict H_{MAX} from species DBH_{MAX} for the 28 species with missing maximum height data.

Data analysis

Any variables demonstrating log-normal distributions were natural log transformed (see below).

a. Light environment

The 42 light intensity measures per plot were averaged to give a mean estimate of light conditions underneath the forest canopy within each plot. We used a two-sample *t*-test to compare mean light intensity between logged and unlogged plots.

b. Taxonomic composition

To describe the taxonomic composition of logged and unlogged plots, we used non-metric multidimensional scaling (NMDS) on a site by species abundance matrix; NMDS is a numerical ordination technique that maximizes the rank-order correlation between distance measures and distance in ordination space (Holland, 2008). The *stress* value for an NMDS indicates how well the ordination summarizes the observed distances among

samples (Holland 2008), with values < 0.2 generally considered a good fit. Species composition for each plot was characterized by its position in ordination space, represented by the scores on the first and second axes of the NMDS. These scores for logged and unlogged plots were then compared using a two-sample *t*-test. We further compared species composition between logged and unlogged plots by using an indicator species analysis to identify species whose patterns of abundance were strongly associated with a particular logging status. The indicator species analysis is appropriate because it relates species abundance values from a set of sampled sites to the classification of the sites into independently predetermined groups (logged/unlogged; (De Cáceres, 2013). The indicator species value is computed for each species independent of other species in the community and estimated as the product of a measure of its sensitivity and fidelity to each logging status category (Legendre and Legendre, 1998). Importance values for each species were estimated as the sum of percentage relative density and relative basal area in all logged plots pooled together and all unlogged plots pooled together. From the importance values, we determined the identity of the ten species that make the most substantial contributions to the density and basal area of the logged and unlogged forest plots, respectively.

c. Structural composition

To compare structural differences between logged and unlogged plots, we calculated

i. plot stem density as number of stems per plot area (200 x 10 m)

ii. basal area as the sum of basal area for all trees in each plot, computed as πr^2 where r is the radius of the tree, estimated as r = DBH/2.

iii. the coefficient of skewness (g_1) to characterize the symmetry of tree size distributions in each plot (Bendel *et al.*, 1989; Wright *et al.*, 2003). When a plot is dominated by an abundance of small trees and a long tail of rare large trees g_1 is positive, and when the plot is dominated by an abundance of large trees and a long tail of rare small trees g_1 is negative (Wright *et al.*, 2003). g_1 is computed as

$$g_1 = \frac{n \sum_i (x_i - \bar{x})^3}{(n-1)(n-2)s^3} \quad \text{Eq. (2)}$$

where n is the number of individuals in a plot, x_i is the logarithm of the DBH for individual i, $\bar{x}_i$ is the mean of x_i, and s is the standard deviation of x_i (Bendel *et al.*, 1989; Wright *et al.*, 2003).

iv. aboveground biomass for each stem using the predictive allometric equations for estimating AGB in moist forest stands provided in Chave *et al.*, (2005). For each tree in a plot, AGB was computed twice, using an equation requiring (Eq. 3), and one not requiring (Eq. 4), height values.

$$\widehat{AGB_{dh}} = 0.0509 \times WD \times D^2 \times H \quad \text{Eq. (3)}$$

$$\widehat{AGB_d} =$$

$$WD \times \exp(-1.499 + 2.1481 * \ln(D) + 0.207 * (\ln(D))^2 - 0.0281 (\ln(D))^3) \quad \text{Eq. (4)}$$

where $\widehat{AGB_{dh}}$ is the estimated AGB based on a given stem's height and DBH, while $\widehat{AGB_d}$ is the estimated AGB based on the stem's DBH. WD (kg/m^3) is the species

average wood density, *D* is the stem DBH (m), and *H* (m) is the stem height. For each stem, *H* was estimated by interpolating from the stem's DBH, based on the KNP forest-wide regression equation predicting height as a function of DBH that is described above in the species functional trait section. The total estimated AGB in a plot is obtained by summing $\widehat{AGB}$ for all stems within the plot. Both $\widehat{AGB}$ estimates were natural log transformed for normality.

d. Functional composition

The functional composition of logged and unlogged plots was calculated for each trait (DBH_{MAX}, H_{MAX}, and WD) as the community weighted mean (CWM) using different weightings: I. relative basal area (BA) and II. relative abundance (ABD). The two weightings provide complementary perspectives on how the forests differ in community attributes by emphasizing contributions from different structural components of the forest, either individuals with large basal area or abundant small stems, respectively (Carreño-Rocabado *et al.*, 2012). Each set of CWM values for each trait was then compared between logged and unlogged plots using a two-sample *t*-test.

Because logging happened in a spatially structured way, logged plots occur in more northerly latitudes than unlogged plots. This distribution results in the problem of simple pseudoreplication, in which 'replicate' plots within the two logging categories are not spatially interspersed across logging categories (Hurlbert, 1984). Consequently, spatial processes could influence forest structure and composition independent of logging effects (Lindenmayer and Laurance, 2012; Ramage *et al.*, 2013). To determine whether geographical space substantially explains some of the variation in forest structure and

composition that is attributed to logging history, we included latitudinal coordinates of each vegetation plot as a covariate in an ANCOVA. This provides a more conservative test for the effect of logging status (environmental predictor) in the presence of latitude, a proxy for spatial predictors, reducing the risk of a Type 1 error (Peres-Neto and Legendre, 2010). However, because latitude was never a significant predictor of any of the community attributes considered when included as a covariate in an ANCOVA (Table A1), we only report the results for *t*-test comparisons of logged and unlogged plots.

All statistical tests were implemented in R version 2.15.1 (R Core Team, 2012), using the packages vegan (Oksanen *et al.*, 2012), FD (Laliberté and Legendre, 2010), and indicspecies (Cáceres and Legendre, 2009).

Results

Light environment (Prediction I): As predicted, logged forest plots had significantly higher light levels than unlogged plots (Fig. 1). However, light levels were not uniformly high within logged plots, as a large proportion of measured areas in logged plots was under shade (e.g. 77% of measured areas within logged plots had less than 5% open light intensity). Higher average light levels in logged plots resulted from light hotspots, i.e. extremely high values of % open light conditions recorded within logged plots (solid black circles in Fig. 1).

Structural composition (Predictions II and III): In total, 2358 stems ≥ 10 cm in DBH were inventoried in all 26 plots. Logged plots had significantly lower stem density contrary to our expectation of higher stem density (prediction II); however, we did find support for

lower total basal area and lower AGB (Table 1) in logged as compared to unlogged forest.

Tree size distributions in logged plots (Fig. 2) had less positive g_1 values than unlogged plots (Table 1), indicating that logged plots were to a lesser extent dominated by an abundance of small trees and had a shorter tail of rare large trees, relative to unlogged plots. These different levels of asymmetry in tree size distributions of logged and unlogged plots were in accordance with prediction III.

Taxonomic composition (Prediction IV): A total of 86 tree species in 39 families were found across all 26 plots. The NMDS recovered two axes (Fig. 3), NMDS1 and NMDS2 with a *stress* value of 0.19, meaning it had a good fit. Logging status was best separated along the first axis of the NMDS (NMDS1; Fig. 3), with logged plots having higher scores than unlogged plots. Taxonomic turnover between logged and unlogged plots was within 2 units on the first NMDS axis.

Only nine species were indicator species showing strong associations with logging status; four were strongly associated with unlogged and five with logged plots (Table 2). Logged and unlogged plots shared six of the ten species with the highest importance values, but in different orders of importance (Table 3).

Functional composition (Prediction IV): Logged and unlogged plots did not differ significantly in functional composition, contrary to our prediction, as both plot types were similar in their community weighted means for all three functional traits when weighted by abundance. On the other hand, basal-area weighted community mean WD was

significantly lower in logged compared to unlogged plots but the difference was small (Table 1).

Discussion

Selective logging is a land-use practice that is increasing in extent and intensity and can alter the conservation value of tropical forests (Asner *et al.*, 2009). Previous investigations on the effects of selective logging on KNP's forests have focused mainly on demographic rates and structural attributes of the forest (Chapman and Chapman, 1997; Chapman and Chapman, 2004; Bonnell *et al.*, 2011). Here, we advance the investigation of the effects of selective logging on KNP's forests by focusing on understory light availability, and structural, taxonomic and functional attributes of the forest 45 years after the selective logging event occurred. We found that on average light levels were higher in logged forest, but with lower stem density, smaller total basal area and AGB, and a dissimilar species composition to unlogged forest. Nevertheless, differences in taxonomic and structural composition of logged forests were not paralleled by differences in community-weighted average trait values; logged plots were functionally analogous to unlogged plots except when community mean WD was basal-area weighted.

Logged forest: higher light environment

Some tropical forests achieve canopy closure after a few decades (Asner *et al.*, 2004). For example, (Nicotra *et al.*, 1999) reported no differences in average light levels between logged and unlogged forest in Costa Rica 15 – 20 years after selective logging. However, this pattern appears to be less true for African forests. Even after 45 years, logged plots

on average had almost double the light intensity of unlogged plots (Fig. 1) likely due to canopy gaps failing to close.

The distribution however of light levels within each plot (Fig. 1) suggests a preponderance of shaded light conditions in both logged and unlogged plots, with a few extreme light hotspots driving average light levels higher in logged forest. The primary source of shade in unlogged plots at 2 m is the closely connected tree canopy, but in logged plots dense herbaceous or shrubby growth overtakes canopy gaps and is a large contributor to the shade at 2 m (Fig. A1 – picture of quantum sensor in shade from shrubby growth). As these shrubs (often *Acanthus pubescens*) are both clonal and browse-tolerant, they are more successful than trees in large canopy gaps, such as was created during the logging event and now maintained by large mammal herbivory in KNP (Struhsaker, 1997; Paul *et al.*, 2004; Royo and Carson, 2006; Lawes and Chapman, 2006; Young and Peffer, 2010).

Logged forest: distinct structural composition

In typical disturbed forests, most stems are in small size classes at high stem densities with few large trees (Denslow, 1995). In KNP, distributions for both logged and unlogged forest approximated the 'reverse J shape' or negative exponential distribution (Richards, 1996), which implies an uneven aged structure, with an abundance of small relative to large-size tree classes (Fig. 2). However, logged plots had less positively skewed distributions than unlogged plots. The less positive skew derived from both an absence of large and a low proportion of small sized stems in logged forest (Fig. 2). This result is consistent with previous reports from KNP that logged plots experienced reduced

recruitment but similar mortality rates of adult trees (≥ 10 cm dbh) to unlogged plots in the first 31 years after logging (Bonnell *et al*., 2011).

KNP logged plots also had fewer total stems per unit area and on average held 44% less AGB than unlogged plots (Table 1). The lower AGB likely resulted from both the low stem density and scarcity of larger trees in logged plots, as large trees make disproportionate contributions to AGB and carbon storage (Lindner and Sattler, 2012).

The absence of large trees in logged plots implies that insufficient time has passed for recovery of biomass, especially through the growth of remnant trees into large size classes. The low number of small trees in logged plots suggests reduced recruitment, which may have resulted from a number of factors. Unfavorable environmental conditions associated with tree damage and canopy loss may have limited recruitment (Chazdon, 2003; Hall *et al.*, 2003). Given that all but a few tree species in KNP perform poorly in large gap conditions (Chapman *et al.*, 1999), sudden crown exposure may have caused physiological stress limiting tree regeneration (Hall *et al*., 2003). Moreover, tree growth and recruitment may have been slowed by early competition from the rapid establishment of dense herbaceous and shrubby vegetation (Donato *et al.*, 2012) and increased elephant activity. Elephants are known to forage extensively on these shrubs (Duclos *et al.*, 2013; Paul *et al.*, 2004; Lawes and Chapman, 2006; Omeja *et al.*, 2014). Based on the measured structural attributes and continued dominance of herb and shrub vegetation, our study supports previous findings that logged forest in KNP is in an arrested state of succession (Chapman and Chapman, 1997, 2004; Bonnell *et al.*, 2011).

The persistence over several decades of the effect of selective-logging on forest structure is not unique to KNP among African forests. For example, Plumptre, (1996) report that 50 years after, logged compartments in Budongo Forest Reserve, East Africa, had not recovered to pre-logging levels in measures of forest structure including mean basal area and crown height. Similarly, Hall *et al*. (2003) report markedly lower basal area and significantly lower stem densities 18 years after logging in a Central African forest. However, in contrast to KNP, another Central African forest showed rapid recovery in AGB within 20 years after logging (Gourlet-Fleury *et al.*, 2013). Reports seem to vary across studies depending on the measure of forest structure and also due to differences in site-specific factors such as selective logging intensity and presence of large mammal herbivory.

Logged forest: divergent taxonomic but analogous functional composition

Taxonomic composition of plots differed depending on logging history (Fig. 3), although the nature of these differences was surprising. We found considerable overlap in important species between logged and unlogged plots; however the order of importance for these overlapping species differed (Table 3). Also, the five species that were closely associated with logged plots (Table 2) were occasional to rare (< 20 stems in total) occurring almost exclusively in logged plots. These results suggest that while the selectively logged environment may have favored the establishment of a few rare disturbance-adapted species, the bulk of the taxonomic differences associated with logging have to do with changes in relative abundances of species.

While we did not find strong taxonomic differences between logged and unlogged forest, these differences may be apparent when contrasting the relative abundances of tree species that were commercially exploited during the logging event. In examining these patterns, however, no obvious differences between 1989 and 2013 can be seen for 11 species commercially harvested in Kibale (Figure 4). While two species (*Celtis africana* and *Strombosia scheffleri*) increased in relative abundance, only *S. scheffleri* had higher relative abundance in unlogged plots. The other commercially exploited species, including the iconic *Parinari excelsa*, maintained a consistent trend of low relative abundances (< 0.025) across logged and unlogged plots (Figure 4). It is unclear whether the lack of recovery for majority of these commercial species is related to regeneration or recruitment, particularly because the two species with increasing abundances represent contrasting ecological strategies. *Celtis africana* is a disturbance-tolerant small-statured generalist with very small seeds and low leaf toughness, while *S. scheffleri* is a shade-loving understory species with larger seeds and high leaf toughness (Chapman *et al.*, 2008; Neuschulz *et al.*, 2013). Moreover, Chapman & Chapman (2004) reported forest-wide fruiting declines for *Parinari excelsa* and *Aningeria altissima* (another commercially exploited species showing poor recovery), which they linked to climate change. Taken together these results suggest that observed taxonomic patterns are generated by multiple perturbations including forest-wide disturbances unrelated to selective logging.

Differences in functional composition between sites with varying logging histories have been found in other studies (Baraloto *et al.*, 2012; Carreño-Rocabado *et al.*, 2012) . In contrast, we do not see a difference in CWM values for WD, H_{MAX}, and DBH_{MAX}

between logged and unlogged plots, except for when WD was basal-area weighted, although this difference was modest (0.03 g/cm^3; Table 1), suggesting that selective logging may have favored the increased growth of species with slightly lower WD.

There are several plausible explanations for this pattern of functionally analogous communities in logged and unlogged forests. First, KNP forest has a small species pool of 86 tree species within 5.2 ha; this is consistent with the general trend of less diversity in African forests relative to tropical forests in other regions (Kreft and Jetz, 2007). A poor species pool can limit trait variation within communities (Mayfield *et al.*, 2010). Moreover, KNP's poor species pool lacks aggressive colonizing tree species (Chapman *et al*., 1999), which tend to have lower WD and smaller H_{MAX}. When comparing KNP to other tropical locations, KNP appears to resemble the species pool for Africa more generally in having a greater incidence of intermediate WD species and an absence of species with extreme WD values (Fig. A2). Even naturally occurring tree fall gaps in KNP are characterized by similar community composition to the forest interior (Zanne and Chapman, 2005), rather than being dominated by pioneer species. Furthermore, Chapman and Chapman (2004) observed a decline in the abundance of the few pioneer species in logged forests in KNP e.g. *Trema orientalis*. In our study, the five species that showed tight associations with the logged forest were small sized and soft wooded, but their modest additions to relative stem density and basal area meant that they had little influence on average community-weighted values. Second, both logged and unlogged forests may be undergoing change triggered by disturbance events independent of the logging event 45 years ago. Such events have recently been reported for KNP, including

changing climates (i.e., longer drought events since the mid-1990s (Hartter *et al.*, 2012) and increased elephant abundance and activity (Omeja *et al.*, 2014).

Caveat

As is common in logging-impact studies, in this study logging history is confounded with geographic space; the logging treatment was implemented as a forestry practice and not for scientific research (Lindenmayer and Laurance, 2012; Ramage *et al.*, 2013). Previous studies of KNP have assumed that compartments within which vegetation plots are located were structurally similar prior to logging, based on historical ground surveys that predate the logging event (Kingston, 1967; Chapman and Chapman, 1997; Bonnell *et al.*, 2011). Here, in addition to the assumption of pre-logging structural similarity of plots, we applied a simple approach to account for pseudoreplication by including latitudinal geographic coordinates for each observation as a covariate in ANCOVA tests. This covariate was not significant for any measure of forest composition and structure (Table A1), increasing our confidence that results we found were due to logging history. However, we are unable to more explicitly test for the effects of spatial processes, and our results should be interpreted with this caveat in mind.

Conclusion

Selective logging is a land-use practice that is becoming increasingly widespread in the tropics, although the extent to which it impacts the taxonomic, structural and functional composition of forests remains unclear. If we assume that unlogged forest is less disturbed than logged forest, from our work, we conclude that 45 years is not enough time for selectively logged forests in KNP to recover in species composition and

structural complexity, but enough time for community-weighted traits to resemble unlogged forest. This functional similarity can be understood in the context of the ecology of Africa generally and KNP more specifically, including a lack of aggressive colonizing trees, a relatively small species pool, concentrated elephant activities, and potential background changes in both forest types unrelated to the selective logging event. Despite the functional similarity in community average WD and adult stature, the dearth of large trees and small stem density reduced the logged forest's capacity for carbon storage, as evidenced by significantly less AGB in logged plots. Likely, the effect of selective logging that has persisted in KNP forest results in part from poor tree recruitment and high mortality of existing trees in the logged plots soon after the logging event.

Consequently, from a conservation standpoint, our results suggest caution should be taken when considering the conservation value of selectively logged forests (Putz *et al.*, 2012; Edwards and Laurance, 2013; Michalski and Peres, 2013; Kormos and Zimmerman, 2014). Surely, given its similar functional trait and not overly distinct taxonomic composition compared to unlogged forest, logged forest in KNP holds greater conservation value than surrounding areas subjected to farming and plantation forestry (Okiror *et al.*, 2012). On the other hand, some argue that for selectively logged forests to have high conservation value they must display rapid recovery following the logging event (Michalski and Peres, 2013). We show in this study that a tropical forest may remain with the imprint of logging for many decades. Furthermore, persistent effects of selective logging have exerted cascading effects on other trophic levels, particularly affecting the population dynamics of primates (Chapman *et al.*, 2010b; Bonnell *et al.*,

2011) and movements of elephants (Omeja *et al.*, 2014). Interestingly, logging extraction levels in KNP ranged from 14 – 17 m^3/ha (Struhsaker, 1997), comparably less than 32.5 m^3/ha reported by Blanc *et al.*, (2009) for a selectively logged forest in French Guiana that rapidly recovered AGB within 40 years. Whether this difference in recovery represents a general contrast between the vulnerabilities to anthropogenic disturbances of mid-elevation and lowland forests or is more due to site-specific differences (e.g. concentrated elephant activities in KNP) remains to be seen. Until we have better answers, strategies for sustainably managing and conserving tropical forests should be informed by local forest dynamics and vulnerabilities to disturbance, rather than blanket 'one size fit all' conclusions on the conservation value of logged forests (Corlett and Primack, 2006).

Acknowledgements

This work was supported by the Whitney Harris World Ecology Center [to O.L.O]; the Webster Groves Nature Study Society [to O.L.O]; IDEA WILD [to O.L.O]; NSERC [to C.A.C]; FQRNT [to C.A.C]; and the National Institutes of Health [grant TW009237 to C.A.C] as part of the joint NIH-NSF Ecology of Infectious Disease program and the UK Economic and Social Research Council. O. L. O. thanks the Uganda Wildlife Authorities for permission to conduct this research; Seezi and Prime for invaluable field assistance; Patrick Omeja, the Chapman lab, and staff of KNP for logistic support; Peter Stevens, Brad Oberle, and Ivan Jiménez for comments on earlier versions of the manuscript.

Tables

Table 1. Mean (± 1 SD) light availability, structural attributes and functional traits for logged (N = 9) and unlogged plots (N = 17), and results from a two-sample t-test, including the test statistic (t) and degrees of freedom (df). Significant tests are in bold (** $P < 0.01$, * $P < 0.05$). Acronyms are defined as follows: CWM = community weighted mean, WD = wood density, H_{MAX} = maximum height, DBH_{MAX} = maximum diameter, ABD= abundance weighted, AGB = aboveground biomass, BA = basal area weighted, and g_1 = coefficient of skewness

Community attribute	**Mean ± 1 SD for logged plots**	**Mean ± 1 SD for unlogged plots**	***t***	***df***
Structural composition				
Total basal area (cm^2)	49265 ± 22021	89210 ± 33182	**-3.67****	23
Stem density ($\#/m^2$)	0.03 ± 0.01	0.05 ± 0.01	**-3.63****	16
AGB (with height; kg)	2262 ± 1139	5091 ± 2876	**-3.56****	23
AGB (without height; kg)	930 ± 426	1840 ± 727	**-4.02****	24
g_1	0.58 ± 0.38	1.20 ± 0.53	**-3.46****	22
Functional composition				
CWM WD_{ABD} (g/cm^3)	0.57 ± 0.04	0.59 ± 0.02	-1.65	12
CWM WD_{BA} (g/cm^3)	0.56 ± 0.03	0.59 ± 0.04	**-2.17***	20
CWM $H_{MAX.ABD}$ (m)	26.9 ± 3.8	27.9 ± 1.9	-0.72	10
CWM $H_{MAX.BA}$ (m)	29.7 ± 5.3	32.2 ± 4.0	-1.25	13
CWM $DBH_{MAX.ABD}$ (cm)	76.3 ± 8.7	76.7 ± 9.3	-0.12	17
CWM $DBH_{MAX.BA}$ (cm)	95.6 ± 23.0	125.8 ± 53.1	-2.01	23

Table 2. Species (Family) with significant logging status associations, species' indicator values, and the probability (*P*) of obtaining as great an indicator value as observed over 999 iterations

Indicator species	**Logging status**	**Indicator value**	***P***
Vepris nobilis (Rutaceae)	Unlogged	0.847	0.006
Trilepisium madagascariense (Moraceae)	Unlogged	0.825	0.016
Leptonychia mildbraedii (Malvaceae)	Unlogged	0.811	0.006
Mimusops bagshawei (Sapotaceae)	Unlogged	0.686	0.024
Rothmannia urcelliformis (Rubiaceae)	Logged	0.758	0.004
Ehretia cymosa (Boraginaceae)	Logged	0.722	0.011
Euadenia eminens (Capparaceae)	Logged	0.719	0.010
Fagaropsis angolensis (Rutaceae)	Logged	0.711	0.046
Kigelia africana (Bignogniaceae)	Logged	0.584	0.039

Table 3. Species (Family) with the ten highest important values (IV) in logged and unlogged plots, and their importance values*

Logged plots		**Unlogged plots**	
Important species	**IV**	**Important species**	**IV**
Celtis durandii[#] (Cannabaceae)	25.0	*Celtis durandii* (Cannabaceae)	21.7
Diospyros abyssinica (Ebenaceae)	24.8	*Funtumia africana* (Apocynaceae)	18.5
Funtumia africana (Apocynaceae)	18.6	*Trilepisium madagascariense* (Moraceae)	18.0
Markhamia lutea[#] (Bignoniaceae)	17.4	*Uvariopsis congensis*[#] (Annonaceae)	14.5
*Celtis africana*** (Cannabaceae)	11.6	*Diospyros abyssinica* (Ebenaceae)	13.4
Premna angolensis (Lamiaceae)	10.9	*Markhamia lutea* (Bignoniaceae)	10.9
*Strombosia scheffleri*** (Olacaceae)	6.1	*Strombosia scheffleri* (Olacaceae)	9.6
Millettia dura (Leguminosae)	6.0	*Aningeria altissima*** (Sapotaceae)	8.9
Trilepisium madagascariense (Moraceae)	5.6	*Vepris nobilis*[#] (Rutaceae)	6.3
Cordia africana (Bignoniaceae)	5.0	*Pseudospondias microcarpa* (Anacardiaceae)	6.0

*Distribution of species importance values was similar for logged and unlogged plots; average (± 1 SD) importance values were 2.38 % (± 4.42) for species in logged and 2.38 % (± 4.82) for species in unlogged forest plots.

**Species extracted for timber during the selective logging event (Struhsaker, 1997); (Bonnell *et al.*, 2011).

[#]Species that may have suffered incidental damage during the selective logging event (Struhsaker, 1997).

Figures

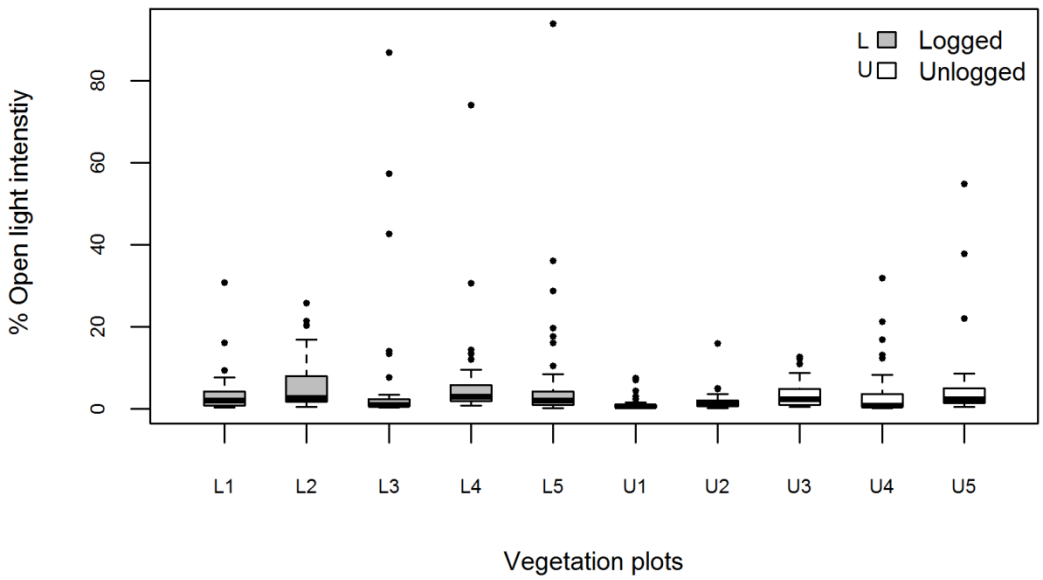

Fig. 1. Percent open light intensity for logged (L1 – L5) and unlogged plots (U1 – U5) in KNP. Each vegetation plot has 42 light intensity measures. Each boxplot shows the median (black horizontal line), the upper quartile (space above black line), the lower quartile (space below black line), minimum (lower whisker) and maximum (upper whisker) values, and extreme values or outliers (solid black circles). Mean percent open light intensity was significantly higher in logged plots ($t = 2.92$, $P < 0.05$).

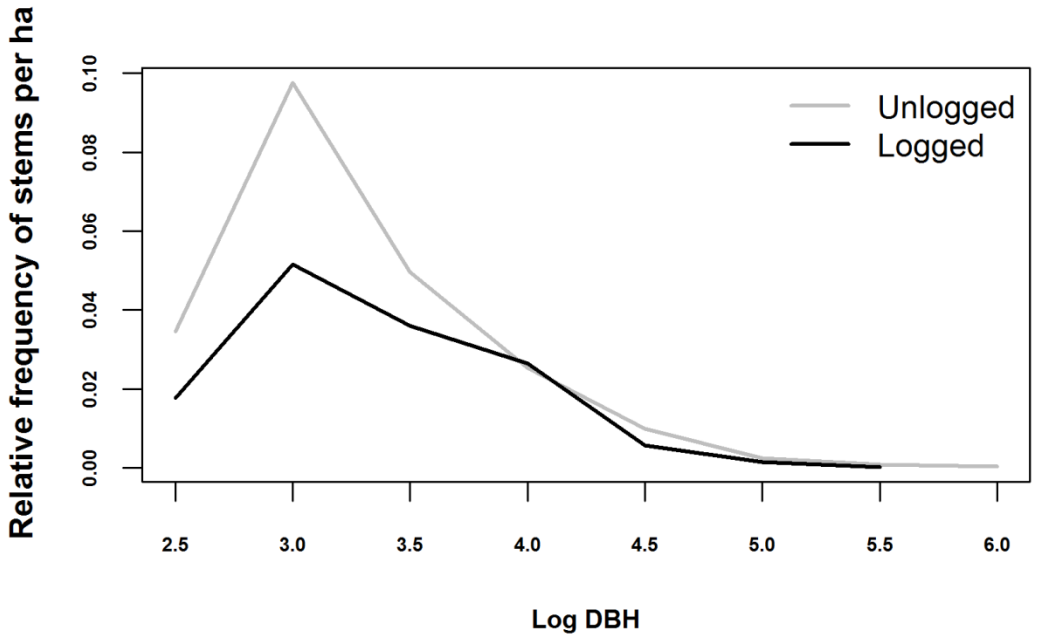

Fig. 2. Diameter distributions for logged and unlogged plots in KNP. Lines show the relative frequencies of stem densities (y-axis) in each log-transformed DBH size class (x-axis). Logged plots (N = 9) are represented by the black line, and unlogged plots (N = 17) by the grey line.

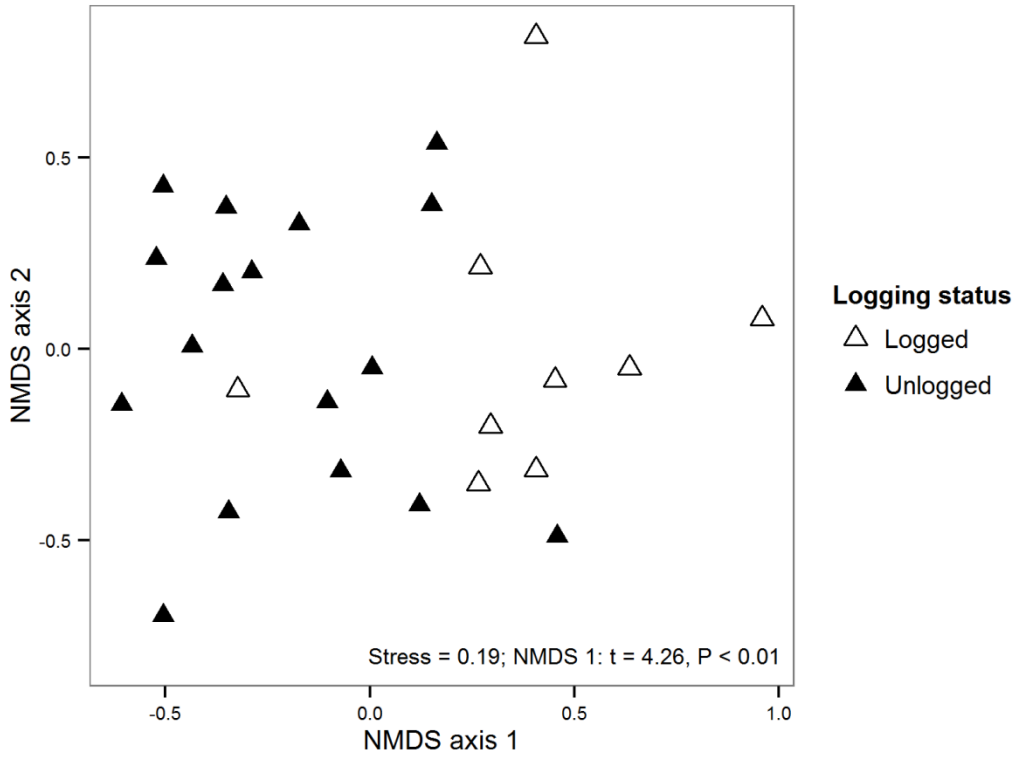

Fig. 3. Ordination of taxonomic composition of logged (*N*=9) and unlogged (*N*=17) plots in Kibale National Park, Uganda. The Non-metric Multidimensional Scaling produced two axes (NMDS1 and NMDS2). Logged plots (open triangles) differed significantly from unlogged plots (solid black triangles) in species composition along the first axis (*t* = 4. 26, *P*<0.01) based on a two sample *t*-test, with most logged plots loading positively on axis 1.

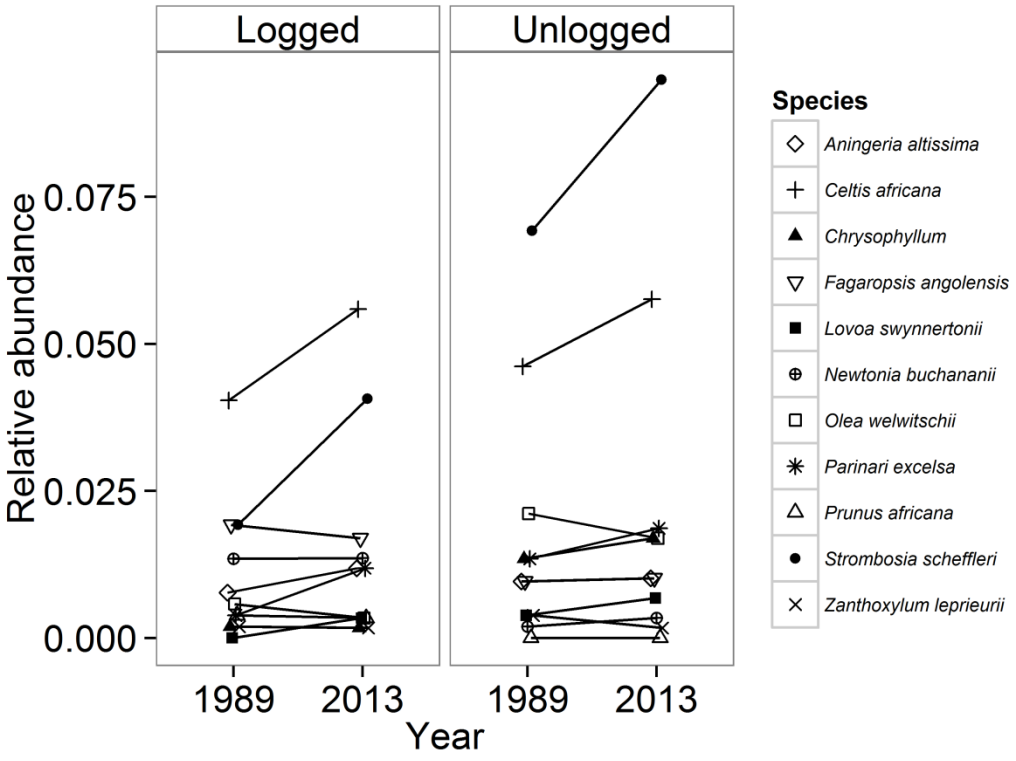

Fig. 4. Trends in relative abundances of 11 tree species commercially logged in Kibale National Park, based on their relative abundances in 1989 and 2013 in logged and unlogged plots. Each species is represented by a different symbol, while lines connect symbols to show trends between relative abundance in 1989 and 2013 for each species.

References

Asner GP, Keller M, Pereira J, Rodrigo, Zweede JC, Silva JNM (2004) Canopy damage and recovery after selective logging in Amazonia: field and satellite studies. *Ecol Appl* 14: 280–298.

Asner GP, Rudel TK, Aide TM, Defries R, Emerson R (2009) A contemporary assessment of change in humid tropical forests. *Conserv Biol* 23: 1386–1395.

Baraloto C, Hérault B, Paine CET, Massot H, Blanc L, Bonal D, Molino J-F, Nicolini EA, Sabatier D (2012) Contrasting taxonomic and functional responses of a tropical tree community to selective logging. *J Appl Ecol* 49: 861–870.

Bendel RB, Higgins SS, Teberg JE, Pyke DA (1989) Comparison of skewness coefficient, coefficient of variation, and Gini coefficient as inequality measures within populations. *Oecologia* 78: 394–400.

Berry NJ, Phillips OL, Lewis SL, Hill JK, Edwards DP, Tawatao NB, Ahmad N, Magintan D, Khen CV, Maryati M, *et al.* (2010) The high value of logged tropical forests: lessons from northern Borneo. *Biodivers Conserv* 19: 985–997.

Blanc L, Echard M, Herault B, Bonal D, Marcon E, Chave J, Baraloto C (2009) Dynamics of aboveground carbon stocks in a selectively logged tropical forest. *Ecol Appl* 19: 1397–1404.

Bonnell TR, Reyna-Hurtado R, Chapman CA (2011) Post-logging recovery time is longer than expected in an East African tropical forest. *For Ecol Manag* 261: 855–864.

Cáceres MD, Legendre P (2009) Associations between species and groups of sites: indices and statistical inference. *Ecology* 90: 3566–3574.

Cannon CH, Peart DR, Leighton M (1998) Tree species diversity in commercially logged Bornean rainforest. *Science* 281: 1366–1368.

Carreño-Rocabado G, Peña-Claros M, Bongers F, Alarcón A, Licona J-C, Poorter L (2012) Effects of disturbance intensity on species and functional diversity in a tropical forest. *J Ecol* 100: 1453–1463.

Chapman CA, Chapman LJ (1997) Forest regeneration in logged and unlogged forests of Kibale National Park, Uganda. *Biotropica* 29: 396–412.

Chapman CA, Chapman LJ (2004) Unfavorable successional pathways and the conservation value of logged tropical forest. *Biodivers Conserv* 13: 2089–2105.

Chapman CA, Chapman LJ, Jacob AL, Rothman JM, Omeja P, Reyna-Hurtado R, Hartter J, Lawes MJ (2010a) Tropical tree community shifts: Implications for wildlife conservation. *Biol Conserv* 143: 366–374.

Chapman CA, Chapman LJ, Kaufman L, Zanne AE (1999) Potential causes of arrested succession in Kibale National Park, Uganda: growth and mortality of seedlings. *Afr J Ecol* 37: 81–92.

Chapman CA, Kitajima K, Zanne AE, Kaufman LS, Lawes MJ (2008) A 10-year evaluation of the functional basis for regeneration habitat preference of trees in an African evergreen forest. *For Ecol Manag* 255: 3790–3796.

Chapman CA, Lambert JE (2000) Habitat alteration and the conservation of African primates: Case study of Kibale National Park, Uganda. *Am J Primatol* 50: 169–185.

Chapman CA, Struhsaker TT, Skorupa JP, Snaith TV, Rothman JM (2010b) Understanding long-term primate community dynamics: implications of forest change. *Ecol Appl* 20: 179–191.

Chave J, Coomes D, Jansen S, Lewis SL, Swenson NG, Zanne AE (2009) Towards a worldwide wood economics spectrum. *Ecol Lett* 12: 351–366.

Chazdon RL (2003) Tropical forest recovery: legacies of human impact and natural disturbances. *Perspect Plant Ecol Evol Syst* 6: 51–71.

Clark JA, Covey KR (2012) Tree species richness and the logging of natural forests: A meta-analysis. *For Ecol Manag* 276: 146–153.

Corlett RT, Primack RB (2006) Tropical rainforests and the need for cross-continental comparisons. *Trends Ecol Evol* 21: 104–110.

De Cáceres M (2013) How to use the indicspecies package (ver. 1.6. 7). *Website Httpcran Rproject OrgwebpackagesindicspeciesvignettesindicspeciesTutorial Pdf Accessed April 2 2013*.

Denslow JS (1995) Disturbance and diversity in tropical rain forests: the density effect. *Ecol Appl* 5: 962.

Donato DC, Campbell JL, Franklin JF (2012) Multiple successional pathways and precocity in forest development: can some forests be born complex? *J Veg Sci* 23: 576–584.

Duclos V, Boudreau S, Chapman CA (2013) Shrub cover influence on seedling growth and survival following logging of a tropical forest. *Biotropica* 45: 419–426.

Edwards DP, Laurance WF (2013) Biodiversity Despite Selective Logging. *Science* 339: 646–647.

Falster DS, Westoby M (2005) Alternative height strategies among 45 dicot rain forest species from tropical Queensland, Australia. *J Ecol* 93: 521–535.

Gibson L, Lee TM, Koh LP, Brook BW, Gardner TA, Barlow J, Peres CA, Bradshaw CJA, Laurance WF, Lovejoy TE, *et al.* (2011) Primary forests are irreplaceable for sustaining tropical biodiversity. *Nature* 478: 378–381.

Gourlet-Fleury S, Mortier F, Fayolle A, Baya F, Ouédraogo D, Bénédet F, Picard N (2013) Tropical forest recovery from logging: a 24 year silvicultural experiment from Central Africa. *Philos Trans R Soc B Biol Sci* 368: 20120302.

Hall JS, Harris DJ, Medjibe V, Ashton PMS (2003) The effects of selective logging on forest structure and tree species composition in a Central African forest: implications for management of conservation areas. *For Ecol Manag* 183: 249–264.

Hamilton A (1991) A Field Guide to Ugandan Forest Trees. Makerere University.

Hartter J, Stampone MD, Ryan SJ, Kirner K, Chapman CA, Goldman A (2012) Patterns and perceptions of climate change in a biodiversity conservation hotspot. *PLoS ONE* 7: e32408.

Holland SM (2008) Non-metric Multidimensional Scaling (MDS). https://www.uga.edu/strata/software/pdf/mdsTutorial.pdf (last accessed 21 October 2013).

Hurlbert SH (1984) Pseudoreplication and the Design of Ecological Field Experiments. *Ecol Monogr* 54: 187–211.

Kasenene JM (1987) The Influence of Mechanized Selective Logging, Felling Intensity and Gap-Size on the Regeneration of a Tropical Moist Forest in the Kibale Forest Reserve, Uganda. Michigan State University.

Katende AB, Birnie A, Tengnäs B (1995) Useful Trees and Shrubs for Uganda: Identification, Propagation, and Management for Agricultural and Pastoral Communities. Regional Soil Conservation Unit, Nairobi, Kenya.

King DA, Wright SJ, Connell JH (2006) The contribution of interspecific variation in maximum tree height to tropical and temperate diversity. *J Trop Ecol* 22: 11–24.

Kingston B (1967) Working Plan for the Kibale and Itwara Central Forest Reserves: Toro District, Uganda. Uganda Forest Dept., Entebbe.

Kormos CF, Zimmerman BL (2014) Response to: Putz et al., Sustaining Conservation Values in Selectively Logged Tropical Forests: The Attained and the Attainable. *Conserv Lett* 7: 143–144.

Kreft H, Jetz W (2007) Global patterns and determinants of vascular plant diversity. *Proc Natl Acad Sci* 104: 5925–5930.

Laliberté E, Legendre P (2010) A distance-based framework for measuring functional diversity from multiple traits. *Ecology* 91: 299–305.

Lasco RD, MacDicken KG, Pulhin FB, Guillermo IQ, Sales RF, Cruz RVO (2006) Carbon stocks assessment of a selectively logged dipterocarp forest and wood processing mill in the Philippines. *0128-1283*.

Lawes MJ, Chapman CA (2006) Does the herb Acanthus pubescens and/or elephants suppress tree regeneration in disturbed Afrotropical forest? *For Ecol Manag* 221: 278–284.

Legendre P, Legendre LFJ (1998) Numerical Ecology. Elsevier.

Lindenmayer DB, Laurance WF (2012) A history of hubris – Cautionary lessons in ecologically sustainable forest management. *Biol Conserv* 151: 11–16.

Lindner A, Sattler D (2012) Biomass estimations in forests of different disturbance history in the Atlantic Forest of Rio de Janeiro, Brazil. *New For* 43: 287–301.

Lwanga J (1996) Trees and Shrubs. In: Kibale Forest Biodiversity Report. Forest Department, Kampala, pp 15 – 36.

Mayfield MM, Bonser SP, Morgan JW, Aubin I, McNamara S, Vesk PA (2010) What does species richness tell us about functional trait diversity? Predictions and evidence for responses of species and functional trait diversity to land-use change. *Glob Ecol Biogeogr* 19: 423–431.

Michalski F, Peres CA (2013) Biodiversity Depends on Logging Recovery Time. *Science* 339: 1521–1522.

Moles AT, Warton DI, Warman L, Swenson NG, Laffan SW, Zanne AE, Pitman A, Hemmings FA, Leishman MR (2009) Global patterns in plant height. *J Ecol* 97: 923–932.

Mouillot D, Graham NAJ, Villéger S, Mason NWH, Bellwood DR (2013) A functional approach reveals community responses to disturbances. *Trends Ecol Evol* 28: 167–177.

Neuschulz EL, Grass I, Botzat A, Johnson SD, Farwig N (2013) Persistence of flower visitors and pollination services of a generalist tree in modified forests. *Austral Ecol* 38: 374–382.

Nicotra AB, Chazdon RL, Iriarte SVB (1999) Spatial heterogeneity of light and woody seedling regeneration in tropical wet forests. *Ecology* 80: 1908–1926.

Okiror P, Chono J, Nyamukuru A, Lwanga JS, Sasira P, Diogo P (2012) Variation in Woody Species Abundance and Distribution in and around Kibale National Park, Uganda. *Int Sch Res Not* 2012: e490461.

Oksanen J, Blanchet GF, Kindt R, Legendre P, Minchin PR, O'Hara RB, Simpson GL, Solymos P, Stevens HMH, Wagner H (2012) vegan: Community Ecology Package.

Okuda T, Suzuki M, Adachi N, Quah ES, Hussein NA, Manokaran N (2003) Effect of selective logging on canopy and stand structure and tree species composition in a lowland dipterocarp forest in peninsular Malaysia. *For Ecol Manag* 175: 297–320.

Omeja P, Aerin JL, Lawes MJ, Lwanga JS, Rothman JM, Tumwesigye C, Chapman CA (2014) Do changes in elephant abundance affect forest composition or regeneration? *Biotropica* 46. doi:10.1111/btp.12154

Osazuwa-Peters OL, Zanne AE, PrometheusWiki contributors (2011) PrometheusWiki | Wood density protocol. http://prometheuswiki.publish.csiro.au/tiki-index.php?page=Wood+density+protocol (last accessed 22 October 2013).

Osmaston H (1959) Working Plan for the Kibale & Itwara Central Forest Reserves, Toro District, Western Province, Uganda. 1st Revision: Period, 1 January 1959-30 June 1965. Uganda Forest Dept., Entebbe.

Paul JR, Randle AM, Chapman CA, Chapman LJ (2004) Arrested succession in logging gaps: is tree seedling growth and survival limiting? *Afr J Ecol* 42: 245–251.

Peres-Neto PR, Legendre P (2010) Estimating and controlling for spatial structure in the study of ecological communities. *Glob Ecol Biogeogr* 19: 174–184.

Picard N, Gourlet-Fleury S, Forni E (2012) Estimating damage from selective logging and implications for tropical forest management. *Can J For Res* 42: 605 – 613.

Plumptre AJ (1996) Changes following 60 years of selective timber harvesting in the Budongo Forest Reserve, Uganda. *For Ecol Manag* 89: 101–113.

Polhill RM (1952) Flora of Tropical East Africa. Balkema.

Putz FE, Zuidema PA, Synnott T, Peña-Claros M, Pinard MA, Sheil D, Vanclay JK, Sist P, Gourlet-Fleury S, Griscom B, *et al.* (2012) Sustaining conservation values in selectively logged tropical forests: the attained and the attainable. *Conserv Lett* 5: 296–303.

Ramage BS, Sheil D, Salim HMW, Fletcher C, Mustafa N-ZA, Luruthusamay JC, Harrison RD, Butod E, Dzulkiply AD, Kassim AR, *et al.* (2013) Pseudoreplication in tropical forests and the resulting effects on biodiversity conservation. *Conserv Biol* 27: 364–372.

Rands MRW, Adams WM, Bennun L, Butchart SHM, Clements A, Coomes D, Entwistle A, Hodge I, Kapos V, Scharlemann JPW, *et al.* (2010) Biodiversity conservation: Challenges beyond 2010. *Science* 329: 1298–1303.

R Core Team (2012) R: A language and environment for statistical computing. *R Found Stat Comput Vienna Austria*. http://www.r-project.org/ (last accessed 22 October 2013).

Richards PW (1996) The Tropical Rain Forest: An Ecological Study. Cambridge University Press.

Royo AA, Carson WP (2006) On the formation of dense understory layers in forests worldwide: consequences and implications for forest dynamics, biodiversity, and succession. *Can J For Res* 36: 1345–1362.

Slik JWF, Verburg RW, Keßler PJA (2002) Effects of fire and selective logging on the tree species composition of lowland dipterocarp forest in East Kalimantan, Indonesia. *Biodivers Conserv* 11: 85–98.

Struhsaker TT (1997) Ecology of an African rain forest: logging in Kibale and the conflict between conservation and exploitation. xxii + 434 pp.

Verburg R, van Eijk-Bos C (2003) Effects of selective logging on tree diversity, composition and plant functional type patterns in a Bornean rain forest. *J Veg Sci* 14: 99–110.

Wright IJ, Ackerly DD, Bongers F, Harms KE, Ibarra-Manriquez G, Martinez-Ramos M, Mazer SJ, Muller-Landau HC, Paz H, Pitman NCA, *et al.* (2007) Relationships among ecologically important dimensions of plant trait variation in seven neotropical forests. *Ann Bot* 99: 1003–1015.

Wright SJ, Muller-Landau HC, Condit R, Hubbell SP (2003) Gap-dependent recruitment, realized vital rates, and size distributions of tropical trees. *Ecology* 84: 3174–3185.

Young TP, Peffer E (2010) "Recalcitrant understory layers" revisited: arrested succession and the long life-spans of clonal mid-successional species. *Can J For Res* 40: 1184–1188.

Zanne AE, Chapman CA (2005) Diversity of woody species in forest, treefall gaps, and edge in Kibale National Park, Uganda. *Plant Ecol* 178: 121–139.

Zanne AE, Lopez-Gonzalez G, Coomes DA, Ilic J, Jansen S, Lewis SL, Miller RB, Swenson NG, Wiemann MC, Chave J (2009) Global wood density database. doi:doi:10.5061/dryad.234

Supporting information for chapter 3

Table A1. Effect of logging status on all community attributes in the presence of a spatial covariate (latitude) with the *F* statistic for main effects of logging status and latitude reported for Analysis of Covariance (ANCOVA) tests run for each community attribute. Significant tests are in bold (** $P < 0.01$, * $P < 0.05$). Acronyms are defined as follows: CWM = community weighted mean, WD = wood density, H_{MAX} = maximum height, DBH_{MAX} = maximum diameter, ABD = abundance weighted, AGB = aboveground biomass BA = basal area weighted, and g_1 = coefficient of skewness.

Community attribute	**Logging status**	**Latitude**
	F	***F***
Structural composition		
Light intensity (% open light intensity)	**11.333***	3.655
Total basal area (cm^2)	**10.261****	0.492
Stem density ($\#/m^2$)	**13.21****	0.420
Relative gap phase	0.034	0.074
g_1	**9.842****	1.294
AGB (with height; kg)	**14.142****	0.131
AGB (without height; kg)	**17.136*****	0.019
Species composition		
NMDS1	**19.028*****	0.522
NMDS2	0.000	1.234
Functional composition		
CWM WD_{ABD} (g/cm^3)	3.44	0.020
CWM WD_{BA} (g/cm^3)	3.906	0.108
CWM $H_{MAX.ABD}$ (m)	0.724	0.004
CWM $H_{MAX.BA}$ (m)	1.823	0.475
CWM $DBH_{MAX.ABD}$ (cm)	0.015	2.746
CWM $DBH_{MAX.BA}$ (cm)	2.523	0.247

Fig A1. Photo of a quantum sensor at 2 m above ground level underneath shade exerted by dense herbaceous growth in logged plot in Kibale National Park, Uganda.
Source: Oyomoare Osazuwa-Peters

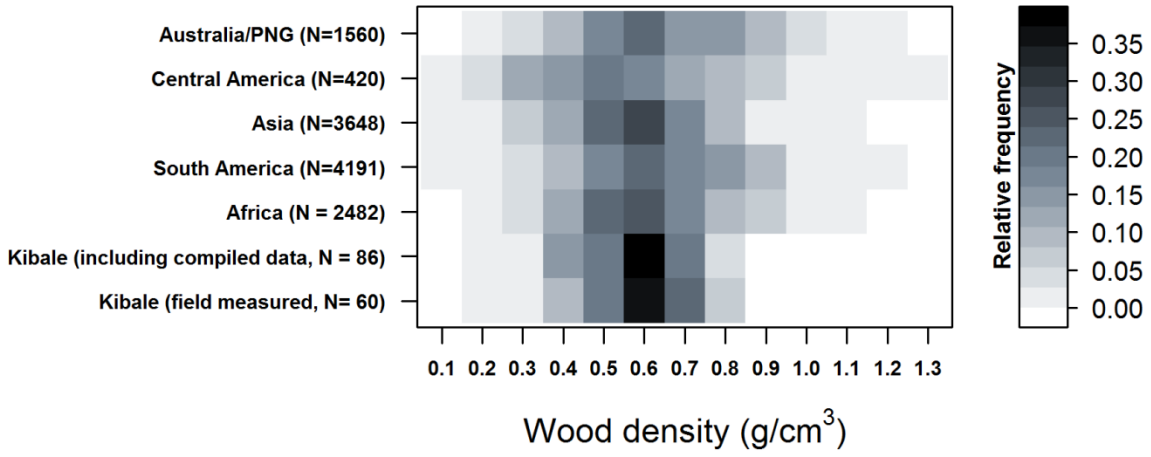

Fig. A2. Map of relative frequencies of wood density values of species in KNP forest for only field measured data (N = 60), and with field measured and compiled data from a subset of the Global Wood Density Database for African region included (N=86), as well as for the Global Wood Density Database subset for tropical Africa (N = 2482), tropical South America (N = 4191), tropical Asia (N=3648), tropical Central America (N=420), and tropical Australia/Papau New guinea (PNG) (N=1560). Color scheme ranges from zero frequency (white) to the highest frequency (black).

Chapter 4

Selective logging: do rates of forest turnover in demography, species composition and functional traits decrease with time since disturbance? – A 45 year perspective

Oyomoare L. Osazuwa-Peters[1], Ivan Jiménez [2], Brad Oberle[3], Colin A. Chapman[4], and Amy E. Zanne[2, 3]

[1]Department of Biology, One University Boulevard, University of Missouri Saint Louis, Saint Louis, Missouri, 63121, USA

[2]Center for Conservation and Sustainable Development Missouri Botanical Garden, P.O. Box 299 St. Louis, MO 63166

[3]Department of Biological Sciences, 2023 G St. NW, The George Washington University, Washington DC, 20052, USA

[4]Department of Anthropology and School of Environment, McGill University, Montreal, Quebec, H3A 2T7, Canada, and Wildlife Conservation Society, 2300 Southern Boulevard, Bronx, New York, USA 10460

Manuscript draft under review in *Forest Ecology and Management*.

Abstract

Selective logging, the targeted harvesting of timber trees in a single cutting cycle, is globally rising in extent and intensity. Short-term impacts of selective logging on tropical forests have been widely investigated, but long-term effects on temporal dynamics of forest structure and composition are largely unknown. Understanding these long-term dynamics will help determine whether tropical forests are resilient to selective logging and inform choices between competing demands of anthropogenic use versus conservation of tropical forests. Forest dynamics can be studied within the framework of succession theory, which predicts that temporal turnover rates should decline with time since disturbance. Here, we investigated the temporal dynamics of a tropical forest in Kibale National Park, Uganda over 45 years following selective logging. We estimated turnover rates in demography, species composition, and functional traits (wood density, maximum height and diameter), using observations from four censuses in 1989, 1999, 2006, and 2013, of stems ≥ 10 cm diameter within 17 unlogged and 9 logged 200 x 10 m vegetation plots. We used null models to account for interdependencies among turnover rates in demography, species composition, and functional traits. We tested predictions that turnover rates should be higher and decrease with increasing time since the selective logging event in logged forest, but should be less temporally variable in unlogged forest. Overall, we found higher turnover rates in logged forest for all three attributes, but turnover rates did not decline through time in logged forest and was not less temporally variable in unlogged forest. These results indicate that successional models that assume recovery to pre-disturbance conditions are inadequate for predicting the effects of selective logging on the dynamics of the tropical forest in Kibale during this interval.

Selective logging resulted in persistently higher turnover rates, which may compromise the carbon storage capacity of Kibale's forest. Selective logging effects may also interact with effects from other global trends, potentially causing major long-term shifts in the dynamics of tropical forests. Similar studies in tropical forests elsewhere will help determine the generality of these conclusions. Ultimately, the view that selective logging is a benign approach to the management of tropical forests should be reconsidered in the light of studies of the effects of this practice on long-term forest dynamics.

Keywords: Beta-diversity, disturbance, functional traits, Kibale National Park, null model, succession, temporal dynamics, tropical forest, turnover rate.

Introduction

Selective logging, the targeted harvesting of timber trees in a single cutting cycle, is rising in extent and intensity on a global scale likely due to its increasing importance as a source of revenue for developing economies (Asner *et al.* 2009). Conservative estimates that do not account for clandestine (but presumably prevalent) logging operations indicate that at least 390 million hectares of tropical humid forests were selectively logged as of 2009 (Asner et al. 2009). In 2011, 403 million hectares of tropical forest were officially reserved for timber production (Putz *et al.* 2012). These figures have prompted the question of whether selective logging has transitioned from a relatively benign land-use practice to a significant threat to the conservation value of tropical forests (Asner *et al.* 2009). Consequently, there is growing interest in understanding the impacts of selective logging on tropical forests, including not only immediate

consequences for forest structure and composition, but also effects on long-term compositional and structural dynamics (Sist *et al.* 2015; Anderson-Teixeira *et al.* 2013).

While the short-term impacts of selective logging on the state of tropical forests have been widely investigated (Cannon *et al.* 1998; Bonnell *et al.* 2011; Gibson *et al.* 2011; Baraloto *et al.* 2012; Putz *et al.* 2012), the long-term effects of selective logging on temporal dynamics of forest structure and composition are largely unknown. These dynamics can be studied within the framework of succession, the temporal change in structure or composition of a group of species co-occurring at a site (Pickett *et al.* 2011; Prach & Walker 2011). A key feature of successional trajectories, central to our understanding of the dynamics of species assemblages, is variation in the rates of temporal change in structure and composition. These rates often referred to as "temporal turnover rates" describe temporal changes in demography, species composition or functional traits. Functional traits are morphological and physiological traits that reflect allocation strategies thought to be important determinants of fitness across environments (Violle et al. 2007). Turnover rates are expected to decrease as succession ensues (Drury & Nisbet 1973; Whittaker 1975; Grime 1979; Bornkamm 1981; Anderson 2007), presumably due to replacement of pioneers at early stages of succession by longer-lived, self-replacing, late-successional species, and a higher resistance to invasion resulting in fewer species being added at later stages of succession (Facelli & D'Angela 1990; Myster & Pickett 1994; Anderson 2007; Walker & del Moral 2008). Declining rates of temporal turnover as succession occurs have been consistently documented across a wide range of species assemblages, including phytoplankton communities (Jassby & Goldman 1974), herbaceous and shrub plant communities (Bornkamm 1981;

Prach et al. 1993; Myster & Pickett 1994; Anderson 2007; Matthews & Endress 2010), forest tree communities (Anderson 2007), and aquatic communities including zooplankton, benthic macroinvertebrates, and fish (Korhonen, Soininen & Hillebrand 2010).

However, because long-term data on temporal change of tree communities are difficult to obtain, only a few studies have used temporal data to investigate the effect of selective logging on the successional trajectories of tropical forests. While it has been shown using chronosequence approaches that stem turnover rates decline with successional stage in a tropical forest (Sheil *et al.* 2000), no study has used long-term data to test the expectation that turnover rates decrease as succession proceeds following selective logging. Most long-term studies of selective logging effects have focused on temporal variation in demography, i.e. recruitment and mortality rates (Sheil *et al.* 2000; Chapman & Chapman 2004; Bonnell *et al.* 2011) and forest structure in terms of stem density (Verburg & van Eijk-Bos 2003), and aboveground biomass and carbon stocks (Blanc *et al.* 2009; Gourlet-Fleury *et al.* 2013). Studies focused on species composition have mainly used ordination methods to establish the direction of temporal change and determine whether selectively logged forests converge on a steady-state through time (Verburg & van Eijk-Bos 2003). For functional traits, Sheil *et al.* (2000) used taxon analysis to test whether the proportion of shade tolerant trees changes as succession progresses after selective logging, while Carreño-Rocabado *et al.* (2012) evaluated changes in the functional diversity of tropical tree communities from 12 traits and the underlying role of demographic processes, over two time points that spanned 8 years following selective logging.

To the best of our knowledge, there are no studies that simultaneously examine the effect of selective logging on temporal turnover rates in demography (mortality and recruitment), species composition and functional traits. Yet, doing so is important for at least two reasons. One is that predictions of succession theory might be supported for only some of these three kinds of turnover rates. Temporal turnover rates in demography and functional traits are expected to show systematic trends as succession proceeds, due to replacement of pioneers with longer-lived species (Walker & del Moral 2008), and because environmental filters are thought to act on traits that determine dispersal, survival, and reproduction in different environments (Shipley 2010). However, temporal turnover rates in species composition might not show systematic trends if several species have similar functional traits and species occurrences are historically contingent on stochastic factors, such as which species arrive first at a site (Fukami *et al.* 2005; Shipley 2010). Thus, temporal turnover rates in demography and functional attributes during forest succession might be more predictable than temporal turnover rates in species composition (Guariguata & Ostertag 2001; Chazdon *et al.* 2007). It follows that support for the prediction of decreasing turnover rates as succession proceeds may depend on whether turnover rate is measured in terms of demography, species composition, or functional traits (Anderson 2007).

A second reason to simultaneously study turnover rates in demography, species composition, and functional traits is that it allows controlling for dependencies between these three kinds of turnover rate and, thus, understanding the extent to which each kind of turnover rate behaves independently as predicted by succession theory. Turnover rates in species composition and functional traits depend at least in part on turnover rate in

demography (Swenson *et al.* 2012). At one extreme, if the demographic turnover rate is zero, and stems neither die nor recruit, then turnover rate in species composition and functional traits are bound to be zero as well. As turnover rate in demography increases it is possible for turnover in species composition and functional traits to increase, but only within the limits imposed by turnover rate in demography. For example, the number of new species entering a site during a given time interval cannot possibly exceed the number of individuals recruited in that site. Likewise, the number of species lost from a site during a given time interval cannot possibly exceed the number of individuals dying in that site. In analogous fashion, turnover rate in species composition limits turnover rate in functional traits (Swenson *et al.* 2012). Thus, when testing if turnover rate in species composition decreases in a decelerating manner while succession occurs, as predicted by succession theory, it is desirable to control for turnover rate in demography. Likewise, when testing if turnover rate in functional traits decreases in a decelerating manner as succession proceeds, it is useful to control for turnover rate in demography and species composition. We are unaware of studies of the effect of selective logging on temporal turnover rates that implement these kinds of controls.

Here, we investigate the temporal dynamics of a tropical forest in Kibale National Park, Uganda during 45 years following selective logging. Given the predictions of succession theory, we test the working hypothesis that turnover rates in demography, species composition and functional traits are declining in selectively logged forest and compare changes in turnover rates to those documented in unlogged forest where we expected little or no change in turnover rates through time. This working hypothesis is reasonable because declining turnover rates characterize successional trajectories in many other

systems (see above). In particular, we examined three predictions about turnover rates derived from the working hypothesis (Fig. 1). First, during the first several years after a selective logging event, turnover rates should be higher in logged forest than in unlogged forest. This first prediction follows from the idea that the selectively logged forests are reset to a relatively earlier stage of succession due to the removal and damage of biomass. The time interval to which this prediction applies depends on the rate of replacement of early successional species by late successional species. In tropical forests, this replacement may take decades (Guariguata & Ostertag 2001; Lebrija-Trejos *et al.* 2010). Second, turnover rates in selectively logged forests should decrease with increasing time since the selective logging event, which indicates that forest stability is increasing as succession ensues. Third, turnover rates in unlogged forest should be less temporally variable than in selectively logged forests. Beyond testing these predictions with raw observed turnover rates in demography, species composition and functional traits, we also conducted tests based on null models that account for dependencies among these three kinds of turnover rates. Specifically, we used null models based on random sampling from a regional species pool (Gotelli & McGill 2006) to account for (i) the turnover rate in species composition expected by chance from the observed turnover rate in demography, (ii) the turnover rate in functional traits expected by chance from the observed turnover rate in demography, and (iii) the turnover rate in functional traits expected by chance from the observed turnover rate in species composition.

Materials and methods

STUDY SITE

This study was conducted in Kibale National Park (here-after Kibale), South-western Uganda, which covers 795 km^2 in area (Chapman *et al.* 2010). It is predominantly mature moist semi-deciduous and ever-green forest, but includes a variety of other habitats including grassland, woodland, lakes and wetlands, secondary forest, and regrowth in areas previously planted with exotic trees (Chapman & Lambert 2000). Kibale receives an average rainfall of 1643 mm annually (1990 – 2013; Chapman and Chapman unpublished data collected at Makerere University Biological Field Station) with two peak rainy seasons from March to May and September to November (Chapman *et al.* 2010). Temperature ranges between an average daily minimum of 15.5^{o}C and daily maximum of 23.7^{o}C. Kibale is divided into compartments which were subjected to varying degrees of logging, and have experienced different restoration efforts (Struhsaker 1997; Chapman *et al.* 2010). Our study involved three compartments within Kibale. The first, K-30 (282 ha), has a recent history that is relatively free of human disturbance, and is typically considered a mature old-growth forest. The second, K-14 (405 ha), was selectively logged between May and December 1969 in a spatially heterogeneous manner, so that some areas (Mikana) experienced heavy logging with the removal and damage of up to 25% of all trees, while other areas were largely untouched. The third, K-15 (347 ha), experienced high intensity selective logging between September 1968 and April 1969 resulting in removal and damage of up to 50% of all trees.

VEGETATION PLOTS

Twenty six permanent vegetation plots were randomly established within the existing trail system in Kibale in December 1989. Each plot is 200 x 10 m with the shorter plot dimension bisected by a trail. These plots were originally established with the purpose of long-term monitoring of tree phenology (Chapman *et al.* 2010). The locations of the 26 plots were unevenly distributed across the three compartments; 11 plots were located in K-30, six were in the lightly logged, and four in the heavily logged (Mikana) parts of K-14, and five were in K-15. We assigned each vegetation plot to one of two categories according to disturbance history: unlogged or selectively logged. We placed the 17 plots in K-30 and the lightly logged areas of K-14 in the unlogged category, and the 9 plots in the Mikana part of K-14 and in K-15 in the selectively logged category. The assignment of plots in the largely untouched areas of K-14 to the unlogged category was informed by earlier work showing that these areas suffered little if any damage from the logging event based on stump and gap enumeration (Kasenene 1987; Chapman & Chapman 1997; Bonnell *et al.* 2011).

DATA COLLECTION

a. Forest composition and structure

The 26 plots have been censused between March and May at four time points: 1989, 1999, 2006, and 2013. Hereafter we refer to these censuses as C_1, C_2, C_3 and C_4 respectively. Censuses of each plot involved following the fate of all trees with diameter at breast height (DBH) $\geq$ 10 cm, including recruitment of new stems and mortality of existing stems (Chapman *et al.* 2010). Trees were determined to species using taxonomic keys (Polhill 1952; Hamilton 1991; Katende *et al.* 1995; Lwanga 1996), and species

names updated using The Plant List (http://www.theplantlist.org/). The census dataset provides information on stem number, species composition, and species abundances for each plot at four time points.

b. Functional traits

We focus on three functional traits thought to be important in successional forest dynamics. First, wood density (WD; g/cm^3), a measure of a tree's dry carbon investment per unit volume, is considered a key indicator of the wood economic spectrum due to its strong connection with several aspects of a plant's ecology including growth rate, carbon allocation strategy, structural stability, hydraulic conductivity, and disease or pest resistance (Chave *et al.* 2009). The other two traits, plant maximum height (H_{MAX}; m) and maximum diameter at breast height (DBH_{MAX}; cm) are measures of adult stature, which is a crucial component of a species light competitive ability and carbon gain strategy (King *et al.* 2006; Wright *et al.* 2007; Moles *et al.* 2009). Both WD and adult stature are thought to vary with species' light requirements and forest successional stage (Falster & Westoby 2005; Chave *et al.* 2009). To estimate DBH_{MAX} we measured diameter at breast height (DBH) as the circumference of a tree trunk at 1.2 m height for all stems in the 26 plots during C_1, C_2, C_3, and C_4. Species DBH_{MAX} was considered the largest DBH value recorded for all individuals of a species from all 26 plots across all four censuses. DBH data was available for all 91 species that occurred in the plots across all censuses.

From within ten randomly selected plots, five of which were in the unlogged category and five in the selectively logged category, we used increment borers to extract wood

cores from 687 upright adult trees. Details of sampling and method for wood density determination are described in Osazuwa-Peters *et al.* (2015). However, we could estimate species mean WD for 61 species out of the 91 species across all censuses; the remaining 30 species had missing mean WD values, but we obtained species, genus, or family level WD means from the Global Wood Density Database subset for African region (Zanne *et al.* 2009) with as fine a taxonomic resolution as was available in the database. There were WD values for 7 of the missing species, genus-level wood density values for 11 species, and family-level wood density values for the remaining 12 species. Consequently, we had two wood density datasets for Kibale's species; one incomplete dataset composed of wood density values measured directly and a second complete dataset that included data compiled from the Global Wood Density Database. These two datasets were used to perform two alternative versions of all analyses involving functional traits. However, we only discuss the results based on the incomplete dataset when they differ from those based on the complete dataset.

Tree height was obtained for 892 trees in the ten randomly selected plots mentioned above, and details can be found in Osazuwa-Peters *et al.* (2015). A species' maximum height was determined as the greatest height recorded across all measured individuals of a species (King *et al.* 2006). This resulted in H_{MAX} estimates for 60 species out of the 91 species that occurred in the plots across all censuses. To obtain estimates of H_{MAX} for all species we used DBH measures that were available for 622 of the 892 stems with height data. In particular, stem height was regressed on stem DBH using this subset of the data to obtain a forest-wide relationship that was then used to interpolate height values for

species with missing height data. The regression relationship (R^2 = 0.31, P < 0.01, N = 622) was as follows:

$$\widehat{H_{MAX}} = 9.753326 + (0.052898 * DBH_{MAX}) \quad \text{Eq. (1).}$$

This relationship was used to predict H_{MAX} from species DBH_{MAX} for the 31 species with missing H_{MAX} values. Consequently, we had two H_{MAX} datasets for Kibale's species; one incomplete dataset composed of H_{MAX} values based on tree height measured directly and a second complete dataset that also included values based on the forest-wide relationship represented by equation 1. These two datasets were used in alternative versions of all analyses involving functional traits. However, we only discuss the results based on the incomplete dataset when they differ from those based on the complete dataset.

FOREST TURNOVER RATES

We quantified turnover rates in demography (mortality and recruitment), species composition, and functional traits. Due to bias associated with census interval variation (the length of the first census interval is 10 years, but 7 years for the second and third intervals), we applied the correction developed by (Lewis *et al.* 2004b) to all estimates of turnover. This correction involves standardizing turnover rate estimates to a common census length using $\lambda_{corr} = \lambda \times t^{0.08}$, where λ is the turnover rate and t is time between censuses in years.

a. Demographic turnover rate

Turnover rate in stem number (T_{SN}) in a given plot was defined as the average of the number of stems gained (recruited) and lost (dead, missing, or broken) between two

consecutive censuses, weighted by the average number of stems in the two censuses and the time interval (*t*) between the two censuses (Anderson 2007):

$$T_{SN} = \frac{\frac{1}{2}\left(\frac{D+R}{t}\right)}{\frac{1}{2}}\left[SN_{Cj} + SN_{Cj+1}\right] \quad \text{Eq. (2),}$$

where *D* is number of dead, missing, or broken stems in a plot between two consecutive censuses; *R* is number of recruited stems between two consecutive censuses; SN_{Cj} is total number of stems counted in the census C_j; and *j* takes the values 1 – 3 (see above section on forest structure and composition).

b. Species composition turnover rate

Rate of turnover in species composition (T_{SC}) was defined as the change in species composition in a plot between two consecutive censuses (*t*), weighted by the time interval between the two censuses. We measured this rate using raw metrics of dissimilarity in species composition, as well as metrics based on a null model that accounted for stem turnover rate.

We used two raw metrics of dissimilarity in species composition. The first was Bray-Curtis index (Bray & Curtis 1957):

$$T_{SCBRAY_{Cj,Cj+1}} = \frac{\Sigma_i|x_{iCj+1} - x_{iCj}| \Big/ \Sigma_i|x_{iCj} + x_{iCj+1}|}{t} \quad \text{Eq. (3),}$$

where x_{iCj} is abundance of species *i* in a given plot at census C_j. The second raw metric was the β component of the Rao's index for taxonomic diversity (De Bello *et al.* 2010):

$$T_{SCRAO_{Cj,Cj+1}} = \frac{100 * (\gamma\ Rao - \bar{\alpha}\ Rao)/\gamma\ Rao}{t} \quad \text{Eq. (4),}$$

where γ *Rao* is total diversity obtained by pooling data from two consecutive censuses of a plot (C_j and C_{j+1}), and $\overline{\alpha}$ *Rao* is the average of two α *Rao* values, each representing diversity during one of two consecutive censuses of a plot. Both γ *Rao* and α *Rao* are sums of the products of the relative abundances of all possible pairs of species. However, the relative abundance of each species is calculated as an average across two consecutive censuses in the case of γ *Rao*, while in the case of α *Rao* only data from a single census is considered (De Bello *et al.* 2010).

Raw metrics of turnover rate in species composition, such as $T_{SC.BRAY}$ and $T_{SC.RAO}$, depend at least in part on turnover rates in demography (see Introduction). It follows that differences between logged and unlogged forests in raw metrics of turnover rates in species composition may be due partially or entirely to stem turnover rates. Thus, we tested the predictions about turnover rates in species composition using a null model that accounts for the effect of observed stem turnover rate on species composition turnover rate, assuming random sampling from a regional species pool (Gotelli & McGill 2006). This null model preserved observed mortality and recruitment rates, as well as observed number of stems in each plot at each census. However, the individual stems that died in a plot during any given time interval, were randomly chosen from the stems found in the plot at the beginning of the time interval. Recruitment was simulated by randomly sampling individuals from a regional species abundance distribution. This distribution included all species found in the 26 plots during all censuses, with abundances equal to the average abundance over the four censuses (following Gotelli *et al.* 2010). We performed 1,000 iterations of the null model for each plot at each census interval ($C_1 - C_2$, $C_2 - C_3$, and $C_3 - C_4$), thus generating 1,000 null turnover values per plot and census

interval. Using this null model we computed turnover rate in species composition as the standardized effect size (*SES*): the difference between observed turnover and expected turnover under the null model (i.e., the mean of 1,000 turnover values generated by the null model), divided by the standard deviation of turnover values generated by the null model. We estimated two *SES* metrics of turnover rate in species composition, based on the two raw metrics: Bray-Curtis ($T_{SCBRAY.SES1}$) and Rao's index ($T_{SCRAO.SES1}$).

c. Functional trait turnover rate

Rate of turnover in functional traits (T_{FC}) was defined as the change in functional trait composition within a plot between two consecutive censuses, weighted by the time interval (*t*) between the two censuses (*t*). We measured rate of turnover in functional traits using raw metrics of dissimilarity in functional traits as well as metrics based on null models that accounted for turnover rates in stem number and species composition.

We used two raw metrics of turnover in functional traits. The first was absolute difference in community weighted mean between two consecutive censuses:

$$T_{|\Delta\, CWM|trait_{Cj,Cj+1}} = \frac{|CWM_{Cj+1} - CWM_{Cj}|}{t} \qquad \text{Eq. (5),}$$

where, CWM_{Cj} is the inter-specific mean of a trait value, weighted by the relative abundance of each species at census C_j. We calculated this metric to measure turnover rate in each of the three functional traits WD, H_{MAX}, or DBH_{MAX}, and refer to the respective measures as $T|\Delta CWM|WD$, $T|\Delta CWM|HMAX$, and $T|\Delta CWM|DBHMAX$.

The second raw metric of turnover in functional traits was the β component of Rao's index for functional diversity (*TFCRAO*) in the Euclidean space defined by the three functional traits (WD, H_{MAX}, or DBH_{MAX}):

$$T_{FCRAO_{Cj,Cj+1}} = \frac{100 * (\gamma_{FD}Rao - \bar{\alpha}_{FD}Rao)/\gamma_{FD}Rao}{t} \quad \text{Eq. (6),}$$

where γ_{FD} *Rao* is functional diversity obtained by pooling data from two consecutive censuses of a plot (C_j and C_{j+1}), and $\bar{\alpha}_{FD}$ *Rao* is the average of two α_{FD} *Rao* values, each representing functional diversity during one of two consecutive censuses of a plot. Both γ_{FD} *Rao* and α_{FD} *Rao* are sums of the Euclidian distances between all possible pairs of species in space defined by the three functional traits, weighted by the product of the relative abundances of the respective species pairs. However, the relative abundance of each species is calculated as an average across two consecutive censuses in the case of γ_{FD} *Rao*, while in the case of α_{FD} *Rao* only data from a single census is considered.

Raw metrics of turnover rate in functional traits depend at least partly on turnover rates in demography and species composition (see Introduction). Therefore, we used two null models to account for the effect of turnover rates in demography and species composition on turnover rate in functional traits. The first null model, hereafter null model 1, is identical to the null model described in the section on species composition turnover rates (above). It accounts for the effect of turnover rates in demography on turnover rate in functional traits, assuming sampling from a regional species pool. The second null model, hereafter null model 2, randomized trait values among species at each census interval, while maintaining the observed species abundance, species richness, and species turnover through time. Thus, null model 2 yielded expected values of turnover rate in functional

traits for observed values of species turnover in a plot, assuming trait values were randomly sampled from the set of observed trait values among all species found in the 26 plots during all censuses. Combinations of values for the three functional traits we studied (WD, H_{MAX}, and DBH_{MAX}) were not altered, but kept fixed so as to preserve observed inter-specific correlations among traits (Schleicher *et al.* 2011). We conducted 1,000 iterations of each null model for each plot and census interval, and calculated standardized effect sizes (*SES*, described above) for each of the raw metrics of turnover rates in functional traits. Extending the abbreviations for these raw metrics, we refer to *SES* values obtained from null model 1 as $T|\Delta CWM|WD.SES1$, $T|\Delta CWM|HMAX.SES1$, $T|\Delta CWM|DBHMAX.SES1$, and $T_{FCRAO.SES1}$. Likewise, we refer to *SES* values obtained from null model 2 as $T|\Delta CWM|WD.SES2$, $T|\Delta CWM|HMAX.SES2$, $T|\Delta CWM|DBHMAX.SES2$, and $T_{FCRAO.SES2}$.

STATISTICAL TESTS OF PREDICTIONS

We evaluated the three predictions described in the introduction for 17 turnover rate metrics (defined above): T_{SN}, T_{SCBRAY}, T_{SCRAO}, $T|\Delta CWM|WD$, $T|\Delta CWM|HMAX$, $T|\Delta CWM|DBHMAX$, T_{FCRAO}, $T_{SCBRAY.SES1}$, $T_{SCRAO.SES1}$, $T|\Delta CWM|WD.SES1$, $T|\Delta CWM|HMAX.SES1$, $T|\Delta CWM|DBHMAX.SES1$, $T_{FCRAO.SES1}$, $T|\Delta CWM|WD.SES2$, $T|\Delta CWM|HMAX.SES2$, $T|\Delta CWM|DBHMAX.SES2$, and $T_{FCRAO.SES2}$. To gauge empirical support for these predictions we used linear mixed effects models (lme) with restricted maximum likelihood ratio method (Bolker *et al.* 2009). These lme models allowed us to express the three predictions of interest in terms of fixed effects, while simultaneously modeling the variance among plots as a random effect. The general structure for the lme models we used was as follows:

$$TR_{iC_j} = (\beta_0 + U_{0,i}) + (\beta_1) \cdot Lo_i + (\beta_2 + U_{2,i}) \cdot Time_{iC_j} + (\beta_3) \cdot Lo_i \cdot Time_{iC_j} + \varepsilon_{iC_j}$$ Eq. (7),

where TR_{iCj} is turnover rate (as estimated by any of the 17 metrics above) in plot i (i = 1,..., 26) measured at census C_j (j = 2, 3, or 4), Lo_i is a dummy variable denoting whether plot i belongs to the unlogged (Lo_i = 0) or logged (Lo_i = 1) category, and $Time_{iCj}$ is the number of years elapsed since the selective logging event when turnover was measured in plot i at census C_j ($Time_{iCj}$ = 31, 38 or 45 years). $Time_{iCj}$ was rescaled by subtracting the length of time that had elapsed since the logging event at census C_2 (31 years). Given this rescaling, the model intercept equals the first turnover rate that we measured. In particular, the first coefficient in equation 7, β_0, represents the average intercept for plots in the unlogged category. In other words, β_0 is the average (across plots in the unlogged category) annualized turnover rate during the first census interval 31 years after the selective logging event. Coefficient β_1 is the difference in average intercept between plots in the logged and unlogged categories. The sum of the first two terms in equation 7, $\beta_0 + U_{0,i}$, is the intercept for plot i in the unlogged category. Likewise, the sum of the first three terms, $\beta_0 + U_{0,i} + \beta_1$, is the intercept for plot i in the logged category. So $U_{0,i}$ is the extent to which the intercept of plot i deviates from the average intercept for the respective category (unlogged or logged). Coefficient β_2 is the average slope relating turnover rate to time since the selective logging event for plots in the unlogged category. Coefficient β_3 is the difference in this slope between the logged and unlogged categories. The value of $U_{2,i}$ is the extent to which the slope of plot i deviates from the average slope for the respective category (unlogged or logged). Finally, ε_{iCj} represents the difference between predicted and observed turnover rate in plot i at census C_j. Terms $U_{0,i}$, $U_{2,I}$, and

ε_{iCj} are random effects, while all other coefficients in equation 7 are fixed effects. Further details of model specification are described in Appendix 1.

Now we can express the three predictions described in the introduction in terms of coefficients in the general model represented in equation 7. From here on, these coefficients are indicated with carets to denote that they are sample-based estimates of population parameters. The first prediction is that during several years after a selective logging event, turnover rate should be higher in selectively logged forest than in unlogged forest. Based on previous studies (see Introduction and Methods sections on forest composition and structure) we assumed that this prediction still applies 31 years after the selective logging event. Thus, in terms of equation 7 the first prediction can be expressed as: $\hat{\beta}_1 > 0$ (Fig. 1). The second prediction is that turnover rate in selectively logged forest should decrease with increasing time since the selective logging event. In terms of equation 7 this prediction can be expressed as: $\hat{\beta}_2 + \hat{\beta}_3 < 0$ (Fig. 1; Appendix 2a for details). The last prediction is that turnover rate in unlogged forest should be less temporally variable than in selectively logged forest. In terms of equation 7 this prediction can be expressed as: $|\hat{\beta}_2| < |\hat{\beta}_2 + \hat{\beta}_3|$ (Fig. 1). To determine empirical support for this last prediction it is necessary to consider the signs of $\hat{\beta}_2$ and $\hat{\beta}_3$. If $\hat{\beta}_3$ and $\hat{\beta}_2$ have the same sign, and $\hat{\beta}_3$ is statistically significant (i.e. it is different from zero), then the third prediction is supported. On the other hand, if $\hat{\beta}_3$ and $\hat{\beta}_2$ have different signs, the prediction is supported only if $|\hat{\beta}_3| - 2^* |\hat{\beta}_2| > 0$ (see Appendix 2b for details).

Because logging happened in a spatially structured way across the study area in Kibale, plots in the logged category occurred in more northerly latitudes than those in the unlogged category (Fig. 2). Consequently, spatial processes could influence forest turnover rates independent of the effects of selective logging (Lindenmayer & Laurance 2012; Ramage *et al.* 2013). To control for the potential effects of unmeasured factors that co-vary linearly with space, we added latitude of each plot as a variable in lme models. The lme models that included latitude had an additional coefficient, β_4, representing the average slope (across plots) of the relationship between turnover rate and latitude. Using spatial variables (e.g., latitude) in this fashion reduces Type I error (Peres-Neto & Legendre 2010) and provides a more conservative test of the predictions of interest. We compared models that included latitude with those that did not using Akaike's Information Criterion corrected for finite sample sizes (AIC_c, Burnham and Anderson 2002). We followed the general rule of thumb that $\Delta AIC_c \leq 2$ indicates similar empirical support (Appendix 3). In all cases when multiple models had similar empirical support, there were no differences in the results of the test of the predictions. Thus, we present only one model for each metric of turnover rate even when multiple models have similar empirical support.

All statistical tests were implemented in R version 2.15.1 (R Core Team 2012). Packages used included *vegan* (Oksanen *et al.* 2012) for Bray-Curtis index, package *FD* (Laliberté & Legendre 2010); (Laliberte & Shipley 2011) for community weighted means, and packages *cluster* (Maechler *et al.* 2012), *ade4* (Dray & Dufour 2007) and a sourced script (rao_script.R) (De Bello *et al.* 2010) for Rao's index. The lme models were performed with the nlme package (Pinheiro *et al.* 2007), caterpillar plots obtained with lme4

package (Bates *et al.* 2013), and ΔAIC_c and AIC_c weights obtained with the AICcmodavg package (Mazerolle 2013).

Results

a. Demographic turnover rate

In accord with the first prediction (Fig. 1), plots in the logged category had a higher intercept for stem turnover rate than plots in the unlogged category ($\hat{\beta}_1 > 0$, Table 1), indicating that stem turnover rate was higher in logged than unlogged forest 31 years after the selective logging event (Fig. 3A). However, contrary to the second prediction (Fig. 1), stem turnover rate for plots in the logged category did not change with time ($\hat{\beta}_2 + \hat{\beta}_3 = 0$, Table 1, Fig. 3A). Moreover, the third prediction (Fig. 1) was not supported because stem turnover rate was not less temporally variable for plots in the unlogged than in the logged category ($\hat{\beta}_3 < 2^* \hat{\beta}_2$, Table 1, Fig. 3A).

b. Species composition turnover rate

Estimates of turnover rate in species composition only partially supported the first prediction of higher intercept for plots in the logged than unlogged category. When measured with raw metrics of species turnover rate, plots in the logged category had higher intercepts than plots in the unlogged category ($\hat{\beta}_1 > 0$ if critical *p*-value = 0.1, Table 1, Fig. 3B and D). These results seemed to reflect the influence of demographic turnover rate on species composition turnover rate (see introduction). In particular, metrics of species composition turnover rate based on null models that control for stem turnover rate revealed either no difference in intercept between plots in the logged and

unlogged categories, or lower intercept for plots in the logged category ($\hat{\beta}_1 \leq 0$, Table 1, Fig. 3C and E).

Estimates of turnover rate in species composition for plots in the logged category did not decrease through time ($\hat{\beta}_2 + \hat{\beta}_3 \geq 0$, Table 1, Fig. 3B−E) and, thus, did not support the second prediction. Indeed, as measured by two raw metrics, turnover rate in the species composition of plots in the logged category tended to increase through time, albeit for one of these metrics the increase was not significant (Table 1). This trend of temporal increase in turnover rates did not seem to result from the effect of demographic turnover rate on species composition turnover rate, because it persisted when species composition turnover rate was measured by metrics based on null models that control for stem turnover rate (Table 1).

The third prediction (Fig. 1) was only partially supported by estimates of turnover rate in species composition. Raw metrics of turnover rate in species composition provided no support for this prediction, because turnover rate was not less temporally variable for plots in the unlogged than in the logged category ($|\hat{\beta}_2| \geq |\hat{\beta}_2 + \hat{\beta}_3|$, Table 1, Fig. 3B and D). However, as measured by one of the metrics that accounts for demographic turnover rate (T*SBRAY.SES1*), turnover rate in species composition for plots in the unlogged category was marginally less temporally variable than that for plots in the logged category ($|\hat{\beta}_2| < |\hat{\beta}_2 + \hat{\beta}_3|$, if critical *p*-value = 0.1, Table 1, Fig. 3C).

c. Functional trait turnover rate

One out of twelve metrics of turnover rate in functional traits (T_{FCRAO}) supported the first prediction of higher intercept for logged than unlogged category ($\hat{\beta}_1 > 0$, Table 1). However, this result seemed driven by the effect of demographic turnover rate on functional trait turnover rate. The metric controlling for such an effect ($T_{FCRAO.SES1}$) did not support the first prediction ($\hat{\beta}_1 \leq 0$, Table 1). None of the other metrics of turnover rate in functional traits provided support for the first prediction (in all cases $\hat{\beta}_1 \leq 0$, Table 1, Fig. 3F−G).

We found no support for the second prediction, as none of the metrics of turnover rate in functional traits decreased through time for plots in the logged category (in all cases $\hat{\beta}_2 + \hat{\beta}_3 \geq 0$, Table 1, Fig. 3F−G). Similarly, we found no support for the third prediction, according to which turnover rate should be less temporally variable in unlogged than selectively logged forest (Fig. 1). As estimated by all twelve metrics, turnover rate in functional traits was not less temporally variable for plots in the unlogged than for plots in the logged category (in all cases $|\hat{\beta}_2| \geq |\hat{\beta}_2 + \hat{\beta}_3|$, Table 1, Fig. 3F and G).

When the analyses were based on the incomplete functional trait dataset, there was no support for any of the three predictions, except in a single case, for prediction III; the unlogged forest was temporally less variable in $T_{|\Delta CWM|WD}$, observed turnover rates for wood density (See Appendix 4).

Discussion

Tropical forests store at least 40% of terrestrial carbon, process six times as much carbon as is released through fossil fuel use, and are epicenters of biodiversity (Lewis *et al.*

2004a). These forests are increasingly being modified by selective logging, but the extent to which this practice causes shifts in temporal dynamics of tropical forest communities remains unclear (Sist *et al.* 2014). Understanding the effects of selective logging on the temporal dynamics of tropical forest will help determine the extent to which tropical forests are resilient to selective logging. It will also be useful to balance the competing demands of sustainable management and conservation of tropical forests, since resilience offers insurance against loss of valued functions (Thrush *et al.* 2009). Succession theory offers a starting point to examine the resilience of tropical forests to selective logging. Based on this theory, we hypothesized that a tropical forest in East Africa had been undergoing recovery to pre-disturbance conditions during 45 years after a selective logging event. We tested three predictions derived from this working hypothesis, focusing on turnover rates of three forest attributes: demography, species composition, and functional traits. Overall, we found higher turnover rates in logged forest than in unlogged forest for all three attributes, lending support to prediction I. However, turnover rates did not decline through time in logged forest, indicating no support for prediction II. Moreover, the unlogged forest was not less temporally variable in turnover rates than the logged forest, indicating no support for prediction III. Below we highlight some caveats before discussing the implication of these results.

Caveats

As is typical of many logging-impact studies (Lindenmayer & Laurance 2012; Ramage *et al.* 2013), the logging history of vegetation study plots within Kibale is confounded with geographic space, with logged plots occupying more northerly locations than unlogged plots (Fig 2). Previous studies on Kibale have assumed structural similarity among plots

prior to logging, based on historical ground surveys that predate the logging event. These historical surveys show that the vegetation plots in this study are all located within the central block of Kibale's forests (Kingston 1967; Bonnell *et al.* 2011). Nevertheless, spatial structure could create spurious relationships between forest turnover rates and selective logging, due to the effects of unmeasured space-related factors (Legendre & Fortin 1989). The presence of spatial structure in ecological data potentially violates the assumption of independent observations, and thus may inflate degrees of freedom of classical statistical models, increasing type I error (Peres-Neto & Legendre 2010). Here we applied a simple approach to account for this potential issue, by including the latitudinal geographic coordinates for each observation as a covariate in linear mixed effects models. This covariate was significant only for turnover rates in species composition (Appendix 5). We emphasize that our approach to control for spatial non-independence of plots assumes a linear relationship between unmeasured spatial factors and the spatial proxy, latitude. Consequently, our approach may not account for complex non-linear spatial processes that may influence forest turnover rates independent of selective logging. This poses a potential problem for empirical tests of predictions I and III, which are based on the assumption that the logged and unlogged plot categories do not consistently differ in ways other than in logging history. If unmeasured processes act in a non-linear, spatially structured way, then an assumption needed to test predictions I and III would be violated. However, even in that case, the test of prediction II would remain valid. The assumption in question is not required for testing prediction II because each logged plot is compared to itself in a temporal series.

There are two other potentially important limitations of this study. First, we only considered stems ≥ 10 cm DBH, and therefore did not study the dynamics of small stems. Small stems are typically more numerous in most forests, and have higher turnover rates than large trees (Stephenson & van Mantgem 2005). Also, small stem dynamics may bear the imprint of selective logging for longer than larger trees because small-sized trees are more susceptible to fine scale variations in environmental conditions and represent the regeneration potential of the forest (Decocq *et al.* 2014). Second, because our first census (C_1) occurred 20 years after the selective logging event, it may be argued that most successional dynamics took place before observations began. However, at C_1, plots in the logged category had lower basal area and stem density (Kingston 1967; Chapman & Chapman 1997, 2004) and a higher abundance of early- to mid-successional species (Bonnell *et al.* 2011) than those in the unlogged category, substantiating the assumption of successional differences between plot categories. These observations in our study site are consistent with the idea that successional dynamics in tropical forests may take decades (Guariguata & Ostertag 2001; Lebrija-Trejos *et al.* 2010).

a. Prediction I: higher turnover rates in logged forest

Our results largely supported the prediction of higher turnover rates in selectively logged forests relative to unlogged forests for the three community attributes we studied. However, for functional traits, higher turnover rates in logged forest were apparent only when the three traits were combined into a single metric, indicating greater turnover rates in biomass for selectively logged forests. For species composition and the multivariate trait combination, this pattern of higher turnover rates in logged forest disappeared when dependencies on stem turnover were accounted for with null models (Figs. 3 B – E, H &

I). This lack of support for prediction I after accounting for stem turnover diverges from theoretical predictions based on the fit of organisms to their abiotic environment (Swenson *et al.* 2012). When observed stem and/or species turnover is accounted for, functional turnover is expected to be higher due to rapid changes in the abiotic environment following an acute disturbance, and lower when the environment is relatively constant (Swenson *et al.* 2012). Contrary to our observations, due to more recent disturbance, higher turnover rates in logged plots should have persisted after accounting for observed stem and species turnover. Nevertheless, our results indicate that the effect of selective logging on turnover rates is largely driven by stem recruitment and mortality, consistent with the idea that succession is essentially a demographic process (Horn 1974). Successional change following disturbance is considered the aggregated outcome of differential demographic responses of constituent species that results from interspecific variation in life history traits (van Breugel *et al.* 2006). Finegan (1996) described successional change as emerging from individualistic temporal patterns of growth and mortality that result in different species populations approaching maturity and decline at different points in succession. In the context of abandoned cornfields, van Breugel *et al.* (2006) demonstrate the demographic basis of succession for tropical rainforest sites in Mexico, based on higher rates of recruitment and mortality during the early stages of succession. Correspondingly, our results suggest that higher turnover rates in species composition and functional traits in logged plots were largely driven by higher rates of stem recruitment and mortality compared to unlogged plots.

b. Prediction II: declining turnover rates in logged forest

Our results did not support the prediction that turnover rates decline temporally in selectively logged forests. According to this prediction, a negative slope should characterize the relationship between time since the selective logging event and turnover rates (Fig. 1), because the logged forest would be recovering from disturbance and increasing in stability as succession ensues (Horn 1974). The absence of a decline in turnover rates through time for all three community attributes in Kibale's logged forests suggests that successional models that assume recovery to pre-disturbance structure and composition do not accurately describe the effects of selective logging on tropical forest dynamics at our site.

In contrast to prediction II, demographic and functional trait turnover rates were largely constant through time, or increased only marginally with time, while species composition turnover rates increased through time (Table 1, Fig. 3). The increasing temporal turnover rates in species composition were not a simple consequence of stochastic processes of recruitment and mortality, because this increasing trend persisted after the effect of stem turnover was accounted for with null models (Table 1; Fig 3 C & E). Thus, opposite to prediction II, logged forest seemed to be increasingly unstable in terms of species composition, despite temporally unchanging turnover rates in demography and functional traits. The absence of parallel trends in turnover rates of species composition and functional traits may be explained by functional redundancy (Fukami *et al.* 2005; Shipley 2010), which would imply that species' that replaced each other over the census intervals in logged plots were functionally similar. The tree species pool of Kibale is characterized by a high frequency of species with intermediate wood density values (0.5 – 0.75 g/cm^3), as well as poor representation of species with very low wood density (< 0.2 g/cm^3) that

might often be colonizing pioneers, and of species with very high wood density (> 0.8 g/cm^3) (Chapman *et al.* 1999; Osazuwa-Peters *et al.* 2015). The high incidence of intermediate wood density species suggests that temporal change in species abundances in logged plots is not necessarily paralleled by change in functional strategies of species, resulting in relatively constant temporal turnover rates in functional traits. This scenario is illustrated in Fig 4, which shows the relatively static distribution of wood density for all stems in the 26 vegetation plots, despite change in species abundances, as highlighted for four species with wood density of 0.7 g/cm^3.

c. Prediction III: temporally less variable turnover rates in unlogged forest

Perhaps the most surprising of our results, was the limited support for the prediction that turnover rates in unlogged forest were temporally less variable than in logged forests. The unlogged forest was expected to be temporally less variable for all three community attributes because it is considered an old-growth forest, free from human disturbance in the recent past and thought to be characterized by late-successional forest dynamics (Chapman *et al.* 2010). Consequently, temporal patterns of turnover rates in unlogged forest would represent background or reference levels, and succession theory predicts they should be less variable than turnover rates in selectively logged forest. Only for null-model based turnover rates in species composition were the unlogged forest plots less temporally variable, providing evidence that successional changes in the taxonomic composition of selectively logged forest were in excess of background turnover rates expected from demographic processes. Temporal changes in Kibale's unlogged forest may well be part of long-term successional dynamics related to large-scale disturbance in the distant past (Chapman *et al.* 2010). But even if that is the case, it would seem

surprising that recently (i.e. 45 years ago) logged forest was not more overtly variable than unlogged forest. An alternative explanation is that there are multiple forest-wide perturbations simultaneously operating on the vegetation in Kibale independent of the selective logging event 45 years ago. Three main sources of forest-wide disturbance in Kibale have been reported including changing rainfall patterns (Hartter *et al.* 2012), concentrated elephant abundance and activities (Omeja *et al.* 2014), and intense competition from non-tree vegetation (Duclos *et al.* 2013). Synergistic interactions among multiple perturbations are thought to result in long-term changes in fundamental aspects of the structure and function of biological communities (Paine *et al.* 1998). Such long-term changes are suggested by global trends in turnover of species composition for a wide range of taxa and biomes during the last 40 years (Dornelas *et al.* 2014).

Conclusion

Much of the focus on the effects of selective logging on tropical forests has been on the state of tropical forests at a single point in time and, to a lesser extent, on the temporal dynamics of demography or species composition. Here, we simultaneously investigated the effect of selective logging on tropical forest dynamics in demography, species and functional trait composition, while accounting for interdependencies among these three kinds of community dynamics using null models. The main take home message from our study is that classical successional models that assume recovery to pre-disturbance conditions seem inadequate for predicting the effects of selective logging on the dynamics of the tropical forest in Kibale. We found no empirical support for decline in turnover rates through time following selective logging. Demographic and functional turnover rates in logged forest plots did not show significant temporal trends, in contrast

to turnover rates in species composition that increased linearly with time since logging. Lastly, many of the temporal turnover rate patterns were driven primarily by demographic turnover rate, with the exception of temporal increases in species composition turnover rates, which remained after accounting for the effect of stem turnover.

Future work may be aimed at determining the generality or uniqueness of our results from Kibale, based on similar studies in tropical forests elsewhere, avoiding when possible confounding spatial location and logging history. Succession is thought to be driven by short-term local drivers (e.g. plant life cycles, nutrient fluxes, and herbivory), but constrained by long-term regional processes such as species pool dynamics (Walker & Wardle 2014). Consequently, results in this study may be shaped by Kibale's specific ecology and constrained by the history of African tropical forests including a relatively small regional species pool and historically few and small disturbances as compared to other tropical regions (Richards, 1996; Chapman *et al*., 1999).

Nevertheless, our results lead to the conclusion that tropical forests are not as resilient to selective logging effects as widely thought (Putz *et al.* 2012; Edwards & Laurance 2013). Selective logging resulted in persistently higher turnover rates in Kibale's forest, which may compromise the carbon storage capacity of these forests. Selective logging effects may also interact with effects from other global change trends, particularly climate change. The synergistic effects of multiple perturbations could potentially cause major long-term shifts in the dynamics of tropical forests. Ultimately, the view that selective logging is a benign approach to the management of tropical forests should be

reconsidered in the light of the studies on the effects of this practice on long-term forest dynamics.

Acknowledgements

This work was supported by the Whitney Harris World Ecology Center [to O.L.O]; the Webster Groves Nature Study Society [to O.L.O]; IDEA WILD [to O.L.O]; NSERC [to C.A.C]; FQRNT [to C.A.C]; and the National Institutes of Health [grant TW009237 to C.A.C] as part of the joint NIH-NSF Ecology of Infectious Disease program and the UK Economic and Social Research Council. C.A.C. thanks Richard Wrangham for help with establishing the plots in 1989. O. L. O. thanks the Uganda Wildlife Authorities for permission to conduct this research; Atwijuze Seezi and Kabagambe Prime for invaluable field assistance; Patrick Omeja, the Chapman lab, and staff of Kibale for logistic support; Euridice Honorio and Tim Baker (University of Leeds) for expert taxonomy advice during field work in Kibale; and Peter Stevens for comments on earlier versions of the manuscript.

References

1.
Anderson, K.J. (2007). Temporal patterns in rates of community change during succession. *Am. Nat.*, 169, 780–793.

2.
Anderson-Teixeira, K.J., Miller, A.D., Mohan, J.E., Hudiburg, T.W., Duval, B.D. & DeLucia, E.H. (2013). Altered dynamics of forest recovery under a changing climate. *Glob. Change Biol.*, 19, 2001–2021.

3.
Asner, G.P., Rudel, T.K., Aide, T.M., Defries, R. & Emerson, R. (2009). A contemporary assessment of change in humid tropical forests [WWW Document]. URL http://si-pddr.si.edu/dspace/handle/10088/18690?mode=full.

4.
Baraloto, C., Hérault, B., Paine, C.E.T., Massot, H., Blanc, L., Bonal, D., *et al.* (2012). Contrasting taxonomic and functional responses of a tropical tree community to selective logging. *J. Appl. Ecol.*, 49, 861–870.

5.
Bates, D., Maechler, M., Bolker, B. & Walker, S. (2013). lme4: Linear mixed-effects models using Eigen and S4. R package version 1.0-4.

6.
De Bello, F., Lavergne, S., Meynard, C.N., Lepš, J. & Thuiller, W. (2010). The partitioning of diversity: showing Theseus a way out of the labyrinth. *J. Veg. Sci.*, 21, 992–1000.

7.
Blanc, L., Echard, M., Herault, B., Bonal, D., Marcon, E., Chave, J., *et al.* (2009). Dynamics of aboveground carbon stocks in a selectively logged tropical forest. *Ecol. Appl.*, 19, 1397–1404.

8.
Bolker, B.M., Brooks, M.E., Clark, C.J., Geange, S.W., Poulsen, J.R., Stevens, M.H.H., *et al.* (2009). Generalized linear mixed models: a practical guide for ecology and evolution. *Trends Ecol. Evol.*, 24, 127–135.

9.
Bonnell, T.R., Reyna-Hurtado, R. & Chapman, C.A. (2011). Post-logging recovery time is longer than expected in an East African tropical forest. *For. Ecol. Manag.*, 261, 855–864.

10.

Bray, J.R. & Curtis, J.T. (1957). An ordination of the upland forest communities of Southern Wisconsin. *Ecol. Monogr.*, 27, 325.

11.
Van Breugel, M., Martínez-Ramos, M. & Bongers, F. (2006). Community dynamics during early secondary succession in Mexican tropical rain forests. *J. Trop. Ecol.*, 22, 663–674.

12.
Cannon, C.H., Peart, D.R. & Leighton, M. (1998). Tree species diversity in commercially logged Bornean rainforest. *Science*, 281, 1366–1368.

13.
Carreño-Rocabado, G., Peña-Claros, M., Bongers, F., Alarcón, A., Licona, J.-C. & Poorter, L. (2012). Effects of disturbance intensity on species and functional diversity in a tropical forest. *J. Ecol.*, 100, 1453–1463.

14.
Chapman, C.A. & Chapman, L.J. (1997). Forest regeneration in logged and unlogged forests of Kibale National Park, Uganda. *Biotropica*, 29, 396–412.

15.
Chapman, C.A. & Chapman, L.J. (2004). Unfavorable successional pathways and the conservation value of logged tropical forest. *Biodivers. Conserv.*, 13, 2089–2105.

16.
Chapman, C.A., Chapman, L.J., Jacob, A.L., Rothman, J.M., Omeja, P., Reyna-Hurtado, R., *et al.* (2010). Tropical tree community shifts: Implications for wildlife conservation. *Biol. Conserv.*, 143, 366–374.

17.
Chapman, C.A., Chapman, L.J., Kaufman, L. & Zanne, A.E. (1999). Potential causes of arrested succession in Kibale National Park, Uganda: growth and mortality of seedlings. *Afr. J. Ecol.*, 37, 81–92.

18.
Chapman, C.A. & Lambert, J.E. (2000). Habitat alteration and the conservation of African primates: Case study of Kibale National Park, Uganda. *Am. J. Primatol.*, 50, 169–185.

19.
Chave, J., Coomes, D., Jansen, S., Lewis, S.L., Swenson, N.G. & Zanne, A.E. (2009). Towards a worldwide wood economics spectrum. *Ecol. Lett.*, 12, 351–366.

20.
Chazdon, R.L., Letcher, S.G., van Breugel, M., Martinez-Ramos, M., Bongers, F. &

Finegan, B. (2007). Rates of change in tree communities of secondary Neotropical forests following major disturbances. *Philos. Trans. R. Soc. B Biol. Sci.*, 362, 273–289.

21.
Decocq, G., Beina, D., Jamoneau, A., Gourlet-Fleury, S. & Closset-Kopp, D. (2014). Don't miss the forest for the trees! Evidence for vertical differences in the response of plant diversity to disturbance in a tropical rain forest. *Perspect. Plant Ecol. Evol. Syst.*, 16, 279–287.

22.
Dray, S. & Dufour, A.B. (2007). The ade4 package: implementing the duality diagram for ecologists. *J. Stat. Softw.*, 22, 1–20.

23.
Duclos, V., Boudreau, S. & Chapman, C.A. (2013). Shrub cover influence on seedling growth and survival following logging of a tropical forest. *Biotropica*, 45, 419–426.

24.
Edwards, D.P. & Laurance, W.F. (2013). Biodiversity Despite Selective Logging. *Science*, 339, 646–647.

25.
Facelli, J.M. & D'Angela, E. (1990). Directionality, convergence, and rate of change during early succession in the Inland Pampa, Argentina. *J. Veg. Sci.*, 1, 255–260.

26.
Falster, D.S. & Westoby, M. (2005). Alternative height strategies among 45 dicot rain forest species from tropical Queensland, Australia. *J. Ecol.*, 93, 521–535.

27.
Finegan, B. (1996). Pattern and process in neotropical secondary rain forests: the first 100 years of succession. *Trends Ecol. Evol.*, 11, 119–124.

28.
Fukami, T., Martijn Bezemer, T., Mortimer, S.R. & van der Putten, W.H. (2005). Species divergence and trait convergence in experimental plant community assembly. *Ecol. Lett.*, 8, 1283–1290.

29.
Gibson, L., Lee, T.M., Koh, L.P., Brook, B.W., Gardner, T.A., Barlow, J., *et al.* (2011). Primary forests are irreplaceable for sustaining tropical biodiversity. *Nature*, 478, 378–381.

30.
Gotelli, N.J., Dorazio, R.M., Ellison, A.M. & Grossman, G.D. (2010). Detecting temporal

trends in species assemblages with bootstrapping procedures and hierarchical models. *Philos. Trans. R. Soc. B Biol. Sci.*, 365, 3621–3631.

31.
Gotelli, N.J. & McGill, B.J. (2006). Null Versus Neutral Models: What's The Difference? *Ecography*, 29, 793–800.

32.
Gourlet-Fleury, S., Mortier, F., Fayolle, A., Baya, F., Ouédraogo, D., Bénédet, F., *et al.* (2013). Tropical forest recovery from logging: a 24 year silvicultural experiment from Central Africa. *Philos. Trans. R. Soc. B Biol. Sci.*, 368, 20120302.

33.
Guariguata, M.R. & Ostertag, R. (2001). Neotropical secondary forest succession: changes in structural and functional characteristics. *For. Ecol. Manag.*, 148, 185–206.

34.
Hamilton, A. (1991). *A Field Guide to Ugandan Forest Trees*. Makerere University.

35.
Hartter, J., Stampone, M.D., Ryan, S.J., Kirner, K., Chapman, C.A. & Goldman, A. (2012). Patterns and perceptions of climate change in a biodiversity conservation hotspot. *PLoS ONE*, 7, e32408.

36.
Horn, H.S. (1974). The ecology of secondary succession. *Annu. Rev. Ecol. Syst.*, 5, 25–37.

37.
Kasenene, J.M. (1987). *The Influence of Mechanized Selective Logging, Felling Intensity and Gap-size on the Regeneration of a Tropical Moist Forest in the Kibale Forest Reserve, Uganda*. Michigan State University.

38.
Katende, A.B., Birnie, A. & Tengnäs, B. (1995). *Useful trees and shrubs for Uganda: identification, propagation, and management for agricultural and pastoral communities*. Regional Soil Conservation Unit, Nairobi, Kenya.

39.
King, D.A., Wright, S.J. & Connell, J.H. (2006). The contribution of interspecific variation in maximum tree height to tropical and temperate diversity. *J. Trop. Ecol.*, 22, 11–24.

40.
Kingston, B. (1967). *Working plan for the Kibale and Itwara Central Forest Reserves: Toro District, Uganda.* Uganda Forest Dept., Entebbe.

41.
Laliberté, E. & Legendre, P. (2010). A distance-based framework for measuring functional diversity from multiple traits. *Ecology*, 91, 299–305.

42.
Laliberte, E. & Shipley, B. (2011). FD: measuring functional diversity from multiple traits, and other tools for functional ecology.

43.
Lebrija-Trejos, E., Meave, J.A., Poorter, L., Pérez-García, E.A. & Bongers, F. (2010). Pathways, mechanisms and predictability of vegetation change during tropical dry forest succession. *Perspect. Plant Ecol. Evol. Syst.*, 12, 267–275.

44.
Legendre, P. & Fortin, M.J. (1989). Spatial pattern and ecological analysis. *Vegetatio*, 80, 107–138.

45.
Lewis, S.L., Malhi, Y. & Phillips, O.L. (2004a). Fingerprinting the impacts of global change on tropical forests. *Philos. Trans. R. Soc. Lond. B. Biol. Sci.*, 359, 437–462.

46.
Lewis, S.L., Phillips, O.L., Sheil, D., Vinceti, B., Baker, T.R., Brown, S., *et al.* (2004b). Tropical forest tree mortality, recruitment and turnover rates: calculation, interpretation and comparison when census intervals vary. *J. Ecol.*, 92, 929–944.

47.
Lindenmayer, D.B. & Laurance, W.F. (2012). A history of hubris – Cautionary lessons in ecologically sustainable forest management. *Biol. Conserv.*, 151, 11–16.

48.
Lwanga, J. (1996). Trees and Shrubs. In: *Kibale For. Biodivers. Rep.* Forest Department, Kampala, pp. 15 – 36.

49.
Maechler, M., Rousseeuw, P., Struyf, A., Hubert, M. & Hornik, K. (2012). cluster: Cluster Analysis Basics and Extensions. R package version 1.14.2.

50.
Mazerolle, M.J. (2013). AICcmodavg: Model selection and multimodel inference based on (Q)AIC(c). R package version 1.33.

51.
Moles, A.T., Warton, D.I., Warman, L., Swenson, N.G., Laffan, S.W., Zanne, A.E., *et al.* (2009). Global patterns in plant height. *J. Ecol.*, 97, 923–932.

52.
Myster, R.W. & Pickett, S.T.A. (1994). A comparison of rae of succession over 18 yr in 10 contrasting old fields. *Ecology*, 75, 387 – 392.

53.
Oksanen, J., Blanchet, G.F., Kindt, R., Legendre, P., Minchin, P.R., O'Hara, R.B., *et al.* (2012). vegan: Community Ecology Package.

54.
Omeja, P., Aerin, J.L., Lawes, M.J., Lwanga, J.S., Rothman, J.M., Tumwesigye, C., *et al.* (2014). Do changes in elephant abundance affect forest composition or regeneration? *Biotropica*, 46.

55.
Osazuwa-Peters, O.L., Chapman, C.A. & Zanne, A.E. (2015). Selective logging: does the imprint remain on tree structure and composition after 45 years? *Conserv. Physiol.*

56.
Paine, R.T., Tegner, M.J. & Johnson, E.A. (1998). Compounded Perturbations Yield Ecological Surprises. *Ecosystems*, 1, 535–545.

57.
Peres-Neto, P.R. & Legendre, P. (2010). Estimating and controlling for spatial structure in the study of ecological communities. *Glob. Ecol. Biogeogr.*, 19, 174–184.

58.
Pickett, S., Meiners, S. & Cadenasso, M. (2011). Domain and propositions of succession theory. *Fac. Res. Creat. Act.*, Paper 21.

59.
Pinheiro, J., Bates, D., DebRoy, S. & Sarkar, D. (2007). Linear and nonlinear mixed effects models. *R Package Version*, 3, 57.

60.
Polhill, R.M. (1952). *Flora of Tropical East Africa*. Balkema.

61.
Prach, K. & Walker, L.R. (2011). Four opportunities for studies of ecological succession. *Trends Ecol. Evol.*, 26, 119–123.

62.
Putz, F.E., Zuidema, P.A., Synnott, T., Peña-Claros, M., Pinard, M.A., Sheil, D., *et al.* (2012). Sustaining conservation values in selectively logged tropical forests: the attained and the attainable. *Conserv. Lett.*, 5, 296–303.

63.
Ramage, B.S., Sheil, D., Salim, H.M.W., Fletcher, C., Mustafa, N.-Z.A., Luruthusamay, J.C., *et al.* (2013). Pseudoreplication in tropical forests and the resulting effects on biodiversity conservation. *Conserv. Biol.*, 27, 364–372.

64.
R Core Team. (2012). R: A language and environment for statistical computing. [WWW Document]. *R Found. Stat. Comput. Vienna Austria*. URL http://www.r-project.org/.

65.
Schleicher, A., Peppler-Lisbach, C. & Kleyer, M. (2011). Functional traits during succession: is plant community assembly trait-driven? *Preslia*, 83, 347 – 370.

66.
Sheil, D., Jennings, S. & Savill, P. (2000). Long-term permanent plot observations of vegetation dynamics in Budongo, a Ugandan rain forest. *J. Trop. Ecol.*, 16, 865–882.

67.
Shipley, B. (2010). *From plant traits to vegetation structure: chance and selection in the assembly of ecological communities*. Cambridge University Press, Cambridge; New York.

68.
Sist, P., Rutishauser, E., Peña-Claros, M., Shenkin, A., Hérault, B., Blanc, L., *et al.* (2014). The Tropical managed Forests Observatory: a research network addressing the future of tropical logged forests. *Appl. Veg. Sci.*, n/a–n/a.

69.
Sist, P., Rutishauser, E., Peña-Claros, M., Shenkin, A., Hérault, B., Blanc, L., *et al.* (2015). The Tropical managed Forests Observatory: a research network addressing the future of tropical logged forests. *Appl. Veg. Sci.*, 18, 171–174.

70.
Stephenson, N.L. & van Mantgem, P.J. (2005). Forest turnover rates follow global and regional patterns of productivity. *Ecol. Lett.*, 8, 524–531.

71.
Struhsaker, T.T. (1997). Ecology of an African rain forest: logging in Kibale and the conflict between conservation and exploitation., xxii + 434 pp.

72.
Swenson, N.G., Stegen, J.C., Davies, S.J., Erickson, D.L., Forero-Montaña, J., Hurlbert, A.H., *et al.* (2012). Temporal turnover in the composition of tropical tree communities: functional determinism and phylogenetic stochasticity. *Ecology*, 93, 490–499.

73.
Thrush, S., Hewitt, J., Dayton, P., Coco, G., Lohrer, A., Norkko, A., *et al.* (2009). Forecasting the limits of resilience: integrating empirical research with theory. *Proc. R. Soc. B Biol. Sci.*, 276, 3209–3217.

74.
Verburg, R. & van Eijk-Bos, C. (2003). Effects of selective logging on tree diversity, composition and plant functional type patterns in a Bornean rain forest. *J. Veg. Sci.*, 14, 99–110.

75.
Walker, L.R. & del Moral, R. (2008). Transition dynamics in succession: implication for rates, trajectories and restoration. In: *New Models Ecosyst. Dyn. Restor.* Island Press.

76.
Walker, L.R. & Wardle, D.A. (2014). Plant succession as an integrator of contrasting ecological time scales. *Trends Ecol. Evol.*, 29, 504–510.

77.
Wright, I.J., Ackerly, D.D., Bongers, F., Harms, K.E., Ibarra-Manriquez, G., Martinez-Ramos, M., *et al.* (2007). Relationships among ecologically important dimensions of plant trait variation in seven neotropical forests. *Ann. Bot.*, 99, 1003–1015.

78.
Zanne, A.E., Lopez-Gonzalez, G., Coomes, D.A., Ilic, J., Jansen, S., Lewis, S.L., *et al.* (2009). Data from: Towards a worldwide wood economics spectrum [WWW Document]. URL http://hdl.handle.net/10255/dryad.234.

Table

Table 1: Empirical support for the three predictions derived from the working hypothesis that logged forest has undergone declining rates of turnover (Fig. 1). The two columns under prediction III correspond to the following two cases: when $\hat{\beta}_2$ and $\hat{\beta}_3$ have the same sign, prediction III is supported if $\hat{\beta}_3 \neq 0$; and when $\hat{\beta}_2$ and $\hat{\beta}_3$ have different signs, prediction III is supported if $|\hat{\beta}_3| - 2 * |\hat{\beta}_2| > 0$. "NA" under any of these columns means the respective case does not apply. Values in bold indicate support for predictions. Significant difference from zero is indicated by superscripts, and critical level of significance indicated as ** = 0.01, * = 0.05, and ˙ = 0.1. Acronyms defined as follows: *T* = turnover, *SN* = stem number, *SC* = species composition, *FC* = functional composition, *LAT* = latitude, *BRAY* = Bray-Curtis index, *RAO* = Rao's index, $|\Delta CWM|$ = absolute difference in community weighted mean, *WD* = wood density, H_{MAX} = maximum height, DBH_{MAX} = maximum diameter at breast height, *SES1* = standardized effect size from Null model 1, and *SES2* = standardized effect size from Null model 2.

Turnover rate	**Metric**	**Predictions**			
		I	**II**	**III**	
		$\hat{\beta}_1 > 0$	$\hat{\beta}_2 + \hat{\beta}_3 < 0$	$\hat{\beta}_3 \neq 0$	$\lvert\beta_3\rvert - 2 * \lvert\beta_2\rvert > 0$
Demographic	T_{SN}	**0.007***	0.00008	NA	-0.00072
Species composition	T_{SCBRAY}	**0.005˙**	0.00043**	NA	-0.00087*
Species composition	$T_{SCBRAY.SES1\_LAT}$	-1.669*	0.132**	**0.107˙**	NA
Species composition	T_{SCRAO} #	**0.705˙**	0.031	0.00331	NA
Species composition	$T_{SCRAO.SES1}$	-0.575	0.104*	NA	0.087
Functional trait	$T_{\lvert\Delta CWM\rvert WD}$	0.00026	0.00001	0.000002	NA
Functional trait	$T_{\lvert\Delta CWM\rvert WD.SES1}$	-0.249**	0.016˙	NA	0.011
Functional trait	$T_{\lvert\Delta CWM\rvert WD.SES2}$	-0.290	0.005	NA	-0.009
Functional trait	$T_{\lvert\Delta CWM\rvert HMAX}$ §	0.078	-0.003	NA	-0.002
Functional trait	$T_{\lvert\Delta CWM\rvert HMAX.SES1}$	-0.096	0.005	0.00267	NA
Functional trait	$T_{\lvert\Delta CWM\rvert HMAX.SES2}$	0.149	-0.032	NA	0.021
Functional trait	$T_{\lvert\Delta CWM\rvert DBHMAX}$ §	0.242	-0.014	NA	0.005
Functional trait	$T_{\lvert\Delta CWM\rvert DBHMAX.SES1}$	-0.015	-0.00052	-0.00042	NA
Functional trait	$T_{\lvert\Delta CWM\rvert DBHMAX.SES2}$	0.173	-0.039	-0.02907	NA
Functional trait	T_{FCRAO} #	**1.086****	0.005	NA	-0.028

Functional trait	$T_{FCRAO.SES1}$	1.526	0.426 ·	NA	0.392
Functional trait	$T_{FCRAO.SES2}$	3.971	0.090	NA	0.075

[#] Turnover rate natural-log transformed to normalize residuals
[§] Turnover rate square root transformed to normalize residuals

Figures

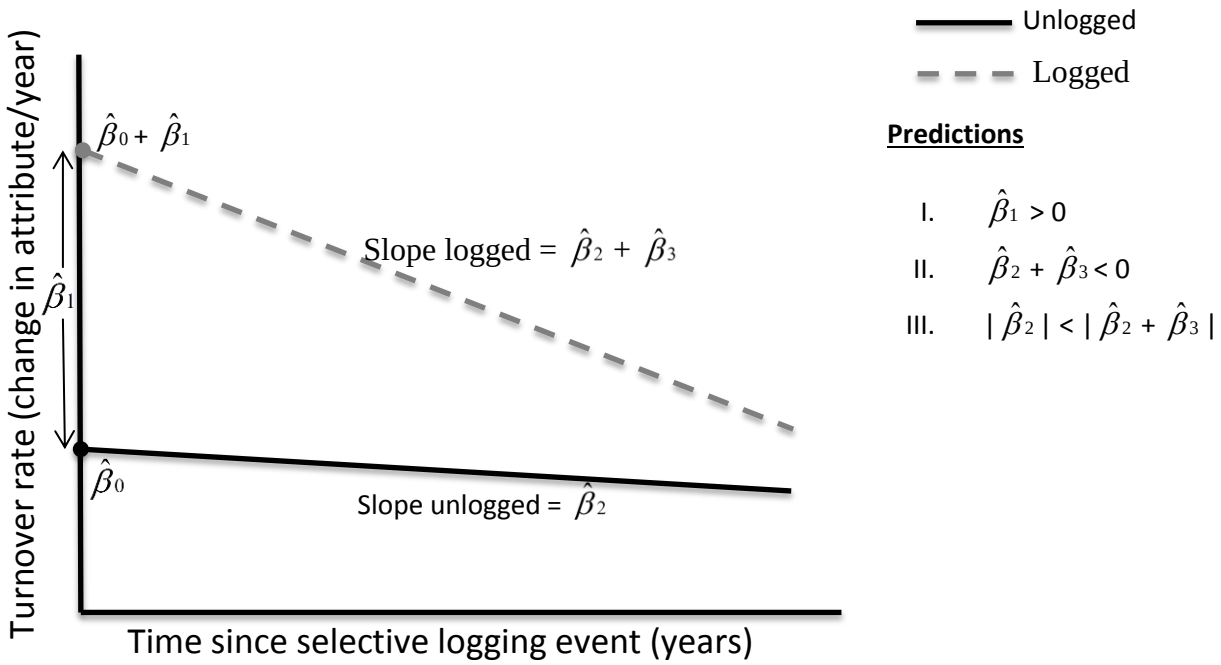

Figure 1: Conceptual figure illustrating predictions based on succession theory. Predictions are expressed in a linear regression framework, focusing on the intercepts and slopes. $\hat{\beta}_0$ is the intercept (i.e. turnover rate when time since selective logging event equals zero) for unlogged plots, $\hat{\beta}_1$ is the difference in intercepts between unlogged and logged plots, such that the intercept for logged plots equals $\hat{\beta}_0 + \hat{\beta}_1$. $\hat{\beta}_2$ is the slope for the effect of time on turnover rates in unlogged plots. $\hat{\beta}_3$ is the difference in slopes between logged and unlogged plots, such that the slope for logged plots equals $\hat{\beta}_2 + \hat{\beta}_3$. Prediction 1: higher turnover rates in logged plots, implies $\hat{\beta}_1 > 0$. Prediction 2: declining temporal turnover rates in logged plots, implies $\hat{\beta}_2 + \hat{\beta}_3 < 0$. Prediction 3: less temporally variable turnover rates in unlogged plots, implies $|\hat{\beta}_2| < |\hat{\beta}_1 + \hat{\beta}_2|$.

Figure 2: Location of study site in Kibale National Park (Kibale), southwest Uganda, East Africa. Left panel shows the location of 26 vegetation plots, northwest of Kibale. Right panel shows the detailed spatial arrangement of logged (N = 9) and unlogged (N= 17) vegetation plots within Kibale.

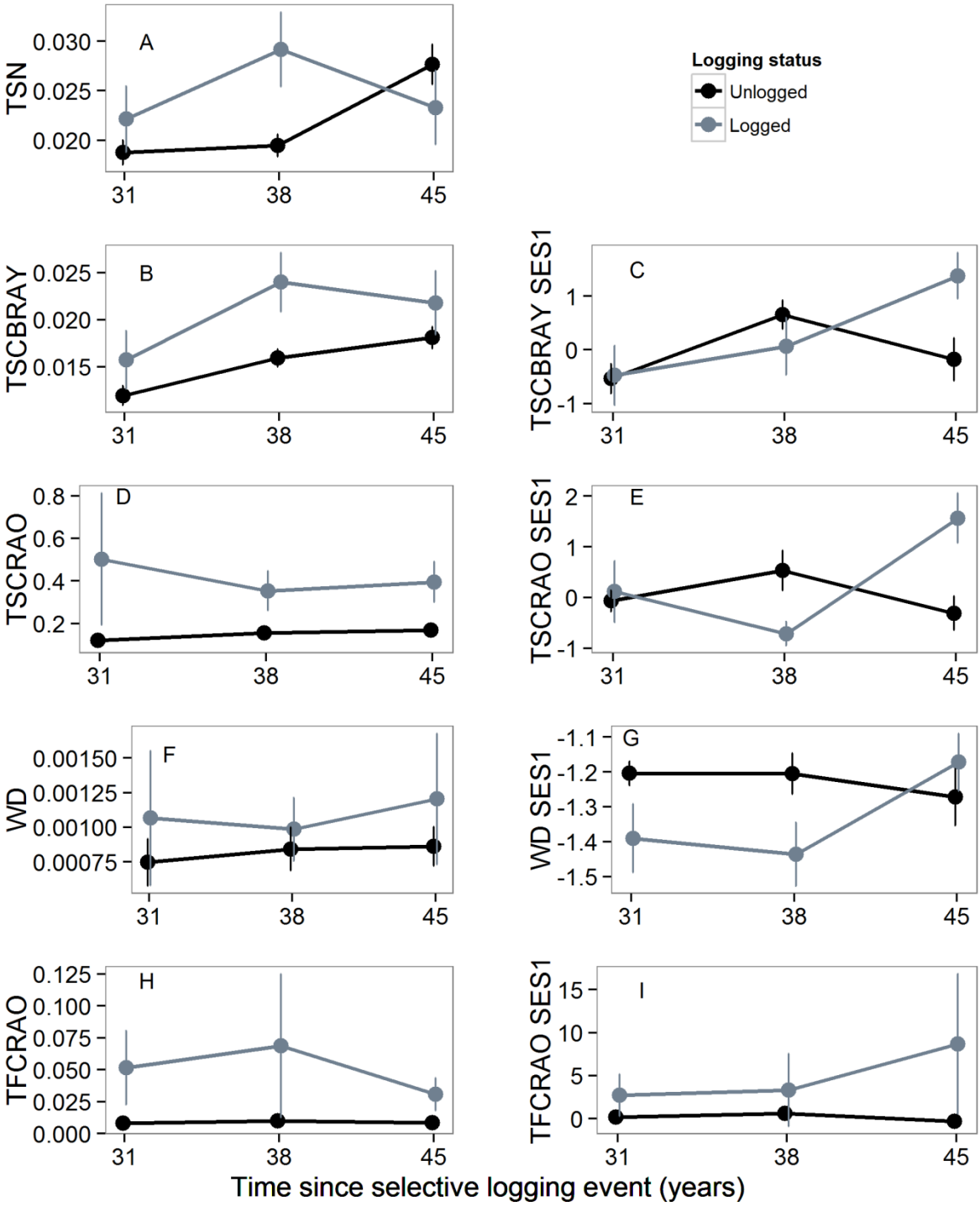

Figure 3: Turnover rates in logged and unlogged plots at three time points since the logging event; A. Turnover rates in stem number. B. Turnover rates in species composition estimated with Bray-Curtis index (T_{SCBRAY}). C. Standardized effect size (SES) for turnover rates in species composition estimated with Bray-Curtis index from Null model 1 (*SES1* T_{SCBRAY}). D. Turnover rates in species composition estimated with

Rao's index (T_{SCRAO}). E. SES for turnover rates in species composition estimated with Rao's index from Null model 1 (*SES1* T_{SCRAO}). F. Turnover rates in wood density (WD). G. SES for turnover rates in WD from Null model 1 (WD SES1). H. Turnover rates in the multivariate trait combination of three traits (T_{FCRAO}), WD, H_{MAX} and DBH_{MAX} I. SES for turnover rates in T_{FCRAO} from Null model 1 (*SES1* T_{FCRAO}). First census interval was from 1989 – 1999, the next census interval was from 1999 – 2006, and the last census interval was from 2006 – 2013, representing 31, 38 and 45 years since the selective logging event, respectively.

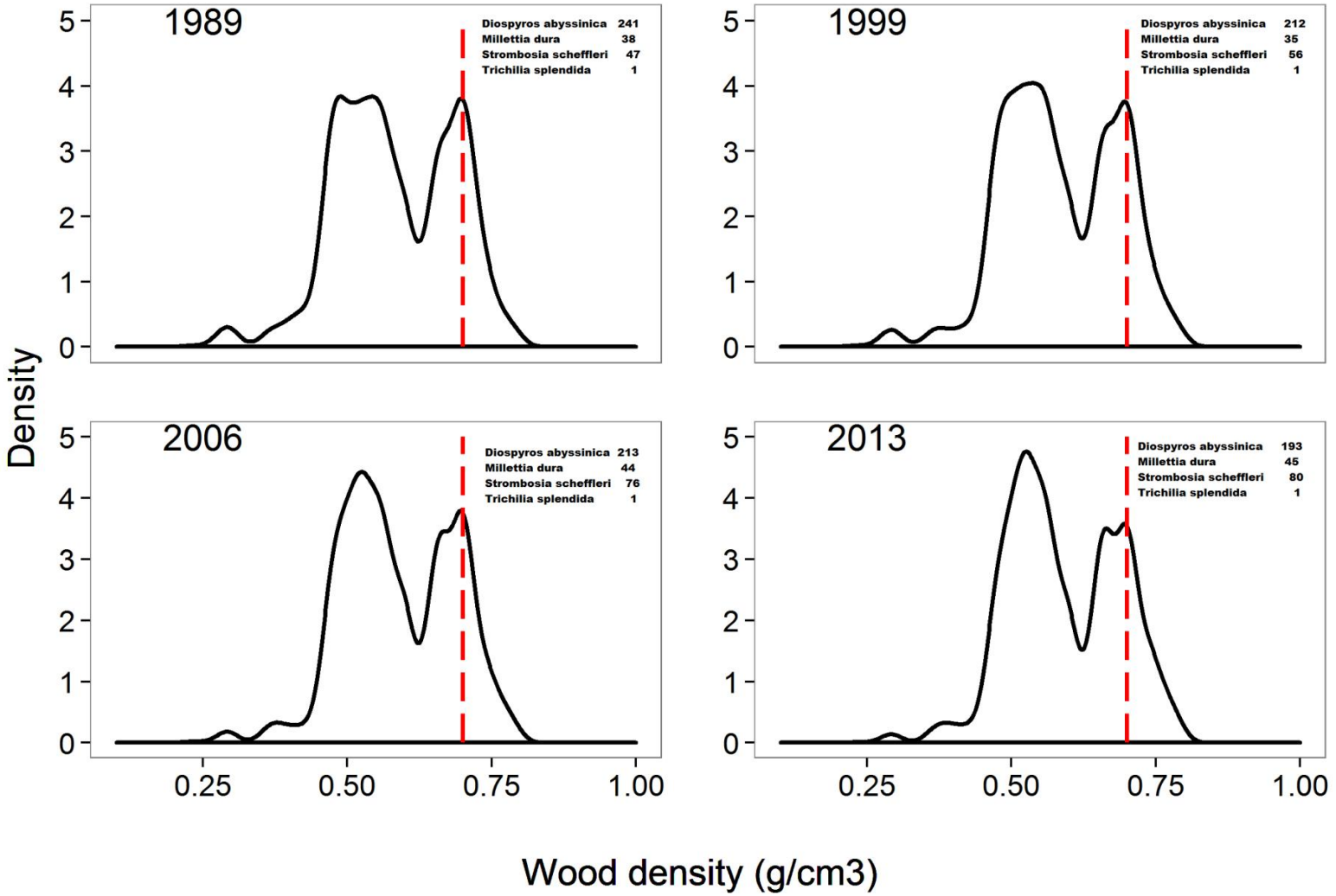

Figure 4: Kernel density estimation showing the distribution of wood density values in Kibale at each census (1989, 1999, 2006 and 2013), where each individual in all 26 vegetation plots was assigned mean wood density values of their species. Wood density distribution remains similar across four censuses despite change in the abundance of species. As an example, notice temporal change in the abundances of the four species (top right corner of graph) with 0.7 g/cm^3 wood density (broken red line).

Supplementary information for chapter 4

Appendix 1a: Specification of three models varying in the structure of random effects, to determine the optimal random structure for the linear mixed model for each estimate of turnover.

Model	**Level-2 equations**	**Assumptions made for the random effects**	**Composite equation**
A: random intercept	$\beta_{0i} = \beta_0 + U_{0i}$ $\beta_{2i} = \beta_2$	$U_{0i} \sim N\,(0, \tau_0^2)$	$\text{Turnover}_{ij} = (\beta_0 + U_{0i}) + \beta_1 \cdot Logging\ status_i + \beta_2 \cdot Time_{ij} + \beta_3 \cdot Logging\ status_i * Time_{ij} + \varepsilon_{ij}$
B: random slope	$\beta_{0i} = \beta_0$ $\beta_{2i} = \beta_2 + U_{2i}$	$U_{2i} \sim N\,(0, \tau_2^2)$	$\text{Turnover}_{ij} = \beta_0 + \beta_1 \cdot Logging\ status_i + (\beta_2 + U_{2i}) \cdot Time_{ij} + \beta_3 \cdot Logging\ status_i * Time_{ij} + \varepsilon_{ij}$
C: random intercept and random slope	$\beta_{0i} = \beta_0 + U_{0i}$ $\beta_{2i} = \beta_2 + U_{2i}$	$\begin{bmatrix} U_{0i} \\ U_{2i} \end{bmatrix} \sim N\left(\begin{bmatrix} 0 \\ 0 \end{bmatrix}, \begin{bmatrix} \tau_0^2 & \tau_{02} \\ \tau_{02} & \tau_2^2 \end{bmatrix}\right)$	$\text{Turnover}_{ij} = (\beta_0 + U_{0i}) + \beta_1 \cdot Logging\ status_i + (\beta_2 + U_{2i}) \cdot Time_{ij} + \beta_3 \cdot Logging\ status_i * Time_{ij} + \varepsilon_{ij}$

As in the main text, *i* denotes the plot (*i* = 1,.,., 26), and *j* the time point of measurement on that plot. β_0 represents the intercept or the estimated average turnover rate for the reference group (unlogged plots) when the predictors equal zero. β_1 is the difference between β_0 and estimated average turnover rate for the comparison group (logged plots). β_2 is the slope for the fixed effect of time on turnover rates for the reference group. β_3 is the slope for the interaction effect of logging status and time, which implies the difference between the slope for the effect of time on turnover rates for unlogged plots and the slope for logged plots. ε_{ij} represents the within plot error which captures the difference between turnover rates on time point *j* in plot *i* and the predicted average turnover rates for the *i*-th plot. ε_{ij} is generally assumed to be normally distributed with variance equals σ^2, which captures within plot variation. U_{0i} is the between-plot random effects, capturing the difference between the intercept of the *i*-th plot and the average intercept. U_{0i} is assumed to belong to a normal distribution *N*, with mean zero and a

variance τ_0 which captures the between individual variation. Similarly, U_{2i} is a random term that captures the difference between the slope for time of the *i*-th plot and the average slope for time. It is also assumed to be normally distributed with mean zero and a variance τ_2. The term τ_{02} is the covariance or joint variability between U_0 and U_2.

Appendix 1b: AIC_c values for models A, B, and C as described in appendix 1a above for each estimate of turnover rate. The optimal random structure for the lme model for each estimate of turnover rate was determined by comparing a random intercept (model A), a random slope (model B), and a random intercept and slope model (model C), and selecting the model with the lowest AIC_c value. Additionally, for each estimate of turnover rate, we examined caterpillar plots of plot level residuals (level 2 residuals) to confirm whether random intercepts and or random coefficients were necessary in the lme model. We conducted model diagnostics on the level-1 residuals to check the validity of model assumptions for lme models. Bold AIC_c values indicate selected model based on lowest AIC_c value, or when there is a tie in AIC_c values, model with the simplest random structure or significant difference from the previous model based on log likelihood ratio test. Acronyms defined as follows: *T* = turnover, *SN* = stem number, *SC* = species composition, *FC*= functional composition, *LAT*=latitude, *BRAY*= Bray Curtis Dissimilarity, *RAO*= Rao's index, $|\Delta CWM|$= absolute difference in community weighted mean, *WD* = wood density, H_{MAX}= maximum height, DBH_{MAX} = maximum diameter at breast height, *SES1* = standardized effect size from Null model 1, *SES2* = standardized effect size from Null model 2. The optimal random structure for the lme models for each estimate of turnover varied; random intercept (Model A) was optimal in 5 cases, a random slope (Model B) in 6 cases, and a random intercept and a random slope (Model C) in 6 cases.

I. Based on dataset for all 91 species including compiled and interpolated data.

	Model A: 1|Plot	**Model B: 0+ cTime|Plot**	**Model C: 1+cTime|Plot**
TSN	**-522.18**	-520.44	-518.77
TSCBRAY	**-568**	-555.58	-564.16
TSCBRAY.SES1	285.27	**285.13***	288.26
TSCRAO	56.85	62.85	**39.42***
TSCRAO.SES1	345.72	345.72	**341.54***
T|ΔCWM|WD	**-875.77**	-869.38	-871.77*
T|ΔCWM| WD.SES1	-2.04	**-6.91***	-4.17
T|ΔCWM| WD.SES2	221.38	**221.18***	224.79
T|Δ CWM|HMAX	-113.57	-113.57	**-124.42***
T|ΔCWM|HMAX.SES1	-28.17	**-28.17***	-24.16
T|ΔCWM|HMAX.SES2	235.05	**235.05***	236.87
T|ΔCWM|DBHMAX	75.78	75.78	**63.64***
T|ΔCWM|DBHMAX.SES1	-71.45	**-71.45***	-69.24
T|ΔCWM|DBHMAX.SES2	**136.39**	136.39	137.21

TFCRAO	**-203.64**	-198.26	-199.77
TFCRAO.SES1	579.53	534.29*	**494.66***
T*FCRAO.SES2*	414.03	547.3	**348.42***

*Significantly different (P < 0.05) from previous model based on log likelihood ratio test.

II. Based on dataset for only the 60 species that had field-measured functional trait data; the optimal random structure for the lme models for each estimate of turnover varied; random intercept (Model A) was optimal in 5 cases, a random slope (Model B) in 4 cases, and a random intercept and a random slope (Model C) in 5 cases. Bold AIC_c values indicate selected model based on lowest AIC_c value, or when there is a tie in AIC_c values, model with the simplest random structure or significant difference from the previous model based on log likelihood ratio test.

	Model A: 1|Plot	**Model B: 0+ cTime|Plot**	**Model C: 1+cTime|Plot**
TSCRAO	-86.894	-82.488	**-90.506***
TSCRAO.SES1	276.96	**274.99***	278.50
T|Δ*CWM*|*WD*	-881.11	**-889.88***	-886.87
T|Δ*CWM*| *WD.SES1*	15.047	**11.684***	14.977
T|Δ*CWM*| *WD.SES2*	215.95	**214.35**	215.80
T|Δ *CWM*|*HMAX*	**-171.20**	-171.20	-167.21
T|Δ*CWM*|*HMAX.SES1*	**-18.915**	-18.915	-14.915
T|Δ*CWM*|*HMAX.SES2*	**233.35**	233.35	237.35
T|Δ*CWM*|*DBHMAX*	70.501	73.542	**64.830***
T|Δ*CWM*|*DBHMAX.SES1*	**-46.077**	-45.155	-42.183
T|Δ*CWM*|*DBHMAX.SES2*	197.80	200.00	**192.26***
TFCRAO	**-251.59**	-241.06	-247.59*
TFCRAO.SES1	510.37	488.54*	**436.81***
T*FCRAO.SES2*	369.27	510.11	**333.17***

Appendix 2: Methods for testing significance of predictions II and III.

2a. Statistical significance for Prediction II, expressed as $\hat{\beta}_2 + \hat{\beta}_3 < 0$, was tested by estimating the confidence intervals (CIs) for the sum of these coefficients. To estimate CIs, the coefficients, $\hat{\beta}_2$ and $\hat{\beta}_3$, their variances, and covariance were extracted from the output of the linear mixed effects models. The variance for the sum of the coefficients $\hat{\beta}_2 + \hat{\beta}_3 < 0$ was calculated by applying the variance rule:

Variance (X+Y) = Variance (X) + Variance (Y) + 2 * Covariance (X, Y)

The standard error for $\hat{\beta}_2 + \hat{\beta}_3$ was estimated as the square root of the variance for the sum of the coefficients. Standard error was then used to estimate CI values at the 90%, 95% and 99% levels by multiplying the standard error by 1.64, 1.96, and 2.58 respectively. The resulting CI values were then used to set the upper and lower bounds of the CIs by adding the CI value to and subtracting the CI value from the sum of the coefficients. The sum of the coefficients, $\hat{\beta}_2 + \hat{\beta}_3$, was deemed to be significantly different from zero at any level when the CIs did not overlap zero.

2b. Statistical significance for Prediction III, expressed as $|\hat{\beta}_3| - 2 * |\hat{\beta}_2| > 0$, was tested by estimating the confidence intervals (CIs) for the difference between coefficients using a similar procedure as in 2a. However, variance for the difference between coefficients $|\hat{\beta}_3| - 2 * |\hat{\beta}_2|$ was calculated by applying another variance rule:

Variance (a*X – b*Y) = (a^2) * Variance (X) + (b^2) * Variance (Y) – 2 * a * b * Covariance (X, Y)

Standard error for $|\hat{\beta}_3| - 2 * |\hat{\beta}_2|$, and CIs at 90%, 95%, and 99% were estimated similarly as described in 2a above. And $|\hat{\beta}_3| - 2 * |\hat{\beta}_2|$ was deemed significantly different from zero when CIs did not overlap zero.

Appendix 3: Delta AIC_c and AIC_c weights for linear mixed effects models with and without latitude testing the effects of logging status and time on different estimates of turnover. Acronyms same as in appendix 1b.

3a. Based on dataset for all 91 species including compiled and interpolated data.

	Model without Latitude		**Model with Latitude**	
Response variable	**ΔAIC_c**	**AIC_c weight**	**ΔAIC_c**	**AIC_c weight**
T_{SN}	0.64	0.42	0	0.58
T_{SCBRAY}	0	0.73	1.94	0.27
$T_{SCBRAY.SES1}$	4.53	0.09	0	0.91
T_{SCRAO}	0	0.74	2.07	0.26
$T_{SCRAO.SES1}$	0	0.74	2.11	0.26
$T\|_{\Delta CWM\|WD}$	0	0.74	2.04	0.26
$T\|_{\Delta CWM\|WD.SES1}$	0.08	0.49	0	0.51
$T\|_{\Delta CWM\|WD.SES2}$	0	0.69	1.62	0.31
$T\|_{\Delta CWM\|HMAX}$	0	0.68	1.51	0.32
$T\|_{\Delta CWM\|HMAX.SES1}$	0	0.77	2.39	0.23
$T\|_{\Delta CWM\|HMAX.SES2}$	0	0.76	2.33	0.24
$T\|_{\Delta CWM\|DBHMAX}$	0	0.74	2.06	0.26
$T\|_{\Delta CWM\|DBHMAX.SES1}$	0	0.71	1.82	0.29
$T\|_{\Delta CWM\|DBHMAX.SES2}$	0	0.76	2.30	0.24
T_{FCRAO}	0	0.74	2.10	0.26
$T_{FCRAO.SES1}$	0	0.77	2.39	0.23
$T_{FCRAO.SES2}$	0	0.78	2.50	0.22

3b. Based on dataset for only 60 species that had field-measured functional trait data.

Response variable	Model without Latitude		Model with Latitude	
	ΔAIC_c	AIC_c weight	ΔAIC_c	AIC_c weight
T_{SCRAO}	0	0.76	2.28	0.24
$T_{SCRAO.SES1}$	0	0.75	2.19	0.25
$T\|_{\Delta CWM\|WD}$	0	0.69	1.6	0.31
$T\|_{\Delta CWM\|WD.SES1}$	0	0.51	0.06	0.49
$T\|_{\Delta CWM\|WD.SES2}$	0	0.77	2.37	0.23
$T\|_{\Delta CWM\|HMAX}$	0	0.65	1.27	0.35
$T\|_{\Delta CWM\|HMAX.SES1}$	0	0.76	2.28	0.24
$T\|_{\Delta CWM\|HMAX.SES2}$	0	0.77	2.42	0.23
$T\|_{\Delta CWM\|DBHMAX}$	0	0.74	2.14	0.26
$T\|_{\Delta CWM\|DBHMAX.SES1}$	0	0.65	1.25	0.35
$T\|_{\Delta CWM\|DBHMAX.SES2}$	0	0.69	1.57	0.31
T_{FCRAO}	0	0.71	1.84	0.29
$T_{FCRAO.SES1}$	0	0.75	2.22	0.25
$T_{FCRAO.SES2}$	0	0.79	2.63	0.21

Appendix 4a: Similar to table 1 in main text, but for 14 metrics based on dataset for only 60 species that had field-measured functional trait data. Values in bold indicate support for predictions.

Turnover rate	**Metric**	**Predictions**				
		I	**II**	**III**		
		$\hat{\beta}_1 > 0$	$\hat{\beta}_2 + \hat{\beta}_3 < 0$	$\hat{\beta}_3 \neq 0$	$\lvert\beta_3\rvert - 2*\lvert\beta_2\rvert > 0$	
Species composition	T_{SCRAO} #	0.464	0.043*	0.01677	NA	
Species composition	$T_{SCRAO.SES1}$	-1.205	0.117**	NA		0.094
Functional trait	$T_{\lvert\Delta CWM\rvert WD}$	-0.00021*	0.00008**	**0.00007***	NA	
Functional trait	$T_{\lvert\Delta CWM\rvert WD.SES1}$	-0.284**	0.023**	NA		0.019
Functional trait	$T_{\lvert\Delta CWM\rvert WD.SES2}$	-0.489	0.055 ·	NA		0.046
Functional trait	$T_{\lvert\Delta CWM\rvert HMAX}$ §	-0.025	0.006	0.004	NA	
Functional trait	$T_{\lvert\Delta CWM\rvert HMAX.SES1}$	-0.179*	0.012 ·	0.011	NA	
Functional trait	$T_{\lvert\Delta CWM\rvert HMAX.SES2}$	-0.474	0.025	NA		0.018
Functional trait	$T_{\lvert\Delta CWM\rvert DBHMAX}$ §	0.074	-0.003	NA		-0.006
Functional trait	$T_{\lvert\Delta CWM\rvert DBHMAX.SES1}$	-0.059	0.002	NA		0.002
Functional trait	$T_{\lvert\Delta CWM\rvert DBHMAX.SES2}$	-0.180	-0.011	-0.002	NA	
Functional trait	T_{FCRAO} #	0.521	0.053*	0.032	NA	
Functional trait	$T_{FCRAO.SES1}$	0.572	0.416*	NA		0.383
Functional trait	$T_{FCRAO.SES2}$	3.003	0.112*	NA		0.096

Turnover rate natural-log transformed to normalize residuals

§ Turnover rate square root transformed to normalize residuals

Appendix 4b: Similar to Fig. 3 in main text, but showing only six metrics of turnover rates based on dataset for only 60 species that had field measured functional trait data.

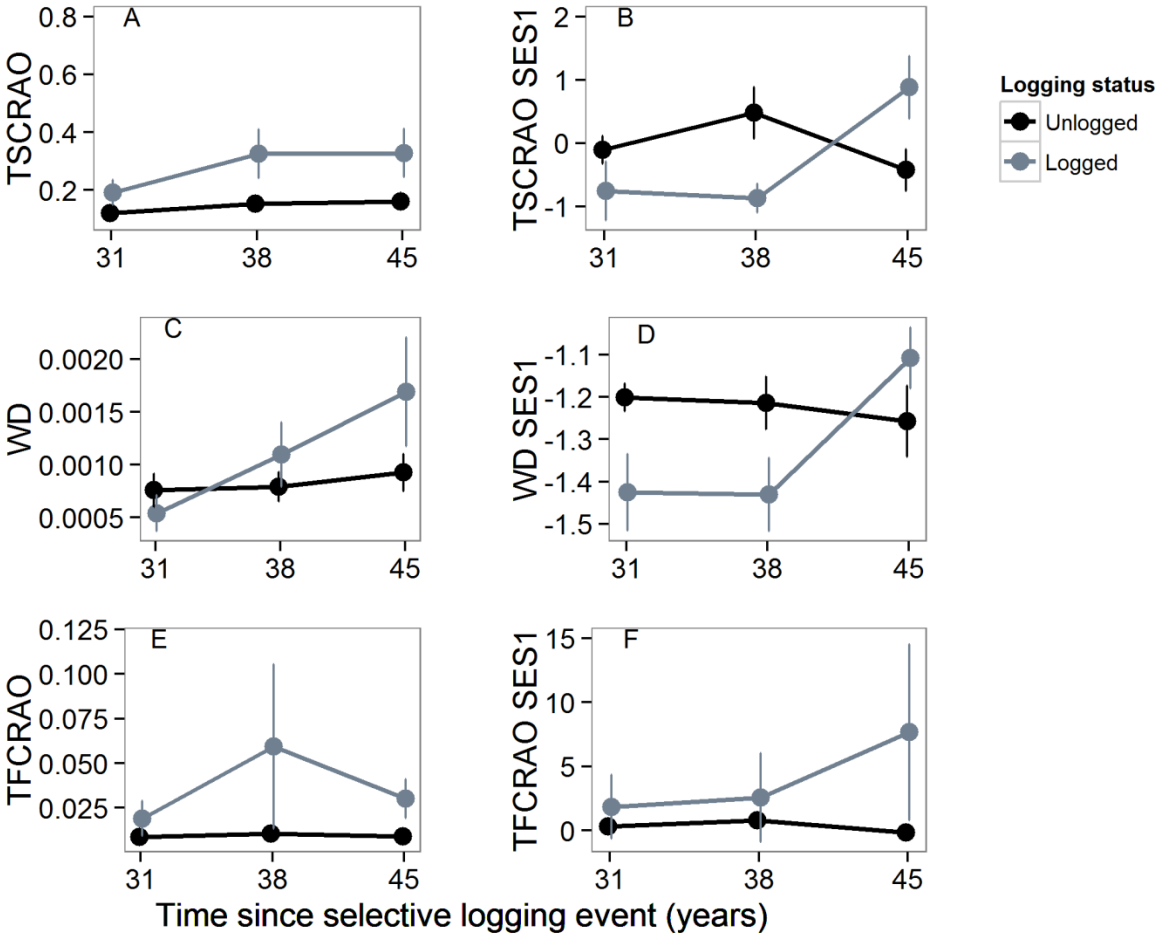

Appendix 5. Results for mixed effect model analysis, testing for the fixed effects of logging, time, the interaction between logging and time, and latitude. Acronyms as in Appendix 1b. For each response variable, there are two models, one with latitude and the other without latitude. Appendix 4 above gives more details on comparisons of models with and without latitude. Estimates in bold have a *P*-value ≤ 0.05.

5a. Based on dataset for all 91 species including compiled and interpolated data.

Model	Unlogged	*P*-value	Logged	*P*-value	Time	*P*-value	Logging status: Time	*P*-value	Latitude	*P*-value
T_{SN}	**0.0175**	0.0000	**0.0068**	0.0439	**0.0006**	0.0008	-0.0006	0.0740		
T_{SN_LAT}	0.1703	0.0577	**0.0125**	0.0110	**0.0006**	0.0009	-0.0006	0.0759	-0.2744	0.0946
T_{SCBRAY}	**0.0122**	0.0000	0.0052	0.0573	**0.0004**	0.0006	0.0000	0.9731		
T_{SCBRAY_LAT}	0.0689	0.4208	0.0073	0.0877	**0.0004**	0.0006	0.0000	0.9733	-0.1018	0.5110
$T_{SCBRAY.SES1}$	-0.2000	0.5165	-0.4053	0.4437	0.0256	0.4713	0.1068	0.0807		
$T_{SCBRAY.SES1\_LAT}$	**-33.9588**	0.0104	**-1.6697**	0.0260	0.0256	0.4513	0.1068	0.0682	**60.6070**	0.0144
T_{SCRAO} [#]	**-2.3104**	0.0000	0.7048	0.0657	0.0274	0.0781	0.0033	0.8985		
T_{SCRAO_LAT} [#]	4.3234	0.6566	0.9532	0.0768	0.0274	0.0804	0.0033	0.8993	-11.9097	0.4992
$T_{SCRAO.SES1}$	0.1717	0.5765	-0.5749	0.2791	-0.0171	0.6303	0.1208	0.0498		
$T_{SCRAO.SES1\_LAT}$	-7.3153	0.5914	-0.8553	0.2535	-0.0171	0.6311	**0.1208**	0.0503	13.4414	0.5856
$T_{\|\Delta CWM\|WD}$	**0.0008**	0.0004	0.0003	0.4579	0.0000	0.6450	0.0000	0.9591		
$T_{\|\Delta CWM\|WD\_LAT}$	-0.0054	0.6053	0.0000	0.9586	0.0000	0.6472	0.0000	0.9593	0.0110	0.5584
$T_{\|\Delta CWM\|WD.SES1}$	**-1.1933**	0.0000	**-0.2485**	0.0042	-0.0049	0.4621	0.0204	0.0723		
$T_{\|\Delta CWM\|WD.SES1\_LAT}$	**-5.0619**	0.0394	**-0.3934**	0.0033	-0.0049	0.4475	0.0204	0.0636	6.9452	0.1195
$T_{\|\Delta CWM\|WD.SES2}$	0.0524	0.8000	-0.2903	0.4145	-0.0139	0.5561	0.0192	0.6309		
$T_{\|\Delta CWM\|WD.SES2\_LAT}$	-8.2449	0.3525	-0.6011	0.2287	-0.0139	0.5547	0.0192	0.6296	14.8960	0.3546
$T_{\|\Delta CWM\|HMAX}$ [§]	**0.2715**	0.0000	0.0781	0.2170	0.0041	0.2936	-0.0067	0.3149		
$T_{\|\Delta CWM\|HMAX\_LAT}$ [§]	1.4113	0.2250	0.1208	0.1241	0.0041	0.2971	-0.0067	0.3184	-2.0461	0.3312
$T_{\|\Delta CWM\|HMAX.SES1}$	**-1.1668**	0.0000	-0.0963	0.2069	0.0026	0.5947	0.0027	0.7467		
$T_{\|\Delta CWM\|HMAX.SES1\_LAT}$	-1.4735	0.4265	-0.1078	0.2997	0.0026	0.5971	0.0027	0.7483	0.5505	0.8689
$T_{\|\Delta CWM\|HMAX.SES2}$	0.3192	0.1639	0.1488	0.7019	0.0103	0.6853	-0.0419	0.3328		
$T_{\|\Delta CWM\|HMAX.SES2\_LAT}$	3.0052	0.7553	0.2494	0.6411	0.0103	0.6871	-0.0419	0.3356	-4.8221	0.7819
$T_{\|\Delta CWM\|DBHMAX}$ [§]	**0.5537**	0.0000	0.2420	0.1486	0.0088	0.3259	-0.0224	0.1412		

Model	Unlogged	*P*-value	Logged	*P*-value	Time	*P*-value	Logging status: Time	*P*-value	Latitude	*P*-value
$T_{\|\Delta CWM\|DBHMAX\_LAT}$[§]	2.2400	0.3990	0.3052	0.1241	0.0088	0.3292	-0.0224	0.1439	-3.0276	0.5279
$T_{\|\Delta CWM\|DBHMAX.SES1}$	**-1.1672**	0.0000	-0.0148	0.8165	-0.0001	0.9798	-0.0004	0.9529		
$T_{\|\Delta CWM\|DBHMAX.SES1\_LAT}$	-2.3299	0.1411	-0.0584	0.5049	-0.0001	0.9799	-0.0004	0.9531	2.0874	0.4630
$T_{\|\Delta CWM\|DBHMAX.SES2}$	-0.0049	0.9851	0.1732	0.7010	-0.0101	0.6714	-0.0291	0.4748		
$T_{\|\Delta CWM\|DBHMAX.SES2\_LAT}$	-3.2492	0.6741	0.0517	0.9235	-0.0101	0.6732	-0.0291	0.4772	5.8244	0.6765
T_{FCRAO}[#]	**-5.1495**	0.0000	**1.0863**	0.0101	0.0223	0.2138	-0.0170	0.5742		
T_{FCRAO_LAT}[#]	-12.1023	0.3448	0.8259	0.1922	0.0223	0.2169	-0.0170	0.5768	12.4822	0.5890
$T_{FCRAO.SES1}$	0.3991	0.6681	1.5261	0.3415	-0.0338	0.8477	0.4599	0.1284		
$T_{FCRAO.SES1\_LAT}$	-4.9097	0.9001	1.3273	0.5426	-0.0338	0.8489	0.4599	0.1314	9.5308	0.8926
$T_{FCRAO.SES2}$	0.2845	0.8613	3.9714	0.1620	-0.0154	0.7785	0.1058	0.2569		
$T_{FCRAO.SES2\_LAT}$	-16.4092	0.7598	3.3462	0.3350	-0.0154	0.7801	0.1058	0.2603	29.9701	0.7572

[#] Natural-log transformed to normalize residuals
[§] Square root transformed to normalize residuals

5b. Based on dataset for only 60 species that had functional trait data.

Model	Unlogged	*P*-value	Logged	*P*-value	Time	*P*-value	Logging status: Time	*P*-value	Latitude	*P*-value
T_{SCRAO} #	-2.3421	0.0000	0.4635	0.1536	0.0260	0.0797	0.0168	0.4997		
T_{SCRAO_LAT} #	2.3917	0.7919	0.6408	0.1782	0.0260	0.0818	0.0168	0.5027	-8.4986	0.6045
$T_{SCRAO.SES1}$	0.1396	0.6136	**-1.2055**	0.0163	-0.0225	0.5085	0.1395	0.0189		
$T_{SCRAO.SES1\_LAT}$	-6.1748	0.6373	**-1.4420**	0.0449	-0.0225	0.5087	11.3362	0.6321	**0.1395**	0.0189
$T_{\|\Delta CWM\|WD}$	**0.0007**	0.0000	-0.0002	0.4069	0.0000	0.5653	0.0001	0.0501		
$T_{\|\Delta CWM\|WD\_LAT}$	0.0076	0.3210	0.0001	0.8923	0.0000	0.5705	0.0001	0.0531	-0.0124	0.3747
$T_{\|\Delta CWM\|WD.SES1}$	**-1.1963**	0.0000	**-0.2841**	0.0018	-0.0040	0.5410	0.0267	0.0196		
$T_{\|\Delta CWM\|WD.SES1\_LAT}$	**-5.0164**	0.0429	**-0.4272**	0.0020	-0.0040	0.5286	0.0267	0.0163	6.8583	0.1272
$T_{\|\Delta CWM\|WD.SES2}$	-0.0199	0.9161	-0.4886	0.1385	-0.0091	0.6928	0.0643	0.1036		
$T_{\|\Delta CWM\|WD.SES2\_LAT}$	1.9693	0.8251	-0.4141	0.3779	-0.0091	0.6954	0.0643	0.1067	-3.5712	0.8244
$T_{\|\Delta CWM\|HMAX}$ §	**0.2808**	0.0000	-0.0251	0.5854	0.0025	0.4082	0.0036	0.4767		
$T_{\|\Delta CWM\|HMAX\_LAT}$ §	1.4388	0.2017	0.0183	0.7686	0.0025	0.4080	0.0036	0.4764	-2.0791	0.3084
$T_{\|\Delta CWM\|HMAX.SES1}$	**-1.1510**	0.0000	**-0.1795**	0.0279	0.0007	0.8961	0.0111	0.1958		
$T_{\|\Delta CWM\|HMAX.SES1\_LAT}$	-1.8185	0.3416	-0.2045	0.0633	0.0007	0.8967	0.0111	0.1984	1.1984	0.7276
$T_{\|\Delta CWM\|HMAX.SES2}$	0.2745	0.2328	-0.4738	0.2320	-0.0079	0.7539	0.0334	0.4384		
$T_{\|\Delta CWM\|HMAX.SES2\_LAT}$	0.2948	0.9755	-0.4730	0.3799	-0.0079	0.7555	0.0334	0.4415	-0.0364	0.9983
$T_{\|\Delta CWM\|DBHMAX}$ §	**0.5562**	0.0000	0.0738	0.5963	0.0084	0.2640	-0.0110	0.3860		
$T_{\|\Delta CWM\|DBHMAX\_LAT}$ §	-1.1824	0.6679	0.0087	0.9599	0.0084	0.2673	-0.0110	0.3892	3.1214	0.5318
$T_{\|\Delta CWM\|DBHMAX.SES1}$	**-1.1663**	0.0000	-0.0598	0.3709	-0.0001	0.9757	0.0025	0.7159		
$T_{\|\Delta CWM\|DBHMAX.SES1\_LAT}$	-2.9989	0.0897	-0.1284	0.1763	-0.0001	0.9758	0.0025	0.7177	3.2901	0.3011
$T_{\|\Delta CWM\|DBHMAX.SES2}$	-0.0329	0.8932	-0.1801	0.6675	-0.0093	0.6644	-0.0021	0.9531		
$T_{\|\Delta CWM\|DBHMAX.SES2\_LAT}$	-7.7259	0.3374	-0.4682	0.3669	-0.0093	0.6665	-0.0021	0.9534	13.8112	0.3446
T_{FCRAO} #	**-5.0997**	0.0000	0.5207	0.1630	0.0213	0.2046	0.0318	0.2661		
T_{FCRAO_LAT} #	-13.7884	0.2447	0.1953	0.7343	0.0213	0.2077	0.0318	0.2693	15.5988	0.4656
$T_{FCRAO.SES1}$	0.5405	0.5721	0.5720	0.7264	-0.0334	0.8093	0.4497	0.0602		
$T_{FCRAO.SES1\_LAT}$	7.8330	0.8587	0.8451	0.7186	-0.0334	0.8100	0.4497	0.0612	-13.0921	0.8691
$T_{FCRAO.SES2}$	0.0326	0.9824	3.0031	0.2408	-0.0165	0.6298	**0.1287**	0.0305		

Model	Unlogged	*P*-value	Logged	*P*-value	Time	*P*-value	Logging status: Time	*P*-value	Latitude	*P*-value
$T_{FCRAO.SES2\_LAT}$	-5.4035	0.9299	2.7995	0.4179	-0.0165	0.6326	**0.1287**	0.0318	9.7594	0.9299

[#] Natural-log transformed to normalize residuals
[§] Square root transformed to normalize residuals